Precise Fish Volume Estimation Using Underwater Helmholtz Resonance

Njane Stephen Njehia

2019

Precise Fish Volume Estimation Using Underwater Helmholtz Resonance

Njane Stephen Njehia

Laboratory of Bio-Sensing Engineering
Division of Environmental Science and Technology
Graduate School of Agriculture
Kyoto University, Japan

2019

Precise Fish Volume Estimation Using Underwater Helmholtz Resonance

Njane Stephen Njehia

This dissertation is submitted to the Graduate School of Agriculture, Kyoto University, in partial fulfilment of the requirements for the degree of Doctor in Agricultural Science

Division of Environmental Science and Technology
Graduate School of Agriculture
Kyoto University

2019

Contents

Chapter I

Introduction

1.1. Precision aquaculture

Feeding the world population which is growing at a rate of 1.1% yearly, and according to the United Nations (UN) (2017) is projected to reach a high of 9.8 billion by 2050 and 11.2 billion in 2100, is not only important and challenging, but also strained by the impacts of climate change. Aquaculture, the rearing of fish, crustaceans, sea weed, and other aquatic organisms, either in extensive (naturally) or intensive systems (controlled) is aimed at providing alternative source of protein for the growing world population, thus hunger eradication, which is one of the 17 Sustainable Development Goals (SGG's) of the United Nations (UN). This will be fuelled by the global fish production which has been steadily increasing since 1950's peaking at 171 million tonnes in 2016, where aquaculture accounted for 46.8% with a total production of 80.03 million tonnes (FAO, 2018). Unlike capture fisheries which has stagnated since the late 1990's, aquaculture production has been steadily increasing and is expected to surpass capture fisheries by 2030 (Fig. 1.1).

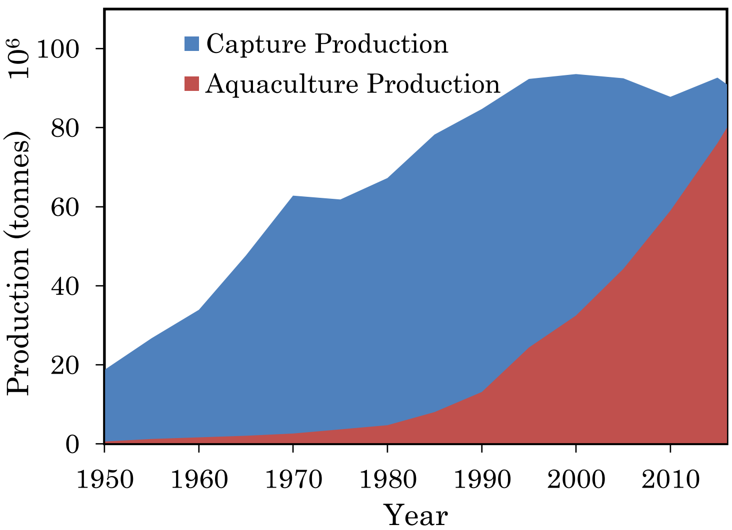

Fig. 1.1. Growth of aquaculture compared to capture fisheries from 1950 to 2016 (FAO 2018).

To realise the optimisation of aquaculture through precise production systems, the informatization of aquaculture is imperative. While precision agriculture, aimed at maximum output based on plant and soil information using sensors, AI (Artificial intelligence) and IoT (Internet of things) has been progressing fast, the informatization of aquaculture is limited, as the growth and production of fish, shellfish and other aquatic products occur in water, thus little has been done to monitor and control both fish and its environs thereof. Not only is there rampant environmental pollution in aquaculture ponds as a result of excessive feed leading to plummeting water quality, but also the high cost of feeding increases the cost of production (Yokoyama et al., 2006).

One of the largest difficulties in informatization and precision aquaculture is the measurement of aquatic products' size in water. Hitherto, the techniques to estimate the size of fish have not yet been developed, and the total volume of fish before landing is unknown. Currently, feeding has been done, based on the sampling of fish *in situ*, manually, a process which is tiresome and can also lead to the death of the fish. Therefore, the development of a rapid technique for fish volume estimation will not only enable efficient feeding based on size determination, but also prevent the use of excessive feeding which is costly and has detrimental effect on the water quality.

1.2. Fish volume measurement techniques and their limitations

Determining the volume of fish and aquatic organisms is an important parameter for monitoring the growth of fish in–situ (underwater), the health condition of the fish (Petrell et al., 1997), the feed consumption patterns and the population density of the fish (Minto et al., 2008). This has not only the possibility of enabling farmers to better plan for harvesting and sales, but to also efficiently utilize their feed (Yokoyama et al., 2006) and eventually could possibly be used to grade the fish. Until recently, fish have been manually sorted on commercial fishing vessels (Kennelly, 1995) based on weight, species and fork length. Furthermore, the length and weight of stream fish have been sampled and measured as a means of conservation (Das and Biswas, 2016).

To do this, the length measurements are taken on the carrier vessel with one person measuring and another jotting down the measurements. However, manual sampling is not only very laborious and time consuming, it is also stressful on the fish (Flos et al., 1988) and may lead to the death of the fish when exposed outside the water for a long period of time.

Hitherto, the non-invasive (without contact) techniques implored underwater for fish size estimation are not only expensive to install and operate, but visual systems have been plagued by water murkiness. An optical stereoscopy could monitor the size, position shape and spatial orientation of a single fish in water (Ruff et al., 1995). But this is limited for single fish volume measurements. The effect of fish sampling position analysed using stereo camera (Shieh and Petrell, 1998) could agree with the physical sampling results but these systems are expensive and cannot sample bottom feeders. Swimmable stereo-video systems that could estimate the length, position and bio mass of fish and operate in areas with low visibilities (Cappo et al., 2003) are expensive to install and need complicated calibration techniques. The fish size and speed in a sea cage could be determined using simple video system. However, inaccuracies occurred when fish swam non-uniformly (Petrell et al., 1997). Edible fishes could be sorted real time while swimming through a narrow channel in a pond but opaqueness due to algae resulted in a need for an artificial source of light (Zion et al., 2007). Colour and shape have been used to sort 23 species of fish with an accuracy of 99% (Strachan, 1994). Furthermore, a computer vision system where fish are transported along a conveyor belt underneath a digital camera, measured the length of the fish and identified whether it was a flat fish or a round fish (White et al., 2006). However, due to water murkiness and low visibility, this method is limited to only the shallow depths, and the use of underwater camera systems is arduous (Spampinato et al., 2008). Though remotely operated vehicles (Underwater ROV's) are used to study behaviour of fish in water (Larsen and Isaksen, 1993), these methods are expensive to install and operate in water. This necessitates the need to develop an alternative non-invasive, efficient and reliable fish volume measurement technique.

The current standard non-destructive measurement methods for precisely determining the volume of irregular shaped products in water are liquid displacement-based methods. However, such methods consume a considerably long time for measurement and are difficult to be applied when fish is in a large water body. Moreover, due to variation in fish size and weight, it makes it difficult to estimate parameters useful for sorting, sizing and grading of which volume is one of these parameters. An alternative method which is fast and non-invasive is necessary to ensure the precise volume estimation of fish and other aquatic organisms. To overcome these challenges, we propose the use of underwater Helmholtz resonance as a technique for fish volume estimation.

1.3. Helmholtz resonance technique for precise fish volume estimation

This technique relies on the change in the effective volume of cavity of the resonator when a sample is inserted into the cavity. By analysing the difference in resonance frequency before and after the sample is inserted, volume can be estimated. The Helmholtz resonance mechanism can be explained by analogy to a mass on a spring. Taking the example of a PET bottle, when air is blown across the top of the neck, a sound can be heard. This is because oscillation of air occurs at the top of the neck of the bottle. The air at the bottle's neck acts as a mass hence has inertia to oscillate and the air in the cavity acts as a spring to provide the stiffness in the cavity. However, due to the inertia at the neck, the air flowing out tends to overcompensate and hence causes the cavity to reduce pressure below that of the external pressure (Zhao et al., 2009; Soedel et al., 1973; Tang, 2005). Helmholtz resonance technique has been used previously for measurement of food samples in air, for example the volume of beans, grapes and apples (Nishizu and Ikeda, 1995). Later, an improved online detection of the samples was developed (Nishizu et al., 2001) and could continuously measure samples and predict their volume moving on a conveyor belt at speeds of 15, 30 and 45 mm/s with an R^2 (R-squared) of prediction of 0.99, 0.99 and 0.97 for wooden blocks, metallic blocks and rice respectively. Since air is less compressible compared to water, this makes it difficult to generate Helmholtz resonance underwater for aquatic products' volume. Furthermore, empirical derivations accompanied by experimental validation are necessary to proof the concept in water.

The same analogy and principle are used in water, where the mass of water oscillates at the top neck of the resonator. The cavity stiffness is provided by the water in the cavity of the resonator as shown in Fig. 1.2. In water, the effect of the density of water ρ_w (kg/m^3) and the neck length l (mL) at the top of the cavity of the resonator, are important parameters in determining the resonant frequency f_o (Hz). Furthermore, when oscillation occurs in the neck underwater, similarly to air, the water rapidly diverges into the cavity and converges into the neck leading to a greater effect of the neck. An additional length l_e (m) which is the end effect of the open end of the neck is utilised to account for the effective longer neck. By utilizing the bulk modulus property of water (K_w) and the dimensional properties of the resonator, an equation that represents the resonance frequency generated is derived as shown in Eq. (1.1) below:

$$f_o = \frac{1}{2\pi}\sqrt{\frac{K_w}{\rho_w} \times \frac{1}{W} \times \frac{S}{l+l_e}} \tag{1.1}$$

When an object, whose volume and bulk modulus are V_o (mL) and K_o (Pa) respectively, is placed inside the resonator, resonance is generated by the bulk water in the neck. The movement of this bulk water at the neck of length x(m), results in a pressure change ΔP (Pa) inside the cavity of the resonator. The resultant resonance frequency when the sample is in the resonator's cavity, f (Hz) is:

$$f = \frac{1}{2\pi}\sqrt{\frac{K}{\rho_w} \times \frac{1}{W-V_o} \times \frac{S}{(l+l_e)}} \tag{1.2}$$

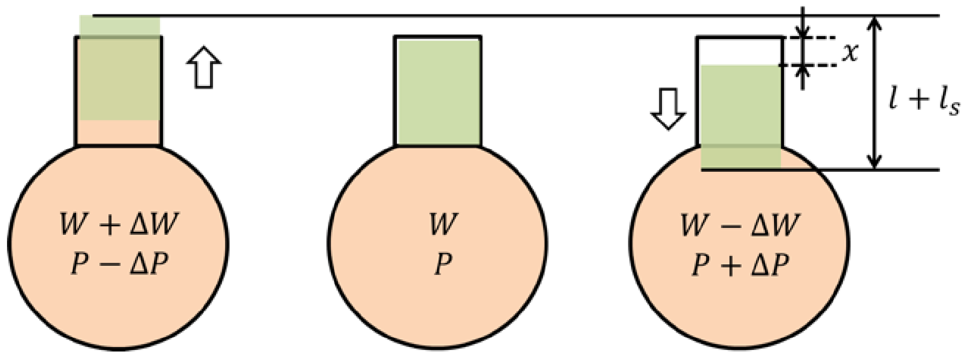

Fig. 1.2. Oscillation of mass of water at the neck resulting in increased pressure in the cavity and Helmholtz resonance occurrence.

When samples whose bulk modulus is less than that of water ($K_o < K_w$) are inserted into the resonator's cavity whose volume, W (mL) is known, resonance frequency decreases as the samples volume increases as shown in Fig. 1.3. However, for samples denser than water ($K_o > K_w$) resonance frequency increases with increased volume of the samples (Fig. 1.3).

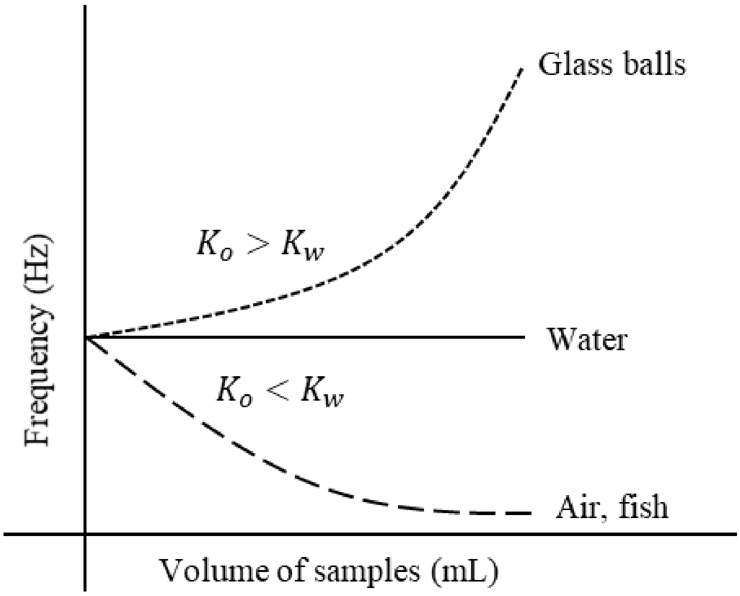

Fig. 1.3. Tendency of resonance frequency with increased volume of denser samples and less dense samples.

A relationship to estimate the volume of aquatic samples V_o (mL), can thus be obtained as shown in the Eq. (1.3) below.

$$V_o = \frac{K_o}{K_o - K_w}\left\{1 - \left(\frac{f_o}{f}\right)^2\right\}W \tag{1.3}$$

However, although the mechanism of Helmholtz resonance has been explained, the actual fish volume measurement in a Helmholtz resonator has yet to be confirmed and explored. This is because the generation of Helmholtz resonance in water is unknown and thus impedes the application thereof. Underwater Helmholtz resonance technique has the potential for application as a fast, non-invasive, accurate method for aquatic products' volume estimation. Study has shown that fish resonate when resonance sound is incident (Ye and Farmer, 1994) and that the fish flesh viscosity (Lo et al., 1979; Raveau and Feuillade, 2014) and the elastic wall of the swim bladder (Feuillade and Werby, 1994; Fine et al., 2016) are responsible for damping of resonance frequency. Therefore utilising underwater Helmholtz resonance technique for fish volume estimation could enable estimation of the density of aquatic products, a useful parameter in sorting and grading (Chen and Sun, 1991; Sun et al., 2010). Aquatic products vary in shape and size and such variation could influence the growth due to dominance in feeding hierarchies and competition for feed (McCarthy et al., 1992). Furthermore determining the volume of aquatic products would reduce the amount of waste that accrues due to organic feed that forms a sludge on the sea bed (Yokoyama et al., 2006). However, to apply this technique underwater, it is important to understand the mechanism of Helmholtz resonance and its principles thereof.

1.4. Underwater closed cavity resonator using water reed technique

In 2011, the laboratory of Bio-Sensing Engineering, Graduate School of Agriculture, Kyoto University succeeded in developing the first underwater Helmholtz resonance technique for aquatic sample volume estimation. Furthermore, the technique was patented and could enable the volume estimation of swimming fish, both in Japan (JP 6103713) and overseas (AO1 K 61/00). The technique involves directing water using a nozzle to an edge on the neck of a cavity (water reed) and because of the oscillation of this mass of water at the neck, the pressure in the cavity changes and because of the difference in the bulk modulus between water and fish, resonance frequency changes. Shinohara et al., (2014) used a closed cavity resonator to estimate the volume of denser samples (glass balls) and less dense samples (air bubbles). Samples were inserted into the closed cavity and closed for measurement to progress. observed that while as the volume of glass balls increased, resonance frequency increased, resonance frequency deceased with increased volume of air. A high linear correlation between the actual and predicted volume of both glass balls and air were obtained. This demonstrated the potential of underwater Helmholtz resonator for aquatic sample volume measurement.

1.5. Limitations of a closed cavity resonator using water reed technique

Normally, for a closed cavity resonator, the neck is utilised for resonance generation (Webster and Davies, 2010). An additional door or a lockable opening must be made for sample insertion and closed or locked once measurement is in progress. This necessitates the need for an additional permanent opening into the cavity of the resonator that can act as an inlet for the samples and in the future underwater applications, be the entrance for live aquatic products, such as fish. A resonator that has another opening would have several advantages, including non-invasive measurement and the ability for future automation when measuring live aquatic products. However, development of an open cavity resonator has been impeded though by the lack of theoretical principles to aid in the optimal design and performance of such an underwater resonator. Thus, we set out to derive a theoretical model for open cavity Helmholtz resonators with an additional opening, and then to experimentally validate the derived empirical models and investigate the implications they have on the performance of this type of resonator.

1.6. Research objectives

The first objective of this study is to develop an underwater Helmholtz resonator with an opening for precise fish volume estimation. Firstly, I design and develop a stainless-steel Helmholtz resonator with an opening on the side where samples can be inserted, and volume measured without locking or closing the resonator. Although the resonator can measure aquatic samples both when closed or open, however, open cavity resonators have potential to improve the limitations of closed cavities since the lock must be opened, the samples inserted and the lock once more closed before sample measurement. However, with the opening, samples can be measured without the need to close or lock the opening. Furthermore, such an opening could act as an inlet for samples, as well as an entrance for live aquatic samples in the future. To generate Helmholtz resonance in such a cavity, I utilise the water reed technique where water flowing through the nozzle and edge attached on the neck of the resonator generates resonance frequencies. To optimise the flow velocity, I evaluate the effect of varied flow velocity over the nozzle and edge of both closed and open cavity resonator for optimised sample product volume estimation. To estimate the volume of samples, I propose empirical models for precise sample volume estimation in the open cavity resonator and simulate the effect of increased volume of both denser and less dense samples, as a lead on fish volume estimation. To validate the simulated empirical models, glass balls are measured as a representative of denser samples while air bubbles are measured as a representative of samples less dense than water. Furthermore, air has acoustic properties similar to fish and can model the behaviour of fish with swim bladder. Finally, as a proof of concept, I will measure the volume of fish in the open cavity resonator. However, to generated Helmholtz resonance in an open cavity, high water flow velocities are needed to overcome the energy lost through the open hole of the resonator. Such high-water velocity not only damage the fish flesh, but fluctuations in resonance frequency occur as a result of unstable shear flows.

To overcome these limitations, the second objective of my research is to develop a new Helmholtz resonance technique for precise fish volume estimation. To do this, I utilise the impedance property of the speaker for resonance generation and a double cavity Helmholtz resonator for precise fish volume estimation. To do this, I firstly, develop the empirical models for by modelling the double cavity resonator as a mass on two springs. While the top cavity, also known as the generating cavity, is for signal generation, the bottom cavity, also known as the sample cavity, is for sample volume measurement. An underwater speaker is attached onto the generating cavity for chirp wave signal (sweep sound) generation. Such a chirp wave signal has an acoustic density higher than white noise enabling peak identification. The diaphragm of the speaker's membrane is used to determine the frequency response of the speaker, thus acting as a transceiver (both transmitting and receiving the signal). The generating cavity is connected by a neck to the sample cavity after which air, which can model the effect of fish with swim bladder, is inserted for measurement. The effect of increased volume of air with resonance frequency is evaluated both empirically and experimentally. As a lead on resonator optimisation for highly sensitive fish volume estimation, the effect of increased cross-sectional area and length of the neck on resonance frequency is investigated. However, since a stainless-steel double cavity resonator is utilised, such a sample cavity is costly to fabricate and thus uneconomical.

For practicability of the double cavity resonator for precise fish volume estimation, the third objective of my research it to improve the double cavity Helmholtz resonator using a light portable acrylic sample cavity for fish volume estimation. Such an acrylic sample cavity is not only cheaper to fabricate and develop but also clear, thus the condition of fish during sample measurement can be monitored. Furthermore, from the results on neck size variation and optimisation resonator, the generating cavity is placed directly onto the sample cavity thus maximising the neck area and minimising the neck length for highly optimised measurement. A chirp wave signal is generated from the speaker connected to the generating, through the neck to the sample cavity, since the acoustic density is higher than white noise (Johansson and Kleiner, 2001; Xu et al., 2010). As a proof of concept, the cumulative volume of the Japanese dace fish (*Tribolodon hakonensis*) and the Japanese rice fish (*Oryzias latipes*) will be measured and estimated and a model correlating the actual and predicted volume will be developed for precise fish volume estimation. However, such a small cavity is limited by the small volume of fish that can be estimated, and since the sample cavity is submerged, a new approach is imminent for onshore aquaculture.

The fourth objective of this study is to develop a Helmholtz resonance technique for total fish volume estimation in large inland aquatic tanks. To do this, I design and develop a generating cavity (connected to a speaker) connected onto the side of an open acrylic tank for total fish volume estimation. This invention, which has been sent for patenting both in Japan (application number 2018-167565) and overseas, will enable easier, faster and with more precision the estimation of the total volume of fish in aquarium and inland tanks. Furthermore, the total fish volume is measured in an open aquarium, a first in the world and a step closer to commercialization. A chirp wave signal will be generated from the generating cavity thus causing the tank to resonate. However, such a large tank may not only be marred by low resonance frequencies, but also such frequencies may not be captured by the speaker due to the limited range of the speaker's frequency sensitivity for detection. A hydrophone is proposed for resonance frequency detection. Japanese dace fish, with cumulative volume are inserted into the tank and the effect of resonance frequency change with cumulative and total fish volume is evaluated. As a lead on the optimisation of the sensitivity of open tank resonator cavities, the effect of the dimeter of the opening with resonance frequency is evaluated.

1.7. Topics of this research

Chapter 1 introduced precision aquaculture for fish volume estimation. Current techniques for fish volume estimation were explored and their limitations described. Helmholtz resonance technique was introduced as a fast, precise and non-destructive technique for fish volume estimation. Hitherto, the measurement of fish volume was limited to a closed cavity, however such a closed cavity resonator is limited as samples must be inserted and closed for measurement to commence. An open cavity Helmholtz resonator that can enable the measurement of fish volume without locking the resonator was introduced.

In chapter 2, the design and fabrication of the open cavity Helmholtz resonators for aquatic and fish volume measurement using water reed technique was explored. The technique which involves directing water to a nozzle and edge on the resonator has potential for aquatic sample volume estimation. Firstly, simulation of empirical model was carried out and validated using samples denser (glass balls) and less dense (air bubbles) than water. To determine the optimum flow for resonance generation, flow velocity was varied, and the optimum flow utilised for sample volume estimation for both closed and open cavity resonators. As a proof of concept, the cumulative volume of the Japanese rice fish (*Oryzias latipes*) popularly known as medaka was measured and the volume estimated. The tendencies of resonance frequency change with increased volume of the samples was obtained, plotted and finally, a linear correlation between the actual and predicted volume of glass balls, air and fish was established.

Chapter 3 introduced a new technique for aquatic sample volume estimation using speaker impedance system utilising a double cavity resonator. To enable the measurement, the empirical models for such a resonator were developed and a stainless-steel double cavity resonator was designed and fabricated. The tendency of resonance frequency change with increased volume of air obtained and a linear correlation between the actual and predicted volume of air was obtained. Furthermore, the effect of the neck connecting the double cavity resonator was investigated

As an improvement of the double cavity resonator system using impedance technique, chapter 4 introduced a light, portable acrylic sample cavity for fish volume estimation. Both small fish (Japanese rice fish) and larger fish, (Japanese dace fish) were measured and their volume precisely estimated. Furthermore, the property of other parts of the fish such as meat and swim bladder resonance were explored as a lead in understanding the resonance property of the fish.

Chapter 5 introduced a new technique for sample volume estimation for inland aquatic tanks. By attaching a generating cavity on the side of the tank, resonance frequency was generated and captured using a hydrophone inserted into the sample cavity. Resonance frequency peak occurred, and such a peak shifted with increased volume of Japanese dace fish in the 4.91 L acrylic tank.

Chapter 6 concluded the research findings that Helmholtz resonator has the possibility to precisely estimate the volume of fish underwater and in inland aquaculture. Furthermore, the prospects of actualisation and commercialisation were explored with a possibility for future upscaling for inland aquaculture tanks. Furthermore, in the future a possibility for underwater sizing and sorting would be possible when using an open-duct type resonator.

References

Cappo, M., Harvey, E., Malcolm, H., Speare, P., others, 2003. Potential of video techniques to monitor diversity, abundance and size of fish in studies of marine protected areas. In: Proceedings of World Congress on Aquatic Protected Areas, Cairns, Australia, pp. 455–464.

Chen, P., Sun, Z., 1991. A review of non-destructive methods for quality evaluation and sorting of agricultural products. Journal of Agricultural Engineering Research, 49, 85–98.

Das, K., Biswas, S.P., 2016. Length-weight relationship and condition factor of a Hill stream fish *Garra gotyla* (Gray) from Noa-dihing river, Arunachal Pradesh. International Journal of Engineering Technology Science and Research, 3, 6.

Food and Agriculture Organisation of the United Nations (FAO), 2018. Meeting the sustainable development goals, the state of world fisheries and aquaculture. Rome, Italy.

Feuillade, C., Werby, M.F., 1994. Resonances of deformed gas bubbles in liquids. The Journal of the Acoustical Society of America, 96, 3684–3692.

Fine, M.L., King, T.L., Ali, H., Sidker, N., Cameron, T.M., 2016. Wall structure and material properties cause viscous damping of swim bladder sounds in the oyster toadfish (*Opsanus tau*). Proceedings of the Royal Society B Biological Sciences, 283, 1841.

Flos, R., Reig, L., Torres, P., Tort, L., 1988. Primary and secondary stress responses to grading and hauling in rainbow trout, *Salmo gairdneri*. Aquaculture, 71, 99–106.

Johansson, T.A., Kleiner, M., 2001. Theory and experiments on the coupling of two Helmholtz resonators. The Journal of the Acoustical Society of America, 110, 1315–1328.

Kennelly, S.J., 1995. The issue of bycatch in Australia’s demersal trawl fisheries. Reviews in Fish Biology and Fisheries, 5, 213–234.

Larsen, R.B., Isaksen, B., 1993. Size selectivity of rigid sorting grids in bottom trawls for Atlantic cod (*Gadus morhua*) and haddock (*Melanogrammus aeglefinus*). In: ICES Marine Science Symposium, pp. 178–182.

Lo, A., Hovem, J.M., others, 1979. An experimental investigation of swim bladder resonance in fishes. The Journal of the Acoustical Society of America, 66, 850–854.

McCarthy, I.D., Carter, C.G., Houlihan, D.F., 1992. The effect of feeding hierarchy on individual variability in daily feeding of rainbow trout, (*Oncorhynchus mykiss*) (Walbaum). Journal of Fish Biology, 41, 257–263.

Minto, C., Myers, R.A., Blanchard, W., 2008. Survival variability and population density in fish populations. Nature, 452, 344–347.

Nishizu, T., Ikeda, Y., 1995. Volume measuring system by acoustic method for agricultural products, 1: Precision and accuracy of volume measuring system by applying Helmholtz resonance phenomena (In Japanese). Journal of the Japanese Society of Agricultural Machinery and Food Engineers, 57, 47-54

Nishizu, T., Ikeda, Y., Manmoto, S., Umehara, T., Mizukami, T., 2001. Automatic, continuous food volume measurement with a Helmholtz resonator. Agricultural Engineering International: The CIGR Journal of Scientific Research and Development, FP01, 004 Vol. III.

Petrell, R.J., Shi, X., Ward, R.K., Naiberg, A., Savage, C.R., 1997. Determining fish size and swimming speed in cages and tanks using simple video techniques. Aquacultural Engineering, 16, 63–84.

Raveau, M.P., Feuillade, C., 2014. Time domain investigations of acoustical scattering from schools of swim bladder fish. The Journal of the Acoustical Society of America, 135, 2177–2177.

Ruff, B.P., Marchant, J.A., Frost, A.R., 1995. Fish sizing and monitoring using a stereo image analysis system applied to fish farming. Aquacultural Engineering, 14, 155–173.

Shieh, A.C.R., Petrell, R.J., 1998. Measurement of fish size in Atlantic salmon (*Salmo salar l.*) cages using stereographic video techniques. Aquacultural Engineering, 17, 29–43.

Shinohara, Y., Kondo, N., Ogawa, Y., 2014. Fish volume estimation using Helmholtz resonance and water reed method. Master's thesis, Kyoto University, Graduate School of Agriculture (Japanese).

Soedel, W., Padilla Navas, E., Kotalik, B.D., 1973. On Helmholtz resonator effects in the discharge system of a two-cylinder compressor. Journal of Sound and Vibration, 30, 263–277.

Spampinato, C., Chen-Burger, Y.-H., Nadarajan, G., Fisher, R.B., 2008. Detecting, tracking and counting fish in low quality unconstrained underwater videos. In: Proceedings of VISAPP 2 2008, 514–519.

Strachan, N.J.C., 1994. Sea trials of a computer vision-based fish species sorting and size grading machine. Mechatronics, 4, 773–783.

Sun, T., Huang, K., Xu, H., Ying, Y., 2010. Research advances in nondestructive determination of internal quality in watermelon/melon: A review: Journal of Food Engineering, 100, 569–577.

Tang, S.K., 2005. On Helmholtz resonators with tapered necks. Journal of Sound and Vibration, 279, 1085–1096.

United Nations (UN), 2017. World population prospects, the 2017 revision. Department of economics and social affairs, New York.

Webster, E.S., Davies, C.E., 2010. The use of Helmholtz resonance for measuring the volume of liquids and solids. Sensors, 10, 10663–10672.

White, D.J., Svellingen, C., Strachan, N.J.C., 2006. Automated measurement of species and length of fish by computer vision. Fisheries Research, 80, 203–210.

Xu, M.B., Selamet, A., Kim, H., 2010. Dual Helmholtz resonator. Applied Acoustics, 71, 822–829.

Ye, Z., Farmer, D.M., 1994. Acoustic scattering from swim-bladder fish at low frequencies. The Journal of the Acoustical Society of America, 96, 951–956.

Yokoyama, H., Abo, K., Ishihi, Y., 2006. Quantifying aquaculture-derived organic matter in the sediment in and around a coastal fish farm using stable carbon and nitrogen isotope ratios. Aquaculture 254, 411–425.

Zhao, D., A'Barrow, C., Morgans, A.S., Carrotte, J., 2009. Acoustic damping of a Helmholtz resonator with an oscillating volume. AIAA Journal, 47, 1672–1679.

Zion, B., Alchanatis, V., Ostrovsky, V., Barki, A., Karplus, I., 2007. Real-time underwater sorting of edible fish species. Computers and Electronics in Agriculture, 56, 34–45.

Chapter II

Underwater Helmholtz resonator with an open cavity for aquatic and fish volume estimation using water reed technique

Abstract

Helmholtz resonators with an opening on the side of the cavity have the potential to improve the limitations of closed cavity resonators as a practical means for determining sample volume underwater. When inserting samples into a closed cavity resonator, a door must be opened, the samples inserted and the door once more closed before commencing measurement. By incorporating an additional opening in the cavity, it could act as east access inlet for samples, as well as an entrance for live aquatic samples in the future. We developed the empirical models, simulated the effect of increased sample volume in the resonators, designed and fabricated a Helmholtz resonator with an opening for sample volume estimation. To develop the model, we utilise samples denser than water, glass balls and less dense than water, air and as a proof of concept the volume of fish is measured in both closed and open cavity resonators. Both the simulation model and the experimental validation indicated that, as the volume of glass balls increased resonance frequency decreased, and as the volume of air, similar to fish increased, resonance frequency decreased. The damping of the resonance frequency was caused by the viscous fish flesh and the elastic swim bladder in the anterior chamber of the model fish, Japanese rice fish (*Oryzias latipes*). By use of empirical equations, a linear regression model R^2 (R-squared) with an accuracy of 0.99 in the open cavity resonator was obtained.

2.1. Introduction

The precise estimation of the volume of fish and aquatic products in water is important for feeding, monitoring the growth of fish and for determine the appropriate time for landing. Until today, fish has been manually sampled, a process which is not only tiresome and may lead to fish death, but also the non-destructive techniques utilised are costly and plagued by water murkiness. We introduce a new rapid measurement technique for aquatic sample volume estimation, known as Helmholtz resonance. This technique has been applied in air for successful measurement of watermelon density (Diezma-Iglesias et al., 2004), liquid volume (Nakano et al., 2005) and food products (Nishizu et al., 2001). However, due to the relative incompressibility of water (compared to air), the theory and the mechanism for resonance generation in water (exploiting differences in the bulk modulus between water and the sample) and its application to *in-situ* water measurements has been left unexplored.

2.1.1. Water reed technique for resonance generation

Underwater Helmholtz resonance can be generated by flow-excited resonance using water reed technique. In this technique, water flows from a nozzle to the edge of the neck at the top of the resonator, where acoustic resonance is generated as shown in Fig. 2.1. The resonance occurs because of unstable separated flows, such as a shear or uneven jet oscillation patterns between the nozzle and the edge, that causes the mass of water at the neck adjacent to such a shear flow to oscillate leading to resonance occurrence. Flow visualizations can be used to explain the mechanism of such flow excited resonance (Ziada, 2001) as periodic vortices normally occur as water passes over the edge. Jumps in the resonance frequency are also associated with this phenomenon as the fluid flow is increased (Brown, 1937a).

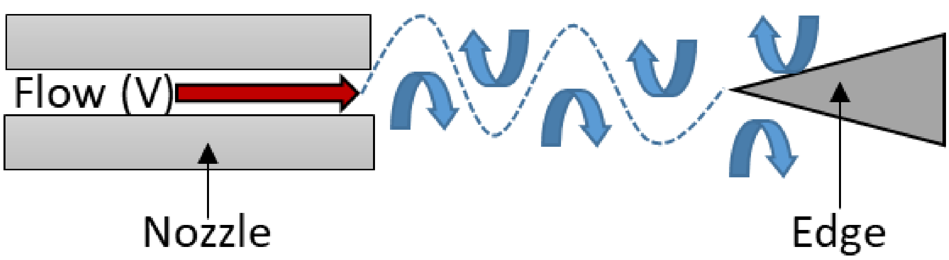

Fig. 2.1. Water jet, through a nozzle hits an edge forming vortex on both sides of the edge.

By characterizing how resonance frequency varies with water flow velocity, optimum flow velocity for sample volume estimation can be realized. The derivation of an edge tone equation is necessary to model the different modes of vibration. The edge tone frequency (f_e) is derived in the Eq. (2.1). The different modes of vibration; 1.0 , 2.3, 3.8 and 5.4 are given as j (Brown, 1937b). By ensuring a constant distance between the nozzle and the edge L (cm), flow velocity V (cm/s) can be varied to indicate the characteristic of such fluid excited resonance.

$$f_e = 0.466j(V - 40)\left\{\frac{1}{(L) - 0.07}\right\} \tag{2. 1}$$

Coupling this phenomenon in water with an open cavity resonator is yet to be examined. In this study, we will utilise water reed technique for resonance generation and for the precise fish volume estimation in a closed and open cavity resonator.

Shinohara et al., (2014) utilised water reed technique for aquatic samples volume estimation. To do this, water flowing at a specified velocity was directed onto the edge and nozzle attached on the neck of a closed cavity resonator as shown in Fig. 2.2 (a). Glass balls were used as a representative of denser samples and air bubbles were used as a representative of samples less dense than water. As the volume of glass balls increased, resonance frequency increased. As the volume of air bubbles increased, resonance frequency decreased. This indicated the potential for underwater Helmholtz resonance measurement for aquatic products volume. However, a such a closed cavity is limited as samples must be inserted and resonator closed before measurement commences. This is not only time consuming and laborious, but also cannot be used for automatic measurement of fish underwater.

To this, an added second opening of the open cavity resonator, is as shown in Fig. 2.2 (b). The volume of the cavity of the resonator is represented as W (mL) while the bulk modulus and the density of the water is K_w (Pa) and ρ_w(kg/m^3) respectively. This resonator has a top neck and a side opening. The top neck has a cross sectional area S_1 (m^2) and length $l_1 + l_{e1}$ (m). The top neck has the mass of water which oscillates and in turn generates the resonance. The opening on the side of the cavity has a cross sectional area S_2 (m^2), and neck length $l_2 + l_{e2}$ (m). For the open cavity resonator, a similar derivation analogy as that of a closed type cavity resonator, can be applied. The Helmholtz resonant frequency f (Hz) when an object is inserted into an open cavity resonator is shown in the Eq. (2.2) below:

$$f = \frac{1}{2\pi} \times \sqrt{\frac{K_w}{\rho_w} \times \frac{1}{W - V_o} \times \left(\frac{S_1}{l_1 + l_{e1}} + \frac{S_2}{l_2 + l_{e2}}\right)} \qquad (2.2)$$

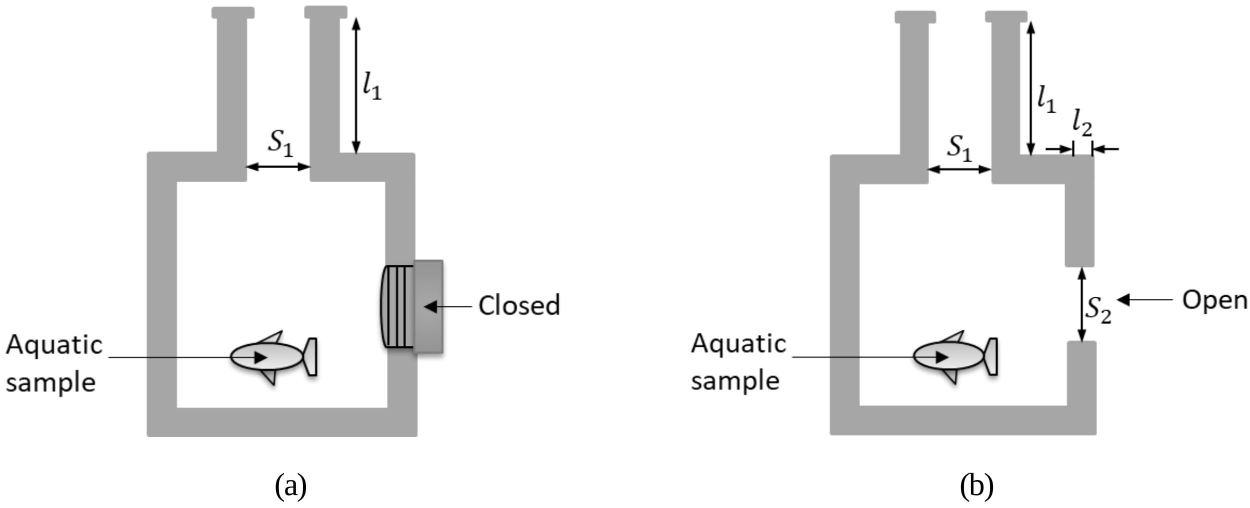

Fig. 2.2. Resonator cavities when (a) closed (b) open for aquatic samples' volume estimation.

In this study, we constructed a stainless-steel type resonating cavity with a neck for resonance generation and a permanent opening on the side of the cavity. The opening acts as an inlet for samples to be inserted (this opening is not closed during measurement) when measurement is underway. The neck, which generates resonance, has a whistle type nozzle and edge attached on top of it. To generate resonance, water is directed to the nozzle and edge at a specified flow velocity. However, in practice, it is difficult to determine the flow velocity at which resonating sounds will be generated due to overtones. We therefore designed an experiment where we compared both closed and open cavity resonators to determine resonance generation parameters when varying the flow velocity. Yet another critical, but unknown, determinant of resonator performance will be the relationship between cavity to sample volume. This is important for future cavity design of the resonator in order to maximize the sensitivity for the expected sample volume given a particular cavity size (Kurdi et al., 2014). To do this, we first developed a theoretical model based on the dimensions of the resonators (both closed and open) to compare their performance. Deyu et al., (2007) has shown that optimally designing a resonator can improve its performance. The models were then used to simulate measurements of samples that are either denser, or less dense than water.

To validate the simulations derived from the empirical models, experimental prototypes of both (the closed and open) cavity resonators were constructed. For samples denser than water, glass balls were used, whereas for samples less dense than water, air was used for sample volume measurement. However, although the mechanism of Helmholtz resonance has been explained, the actual fish volume measurement in a Helmholtz resonator has yet to be confirmed and explored. In this study, as a proof of concept, fish volume was measured and estimated using both closed and open cavity Helmholtz resonators. In addition, these open cavity resonators have the potential to be utilized to sort fish in-situ (water) based on volume differences in actual practical application. Furthermore, this could be applied to individual fish volume estimation, hence enabling individual grading where growth differences occur within similarly reared fish species.

2.2. Materials and devices

2.2.1. Materials: Glass balls and air

Glass balls were chosen as a representative of sample that is denser than water. The glass balls were spherical with a diameter 17 ± 0.5 mm. Amplitude domain indices are relevant when choosing the size or diameter of the glass balls (Grassi, 2005). Each glass ball had a volume of 2.57 mL. The bulk modulus of glass (silica glass) is 3.7×10^{10} Pa. Silica glass balls were chosen because of their low vibrational response, and high strength to weight ratio (Wang et al., 2004). Air bubbles were used as a model sample that is less dense than water, such as a fish's air-filled swim bladder. Air has a bulk modulus of 1.4×10^{5} Pa (20 °C, 1 atm.). The volume of air directly inserted into the resonator was measured by use of a syringe. Once inserted into the resonator, the air gathered at the upper corner of the resonator's cavity.

2.2.2. Japanese rice fish

28 Japanese rice fish, popularly known as "medaka" (*Oryzias latipes*) were bought from Hamaichi bait manufacturer company in Wakayama, Japan. These fish inhabits both fresh and brackish waters throughout Asia and South East Asia (Iwamatsu, 2004). The fish were two months old after hatching with an average fork length of 25 ± 5 mm and an average volume of 0.26 ± 0.06 mL. In the closed cavity resonator, 28 fish (with a total volume of 7.277 mL) were utilised while in the open cavity, a total of 9 fish (with a total volume of 2.245 mL) were utilised for measurement. Japanese rice fish are omnivorous eurythermal fish which can survive in ponds and outdoor environments where they feed on zooplankton and phytoplankton (Shima and Mitani, 2004). However, the fish were kept in a fish tank measuring 1200 × 600 × 600 mm and were fed synthetic food.

2.2.3. Helmholtz resonators: Closed and open cavities

A stainless-steel cavity resonator with an internal volume of 729.0 mL and an external dimension of 100 × 100 × 100 mm, similarly to that developed by Njane et al., (2018) was fabricated and utilised as shown in Fig. 2.3. The wall of the resonator's cavity was 10 mm and the neck connected to the cavity of the resonator was 75 mm long with an internal diameter of 30 mm.

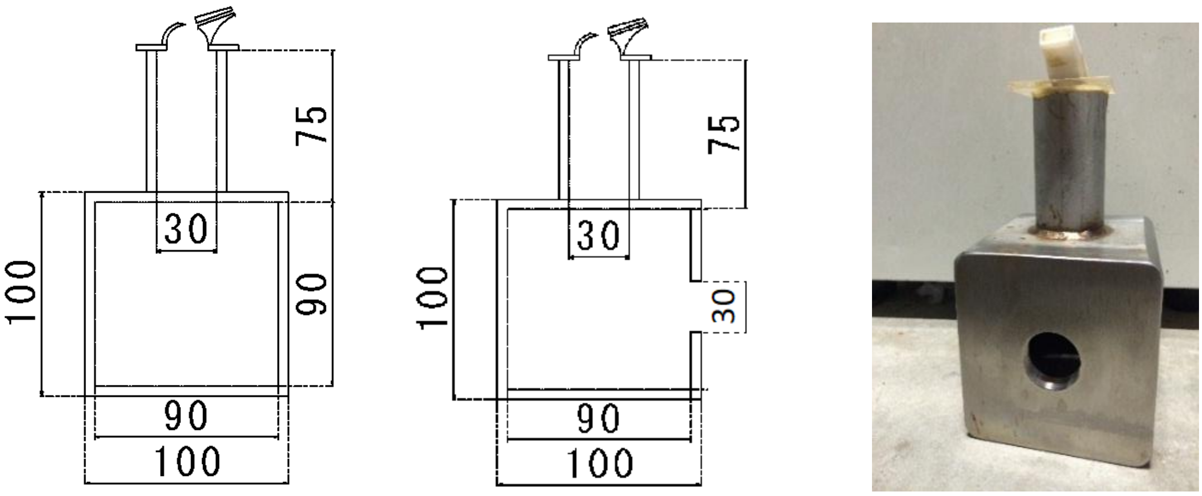

(a) (b) (c)

Fig. 2.3. Stainless-steel Helmholtz resonator (a) closed cavity (b) with an opening on the side of the cavity (c) the image of the open cavity resonator (dimensions in mm).

An open cavity resonator with an opening on the side of 5 mm in depth (same as resonator's thickness) and had a diameter of 30 mm, which is the same as the cavity wall thickness, was incorporated (Fig. 2.3 (b and c)). This was the opening where samples were inserted and was left open during sample volume measurement. To generate resonance at the neck and in the resonator's cavity, an acrylic whistle type nozzle and edge, was attached onto the top part of the resonator's neck as shown in Fig. 2.4. The nozzle was 38 mm long with a clearance of 5 mm to the edge of the whistle. The nozzle, 38 mm long was inclined at an angle of 30 degrees from the horizontal plate. The nozzle had a cross sectional area of 1.328 cm^2, and the distance between the jet and the edge was 5 mm. Water flowing through the nozzle was directed to the edge hence creating vortex on both sides of the edge. The mass of water at the neck oscillated, hence generating resonance.

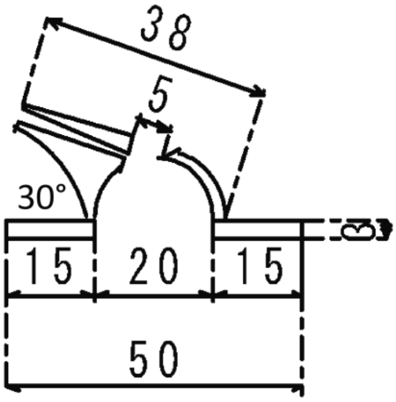

Fig. 2.4. The whistle-type acrylic nozzle and edge attached on the neck of the resonator (dimensions in mm).

2.2.4. Supporting devices

A magnetic drive water pump (MD-70 RM, IWAKI CO., LTD, Japan) was used to generate water flow from the water tank to the resonator. The pump had a maximum flow rate of 62 L/min. From the pump, a stainless-steel pipe, with an outer diameter of 26 mm and an inner diameter of 19 mm was used to connect the pump and the nozzle pipe. The head maximum was about 8 m. The pump flow rate used during the experiment was between 3.0 L/min– 18 L/min. The specifications of the pump are shown in Table 2.1.

Table 2.1 Water pump specifications used for measurement.

Parameter	Specification
Flow Rate	5 – 62 L/min
Pump Setting	Any flow rates
Power Capacity	AC 100 V 50/60 Hz
Length of Pipe	1500 mm, max head 300 mm

To determine the water flow rate into the resonator, a water flow sensor (Keyence FD-M Series, KEYENCE, Japan) was attached onto the stainless-steel pipe. This is a non-wetted electrode electromagnetic flow sensor that estimates the water flowrate passing through the pipe in L/min, with an accuracy of 0.01 L/min. The flow sensor uses electrostatic capacitance and there are no electrodes used inside the pipe, hence the effect of deposits flowing in the pipe were minimised. An elastic horse pipe with an external diameter of 20 mm and an internal diameter of 15 mm was used to connect water from the stainless-steel pipe to the acrylic edge and nozzle attached onto the neck of the resonator's cavity.

A highly sensitive hydrophone (AQ-020, Aqua Sound Inc. Kobe, Japan) was used to capture the sound signal from the resonator. The knob of the hydrophone (diameter of 30 mm) was placed on the neck at the top of the resonator to capture the tones as the resonance frequencies were generated. The specifications of the hydrophone are shown in Table 2.2. The hydrophone was connected to an amplifier (Aqua feeler SH20K, Aqua Sound Inc. Kobe, Japan) for signal gain amplification. A Hi-speed USB (Roland UA-101 USB, Roland, Japan) sound interface device was utilized to connect the hydrophone through the amplifier to the computer. The sound interface functions as a stereo audio interface with a sampling frequency of 48 kHz and a signal processing specification of 24 bits with a signal to noise ratio of 107 dB for the output and 101 dB for the input channel.

Table 2.2 Specifications for the hydrophone used for measurement.

Parameter	Specification
Frequency Range	20 Hz-20 kHz
Reception Sensitivity	195 dB (re 1V/μPa
Capacitance	10000 pF (10 m cable length)
Maximum Water Depth Length	50 m

2.3. Methodology for glass balls and air volume measurement

2.3.1. Flow variation with sample volume measurement

To analyse the effect of flow excited over the resonator's cavity, water flow was regulated from 35 - 565 cm/s. The signal was captured by a hydrophone, and post signal processing performed with Fast Fourier Transform function using spectrum analysis (volume spectrum analyser, developed using Microsoft Foundation Class library, MFC 6.0 using Visual C++) to extract the resonant peaks in both resonator cavities. The water temperature in the experimental tank was maintained at 20 °C.

2.3.2. Glass balls and air volume measurement

To measure the volume of samples less dense than water, atmospheric air, which is less dense than water, was injected into the cavities over the resonators, using a syringe with a needle. The air bubbles occupied the top corner of the resonator's cavities. For samples denser than water, glass balls with an increasing aggregate volume were inserted into the cavities of the resonators. Water flowed into the edge part of the resonator's neck at a flow velocity of 140 and 423 cm/s, for the closed cavity and the open cavity resonator, respectively, to generate the peak frequencies as shown in Fig. 2.5. At each resonant frequency, five replicate measurements were taken and the relationship between volume of samples and average resonant frequency was plotted. A water cooler was utilised and the water temperature in the experimental tank was maintained at 20 °C.

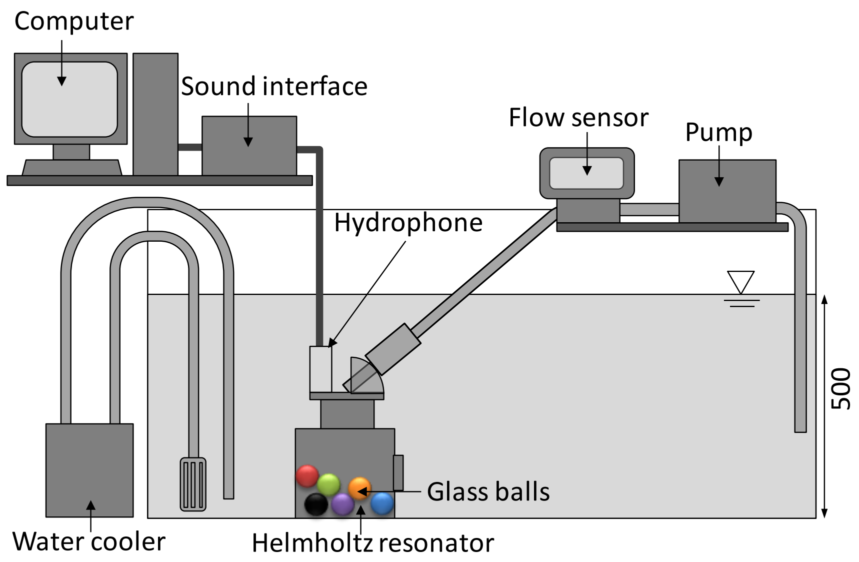

Fig. 2.5. General experimental set up of resonator with devices connected in water for sample volume estimation.

2.3.3. Simulation of empirical models

The proposed empirical model Eq. (2.2) was simulated and the effect of increased samples volume with the tendency of resonance frequency was evaluated. To do this, both samples denser and less dense than water were utilised in the simulated empirical model in both the closed and open cavity resonators. The water temperature was assumed to be about 20 °C.

2.4. Methodology for fish volume measurement

The Japanese rice fish of known volume (measured by water displacement method) were inserted into both the closed and open type resonator's cavities for measurement as shown in Fig. 2.6 (a). In the closed cavity resonator, the fish were inserted, and the cavity locked when measurement was in progress as depicted in Fig. 2.6 (b). However, in the open cavity resonator, fish samples were inserted, and the cavity left open when measurement was underway as indicated in Fig. 2.6 (c). Water temperature in the tank was maintained at 20 °C. A water flow speed of 4 L/min for the closed cavity resonator and 14 L/min for the open cavity resonator respectively was generated from the pump and directed to the nozzle and edge on the top part of the resonator's neck. The flow rates were determined by analysing the region of maximum resonance frequency generation over varied flow speed (Njane et al., 2018).

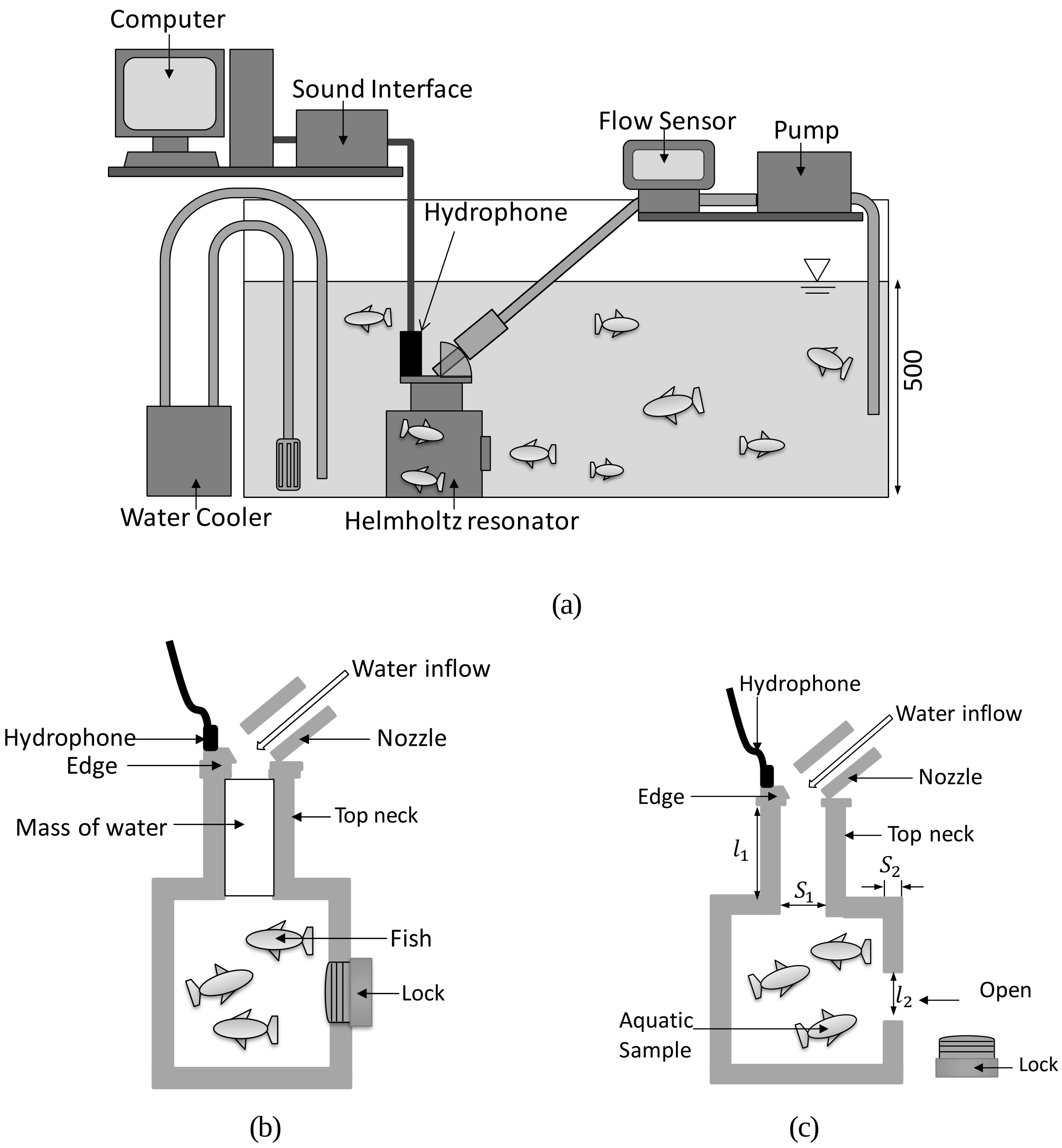

Fig. 2.6. General experimental set up consisting of (a) Helmholtz resonator submerged in a water tank containing fish, water pump, flow sensor, hydrophone, sound interface and computer (b) closed cavity Helmholtz resonator and (c) open cavity Helmholtz resonator.

As a result of water flow hitting the edge at the top of the neck of the resonator, the mass of water in the neck of the resonator oscillated, resonance occurred, and resonant tones could be heard. The signal was captured by a hydrophone attached close to the neck of the resonator and sent to the computer *via* the sound interface. The time domain signal was converted to a frequency domain signal using a Fast Fourier Transform (FFT) algorithm in a volume spectrum analyser. The volume spectrum analyser was developed using a Microsoft Foundation Class library, MFC 6.0 using Visual C++. In the closed cavity resonator, Helmholtz resonance is dominated by a peak with high amplitude, as shown in Fig. 2.7 (a). Similarly, in the open cavity resonator, Helmholtz resonance frequency is characterised by high amplitude peak. However due to the opening in the resonator's side, higher frequencies are speculated in the open cavity resonator compared to those in a closed cavity type as shown in Fig. 2.7 (b).

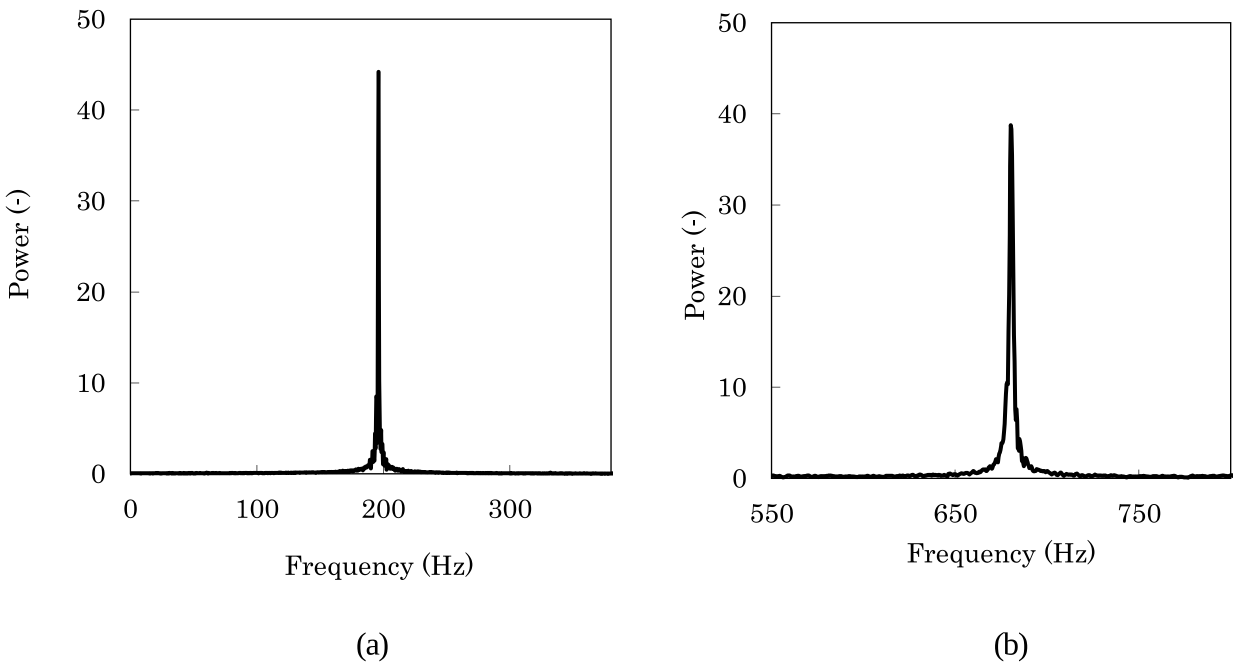

Fig. 2.7. Resonance frequency peak characterised by high amplitudes in (a) closed cavity resonator and (b) in an open cavity resonator.

2.5. Results and discussion for glass balls and air volume measurement

2.5.1. Variation of water velocity with resonance frequency in both closed and open cavity resonators.

As water velocity increased, the characteristic property of the resonant frequency was observed to vary as shown in Fig. 2.8. Different modes of vibration could be observed as flow increased. As flow velocity increased from 35 cm/s to about 100 cm/s, frequency also increased. This is a natural edge-nozzle characteristic with resonant frequencies and the edge tone being observed (Zoccola, 2004). In this situation, there are symmetrical oscillations of the vortex on both sides of the edges. At this point, acoustic Helmholtz resonance frequencies are not yet excited (Nariaki, 2001). However, as flow velocity increased from 105 cm/s to 176 cm/s, a gradual increase in resonant frequency was observed. Over this flow velocity range, the edge tone was coupled with resonant frequency and Helmholtz resonance was observed. In this region, the second mode of vibration, as well as Helmholtz resonance, occurred. Two distinctive shear layers were present intermittently and different flow velocities generated this resonance frequency (Ma et al., 2009). At flow velocity of about 105, 246 and 282 cm/s a Helmholtz resonant frequency of about 279 Hz was observed. By simulation of empirical model, when no sample is in the resonator's cavity, Helmholtz resonance frequency was plotted. The Helmholtz resonance at the lowest flow velocity (105 cm/s) was used as the optimum flow velocity for resonance generation and was also utilized for sample volume measurement. Lower flow velocities that excite Helmholtz resonant frequencies would be ideal to lower friction head (friction loss on water flowing in the pipe) and less fluctuations in flow velocities.

Over the flow velocity range of 176 - 282 cm/s, there was a gradual drop in resonant frequency. Jumps in frequency occurred and the second mode of vibration occurred. The number of vortex on one side of the edge increased leading to asymmetrical oscillation of the vortices on the edge (Cattafesta et al., 2008). However, from 282 to 493 cm/s, resonant frequency increased linearly with flow velocity increase. This is because the number of vortices forming on the sides of the edges increased, and both even and uneven vortex were formed on the edge. This led to the formation of both symmetrical and asymmetrical oscillations on both sides of the edges.

This is a characteristic behaviour of the nozzle and edge and is not dependent on the presence of a resonating cavity.

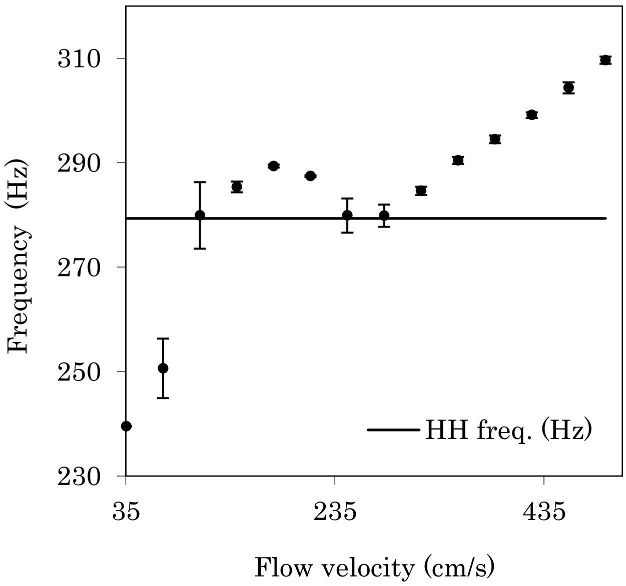

Fig. 2.8. Frequency vs. flow velocity in a closed cavity resonator. At different flow velocity, resonance occurs in the region plotted as HH (Helmholtz frequency).

This vibrational mode behaviour in the closed type resonator indicates the importance of characterizing the flow and using both empirical equations and flow variations to determine the optimum flow for sample volume estimation. When edge tone frequencies are coupled with resonant frequencies, acoustic constraints occurs thus limiting the resonance frequency selection (Glesser et al., 2008). Only flow velocities in the regions where Helmholtz resonance frequency occurs have the potential to be utilized for sample volume estimation.

By increasing the flow velocity on a resonating cavity, a graph of frequency against flow velocity was obtained, as shown in Fig. 2.9 below. From a flow velocity of 352.8 cm/s to about 388.08 cm/s, frequency increased with increased flow velocity. This was due to symmetrical oscillations of the vortices on both sides of the edges, a natural characteristic of the nozzle to edge flow phenomenon. A single jump in frequency was observed in the region of Helmholtz resonant frequency excitation over the range of the flow velocity investigated. An axial mode is excited by the shedding vortex hence frequency does not increase continuously linearly (Petrie and Huntley, 1980). Helmholtz resonant frequency was excited by the first shear layer at about 388 cm/s flow velocity. Unlike the closed cavity resonator, lesser jumps of frequencies were observed. Therefore, any flow velocity above the Helmholtz resonance excitation, can be utilized for sample estimation.

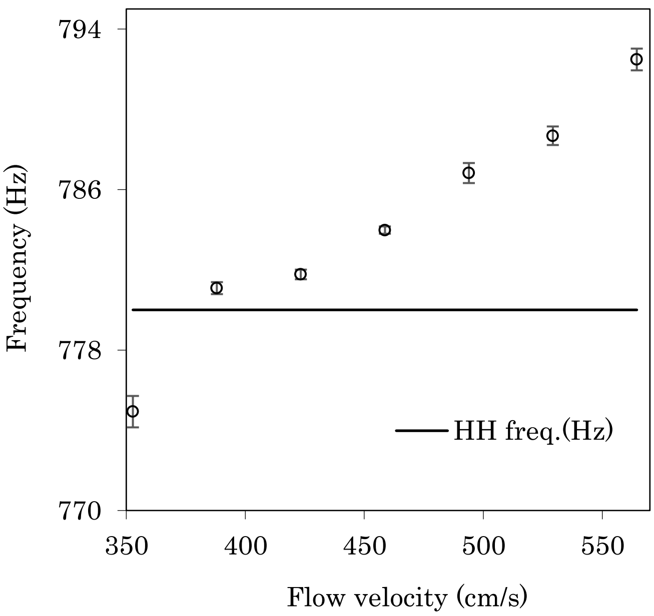

Fig. 2.9. Frequency vs. flow velocity in an open cavity resonator with Helmholtz resonance occurring at 388 cm/s (Helmholtz frequency marked as HH).

As flow velocity increased from 423 cm/s to 564 cm/s, frequency increased proportionately. There was an excitation of stable shear layers and hence self-excited oscillations were diminished. Considering a similar flow velocity range, higher resonance frequencies were observed in the open cavity resonator than in the closed cavity resonator. An increase in the stiffness of cavity of the open resonator occurred. The open hole acted as a source of energy loss; hence the higher vibration power was necessary to generate resonance in this cavity. This led to increased frequencies over similar flow velocities. Hence higher frequency modes can retard the self-sustained oscillations (Billon et al., 2005). In a flow excited resonance, acoustic fluctuations are enhanced by the acoustic energy provided by the resonance (Glesser et al., 2008). Similar to empirical model simulations, flow excited resonance exhibited higher frequencies in the open cavity compared to the closed cavity resonator, over a similar range of flow velocities (Nelson et al., 1983). A possible application would be where wider bandwidths of attenuation are required (Griffin et al., 2001).

By using an open cavity resonator, jumps in frequency can be avoided during sample volume estimation. This provides a wide range of flow velocities that can be chosen to estimate the volume of samples. Characterizing of the flow pattern both empirically and experimentally would not be necessary when determining the optimum flow velocity for sample volume estimation.

2.5.2. Volume of air and glass balls measurement in both closed and open cavity resonators

To validate the performance of the proposed model, experiments utilizing the property of air (less dense than water) were carried out. Similar patterns of frequency decrease with increased volume of air were observed in both cavities of the resonators, as shown in Fig. 2.10. This is because the bulk modulus of air is less than that of water, thereby damping the signal in the cavity of the resonator. When the air is exposed to sound pressure at varying frequencies, the magnitude and sharpness of the resulting resonance is associated with energy loss (Sand and Hawkins, 1973). As predicted in the simulated empirical equations, higher frequencies in the open cavity resonator were observed. This is a result of reduced oscillation of the mass of water at the neck of the resonators, which lead to increased stiffness of the cavity walls. Previous research that increased the hole size of an open-ended tube also indicates an increase in resonant frequency is to be expected (Pippard, 1989). Thus, this confirms that a resonator with an open cavity performs as well as a closed cavity one, with the additional benefit of being able to input and estimate sample volume without having to open and close a door.

Since air in a swim bladder of a fish presumably exhibits similar properties, future applications can utilize this phenomenon non-invasively to estimate the volume of fish. For the future design of such a resonator, a larger cavity to sample volume ratio would be preferred to increase the sensitivity of sample volume estimation. While air bubbles can be used to model the behaviour of a fish swim bladder in water, the spherical bubbles may satisfy the boundary conditions for a sphere. However, the shape of the swim bladders may not be modelled as spherical, since swim bladders vary in shape, size and orientation inside the fish (Clay and Horne, 1994).

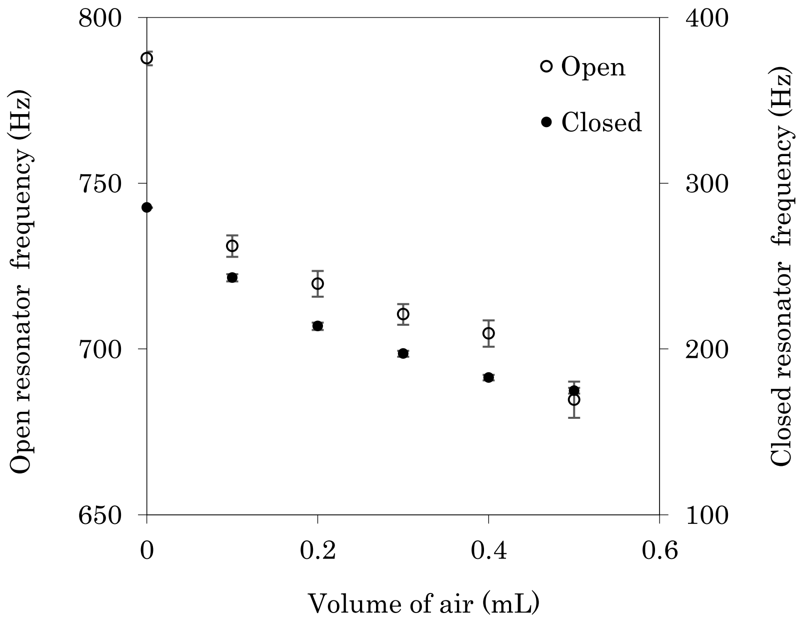

Fig. 2.10. Resonance frequency decrease with increased volume of air in both closed and open cavity resonators.

We also validated the performance of the proposed model using glass balls as a representative of samples denser than water. Resonant frequency increased with increase in the volume of glass balls, as shown in Fig. 2.11. This is because, the bulk modulus of the glass balls is higher than water. In this system, water had inertia only in the neck part. In the cavity, water is considered compressible. As was observed in the simulation, the resonator with an open cavity had higher frequencies compared to that of a closed type cavity (Koju et al., 2014). This was caused by the increased stiffness inside the resonator due to the opening at the side of the cavity. Similarly, this resonator had the same accuracy of measurement as that of the closed cavity, with an additional advantage of the samples being easily inserted into the cavity and the volume estimated without the need to close or lock the resonator. In future designs with a second opening to the cavity of the resonator, this opening could act as an inlet for aquatic products' estimation. However, for accurate volume estimation, deflection losses need to be accounted for in order to accurately predict the volume of samples, especially due to discrepancies between estimated and actual volume of sample (Moloney, 2004).

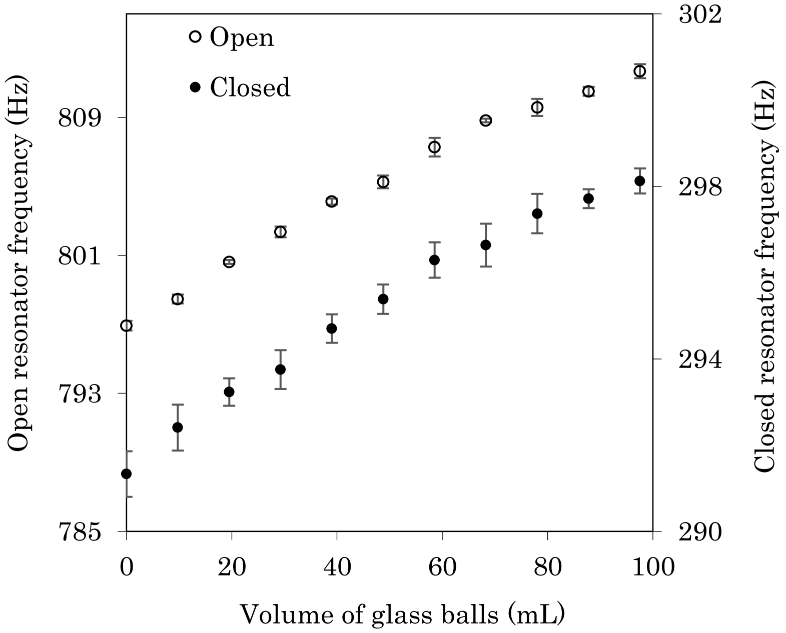

Fig. 2.11. Resonance frequency increase with increased volume of glass balls in both closed and open cavity resonators.

2.5.3. Simulation of empirical models in both closed and open resonator cavities

The effect of an opening on the side of a cavity compared to that which has none was simulated as shown in Fig. 2.12. To verify the model behaviour, we used samples which were denser than water, as well as samples less dense than water. The effect of increased volume of these samples with resonance frequency was modelled using the Eq. (2.1) in both closed and open cavity resonators. Glass balls were used to model samples denser than water. In the proposed simulated model, resonant frequency increased as the volume of glass balls increased, as shown in Fig. 2.12 (a). This is because the bulk modulus of glass balls is higher than that of water (bulk modulus of glass balls, 3.7×10^{10} Pa and water, 2.2×10^{9} Pa (20 °C, 1 atm.)). Furthermore, it was observed that as the volume of the denser sample materials increased, the sensitivity of the resonator for volume estimation increased. As the volume of sample approached that of the cavity, a rapid increase in resonant frequency was observed. This means that the cavity to sample volume ratio should be close to unity to increase the sensitivity of the measurement of denser samples than water. For samples less dense than water, air was used as a representative sample. Unlike the dense glass balls, as the volume of air increased, resonant frequency decreased, as shown in Fig. 2.12 (b). Moreover, sensitivity decreased with increased sample (air) volume. For future design of resonators, a large resonator cavity size relative to sample size would be preferred.

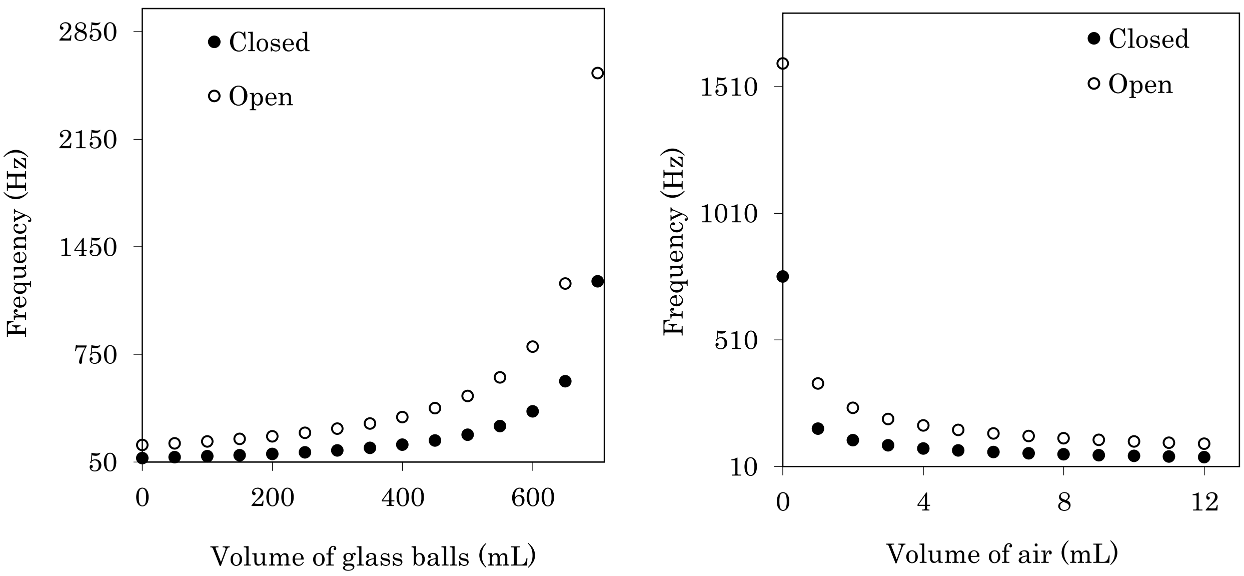

(a) (b)

Fig. 2.12. Simulation of resonance frequency against (a) volume of glass balls (b) volume of air in both closed and open cavity resonators.

In the simulations of empirical models for both denser and less dense samples, higher frequencies were observed in the open cavity resonator. This is because the opening at the side of the cavity of the resonator acted as a counter spring constant against the already suppressing spring constant of the mass at the top neck of the resonator. This makes the top neck and the opening act like two plugs moving in anti-phase hence generating compressions and expansions. The opening on the side of the cavity alters the resonant frequency and the transmission losses (Selamet and Lee, 2003). Because of the increased spring constant, which is inversely related to the volume of the cavity, this resulted in increased frequencies. Future resonator design optimizations will need to consider the effects of these higher frequencies. However, trade-offs will need to be made between power output and the physical dimensions of the resonator (Henriquez and Young, 1980). Design optimization would facilitate measurement of samples across a desired frequency range. Resonance frequency increases with the increases in cross sectional area (Chanaud, 1994). However, as the cavity volume increases, while maintaining the same neck area, resonance frequency will decrease. Also, the smaller the neck diameter, the lower the natural resonant frequency of vibration (Neville and Thomas, 2010).

2.5.4. Prediction of samples volume in both closed and open cavity resonators

From frequency changes in both cavities of the resonator because of increased sample volume, a correlation was made to predict the volume of air and glass balls measured in situ. The proposed empirical model assumed a rigid wall of the resonator. However, from the prediction, there was a low correlation between the predicted and the actual volume of samples. When samples were introduced into the resonator, there was increased compression inside the cavity of the resonator (Griffin et al., 2001). The resonator's cavity experienced vibrational changes hence leading to a small change in the volume of both the sample and the cavity. To compensate for resonator's deflection, a correction factor E_r (Pa) was introduced. It can also be represented as shown below in Eq. (2.3).

$$E_r = \frac{K_w K_o\left\{1-\left(\frac{f_o}{f}\right)^2\right\}}{V_o(K_o - K_w) - K_o W\left\{1-\left(\frac{f_o}{f}\right)^2\right\}} \quad (2.3)$$

The bulk modulus of water and the aquatic sample are K_w (Pa) and K_o (Pa) respectively. The resonance frequency of the resonators without the aquatic sample (only water in the cavity) is f_0 (Hz) while the resonance frequency after aquatic sample is measured is f (Hz). The sample cavity volume is W (mL). By analysing the frequency changes, a comparison was done on the E_r (Pa) values in both the closed and open cavities of the resonator for denser and less dense samples as shown in Fig. 2.13 (a and b). The resonator's deflection values were higher in the closed resonator cavity. With a closed cavity resonator, there was a resultant increase in pressure in the cavity, hence increased resonator's wall deflection. However, in the open cavity resonator, the opening acted as an energy loss pathway for the increased pressure, hence decreasing the effects of the resonator's wall deflection. Lower values of the deflection values were observed when samples less dense than water were used. The air absorbed some of the acoustic energy present inside the cavity of the resonator (Lo et al., 1979).

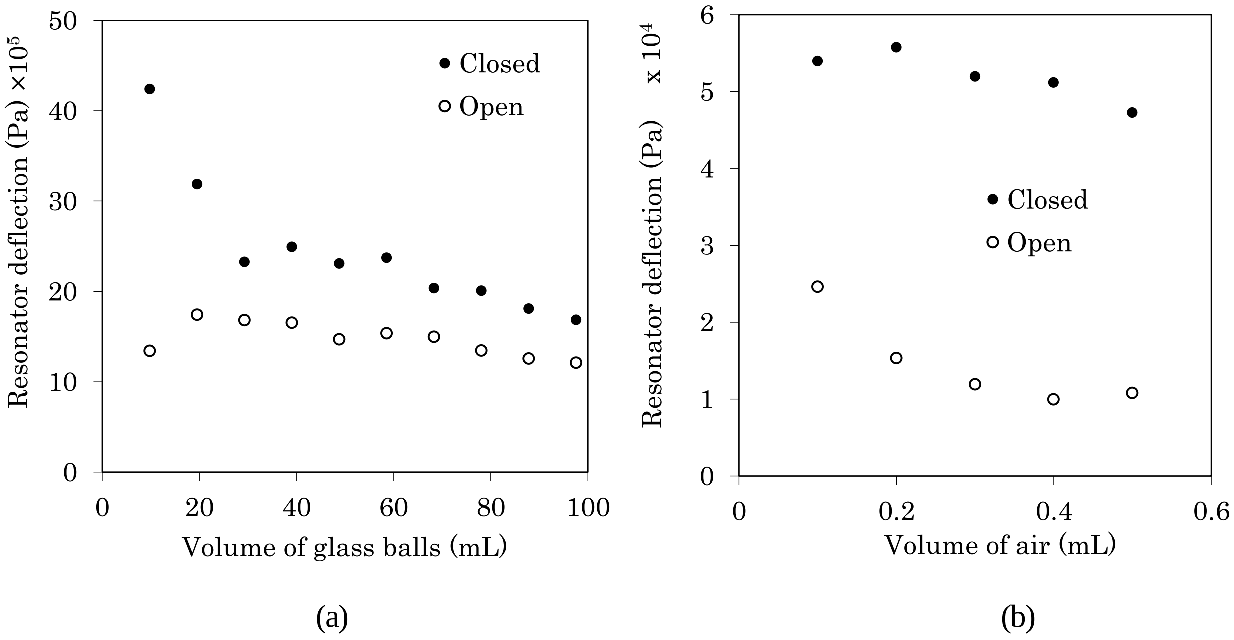

Fig. 2.13. Resonator deflection in both closed and open cavity resonators (a) when glass balls (denser than water) and (b) when air (less dense than water) are used.

By compensating for the deflection losses in the walls of the resonator's cavity, we developed an improved model that could precisely predict the volume of samples. The new equation, an improvement from equation 4 was shown below in Eq. (2.4):

$$V_o = \frac{K_w K_o + E_r K_o W}{W(K_o - K_w)} \left\{1 - \left(\frac{f_o}{f}\right)^2\right\} W \tag{2.4}$$

We utilised the improved model to predict the volume of samples, and the relationship between the predicted and actual volume of glass balls and air in both resonators is as shown in Fig. 2.14.

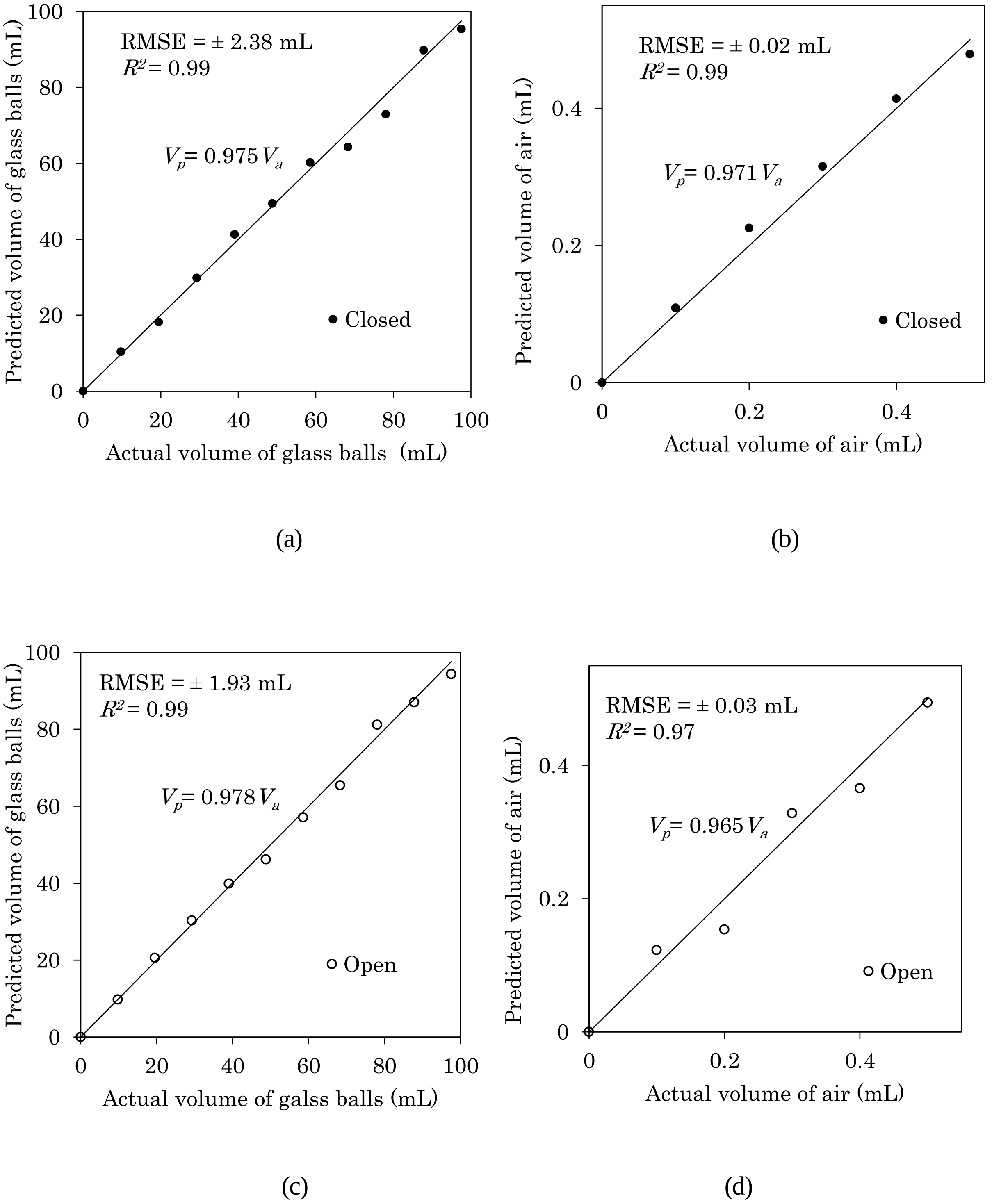

Fig. 2.14. Correlation between the predicted and the actual volume of (a) glass balls and (b) air in closed cavity resonator and (c) glass balls (d) air in open cavity resonator.

The linear regression model for denser samples (such as glass balls) accounted for R-squared (R^2) of 99.7% of the variance from the actual samples' volume in the open cavity resonator (see Table 2.3). For the less dense samples (such as air), the linear regression model, R-squared (R^2) accounted for 97.5% and of the variance with the actual samples' volume in the open cavity resonator. Similar to the closed cavity resonator, the open cavity resonator had a high linear correlation between the predicted actual volume of samples measured. The higher accuracy and precision of the open cavity would be preferred when estimating the volume of both less dense denser samples in water. Furthermore, the open cavity resonator has potential to be utilized as inlet for aquatic samples volume measurement.

Table 2.3 Linear regression model results of closed cavity resonator.

Resonator	**Samples**	R^2	**RMSE (mL)**	**Coefficients**
Closed	Glass balls	0.995	2.384	0.975
	Air	0.993	0.017	0.971
Open	Glass balls	0.997	1.932	0.978
	Air	0.975	0.032	0.965

2.6. Results and discussion for fish volume measurement

2.6.1. Resonance frequency with increased volume of fish in both closed and open cavity resonators

As the volume of the fish increased inside the closed and open cavity resonators, the characteristic property of the corresponding resonance frequency was measured as shown in Fig. 2.15. From the simulation of the empirical model, as the volume of fish increased in the closed cavity resonator, resonance frequency decreased. From 0 to 4 mL, a high sensitivity of measurement was characterised by a rapid drop in resonance frequency. However, with further increased fish volume, from 4 to 7.28 mL, sensitivity decreased and a gradual drop in resonance frequency was observed.

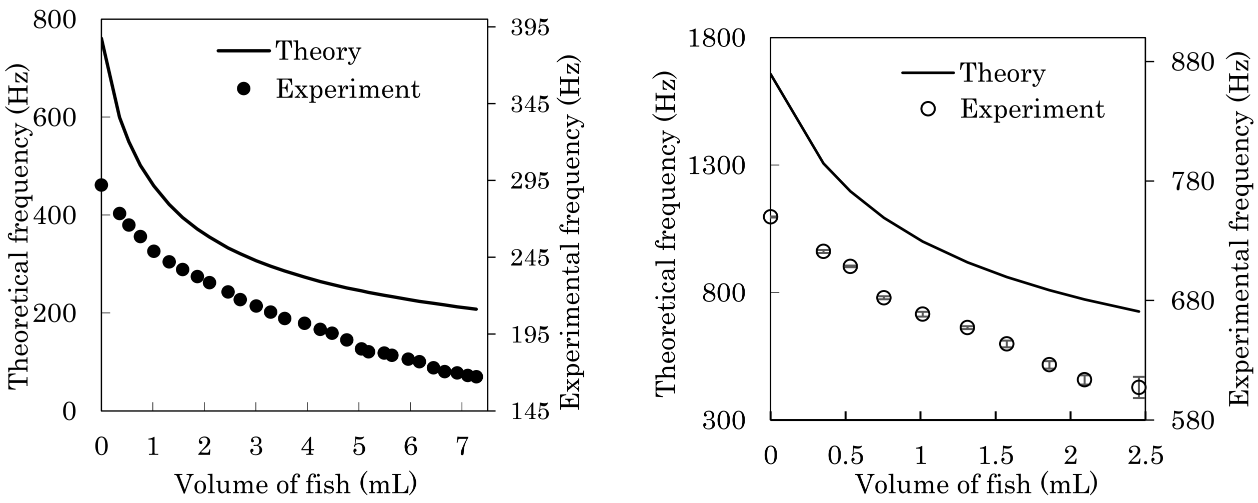

(a) (b)

Fig. 2.15. Theoretical simulation and experimental validation of resonance frequency vs. increased volume of fish in (a) a closed cavity and (b) an open cavity resonator.

Similarly, in the experimental findings, as the volume of fish increased in the closed cavity resonator, resonance frequency decreased. A rapid decrease in resonance frequency was observed as the fish volume increased. Fish behave acoustically similar to air bubbles under resonance frequency leading to damping (Frinking and Jong, 1998). A closed cavity resonator has a high sensitivity which allows for more samples to be measured over a constant cavity volume. However, unlike the simulation of empirical model, lower resonance frequencies were observed when actual fish measurement was carried out in the closed cavity resonator (see Fig. 2.15 (a)). This was attributed to the deflection of the resonator's wall when sample volume measurement is in progress thus leading to lower frequencies compared to the model (Njane et al., 2018).

In the open cavity resonator, as the volume of fish increased resonant frequency decreased in both theoretically and experimentally as shown in Fig. 2.15 (b). When validated experimentally, higher resonance frequencies were observed in the open cavity resonator compared to those observed in the closed cavity resonator. This is because the opening on the side of the cavity led to increased resonator stiffness (Selamet and Lee, 2003). To generate resonance and overcome this stiffness, a higher water flow speed was utilised (14 L/min in the open cavity resonator compared to 4 L/min in the closed cavity resonator). With increased flow speed, the vortex formed on both sides of the edges also increased leading to increased oscillation of mass of water at the resonator's neck, thus resulting to increased resonance frequency. Similar to the closed cavity resonator, higher frequencies were observed in the simulation model compared to the experimental findings of the open cavity resonator. Deflection of resonator walls occurred similarly in the open cavity resonator.

In the open cavity resonator, lesser total volume of fish (2.457 mL in the open cavity resonator compared to 7.277 mL) was sampled over a similar capacity of the resonator (729 mL) as that of the closed cavity resonator. This is because the opening on the side of the cavity led to increased resonator stiffness thus reducing the effective volume of the resonator's cavity. The reduced effective volume leads to decreased sensitivity as fish volume is increased in the resonator's cavity. Higher cavity to sample volume ratio is preferred to attain a high sensitivity for resonance frequency change when fish volume is increased in the resonator's cavity. Furthermore, higher frequencies in the open resonator's cavity were observed due to high water flow velocities needed to generate the resonance frequency. Njane et al., (2018) observed that open cavity resonator's are bound to experience jumps in frequency due to edge tones resulting from the increased vortex forming below and above the edge on the neck of the resonator's cavity. Such uneven vortex lead to fluctuating frequencies (indicated by the increased error bar) with increased volume of fish. For future design optimization of an open cavity resonator, a larger resonator's cavity to fish volume ratio is necessary to increase the sensitivity thus allowing more fish volume to be measured in the specified cavity volume. However, trade-offs must be made since larger cavities would require high water flow speed to generate resonance and this may lead to unstable shear vortex hence increased fluctuation of resonance frequency. High water flow speeds incident on the fish may also pose a risk in damaging the muscles of the fish.

2.6.2. Swim bladder resonance in both closed and open cavity resonators

In both the closed and open cavity resonators, resonance frequency decreased with increased volume of the sampled teleost fish, Japanese rice fish. Most teleost fish have a swim bladder, a hydrostatic organ which maintains neutral buoyancy in water, for respiration, for detection of water pressure changes and for producing sound (Wahlberg and Westerberg, 2003). Depending on the size of the fish, the swim bladder can vary in their orientation, the angle to the body axis position and their anatomical structure. In most fish, the swim bladder is located between the alimentary canal and the kidney of the fish. When sound is incident on the fish, some of the energy is absorbed by the swim bladder, while the rest is scattered in all directions (McCartney and Stubbs, 1971). The size of the swim bladder is a reliable indicator of fish volume because of the property of the swim bladder to resonate when sound is incident upon it (Fine et al., 2001). It was observed that when resonance frequency was excited in the resonator's cavity and the resonance sound was incident on the fish, damping occurred. This damping was caused by viscosity of fish flesh and the elastic nature of the swim bladder (Lo et al., 1979). In the swim bladder of most teleost, Oxygen and Nitrogen constitute a very high percentage of the mixed gas (Foote, 1980). Therefore, the acoustic and physical properties of the swim bladder are assumed to be similar to that of air bubbles in water. Previous research has shown that measurement of resonance frequency of small air bubbles gives a reasonable approximation of the resonance frequency of the swim bladder (Love, 1978). Didenkulov et al., (2015) observed that bubble concentration in the resonator affects the sound velocity and damping and thus results in reduction of the acoustic radiation power. A confirmation experiment revealed that by cutting the fish open in water to release air from the swim bladder in the intact fish, the air bubbles could be collected at the top of a beaker inside the water. Using a graduated syringe with a needle, air could be extracted from the beaker and the volume estimated. A correlation between the extracted volume of air in the swim bladder V_s (mL) to the volume of the fish V_f (mL) was plotted as shown below in Fig. 2.16.

An average ratio of 9.473% of volume of air inside the swim bladder, to the total volume of the sampled fish was obtained. This ratio varies depending on the species of the fish and the size of the fish, ranging between 5-10% of the total volume of the fish (Alexander, 1959). The ratio of fish swim bladder volume to the total volume of the fish is paramount for determining the bulk modulus of the fish. This is because both the viscous muscles of the fish and the elastic property of the swim bladder affect the bulk modulus of the fish. The bulk modulus of fish K_o (Pa) was calculated, as shown in Eq. (2.5) where the bulk modulus of the fish meat, K_m is 2.4×10^9 Pa and that of air K_a is 1.4×10^5 Pa.

$$K_o = \frac{1}{\frac{1-0.095}{K_m}+\frac{0.095}{K_a}} \tag{2.5}$$

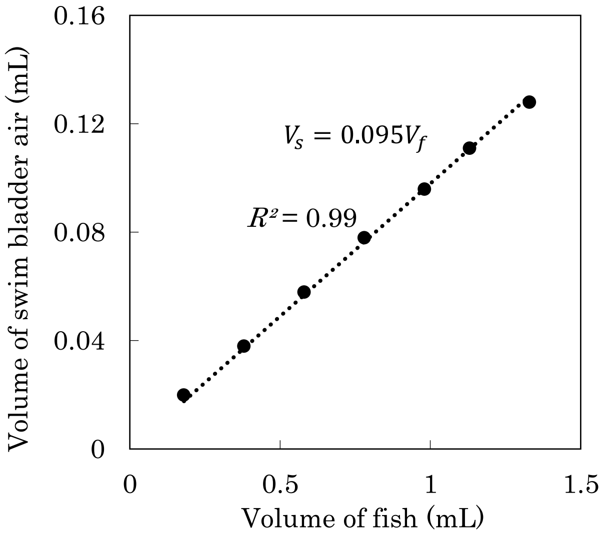

Fig. 2.16. Volume of air extracted from the swim bladder in comparison to the total volume of the fish.

From the correlation in the Eq. (2.5), the bulk modulus of the sampled fish was estimated to be 1.472×10^6 Pa. As can be observed, the calculated bulk modulus of fish is less than that of water, but greater than that of air. Damping would occur on the fish, but air bubbles would be damped more. Similar to phenomenon of air bubbles in water, resonance frequency decreases with increased volume of fish (Njane et al., 2018). In this experiment, a water depth in a tank of about 500 mm height from the ground was maintained. This is because scattering amplitudes may also be dependent on the orientation of the fish relative to the distance of the excitation beam (Clay and Horne, 1994). The swim bladder can be regulated, and the fish tends to maintain a constant volume by absorbing or releasing gas. This means that the buoyancy of the fish is the same at different depths. However, when a fish rapidly moves down through a column of water, there is not enough time for the swim bladder to equilibrate. However, if the fish moves slowly from one depth to another allowing time for the swim bladder to adjust its level, then a constant volume of gas is in play (Alexander, 1959; Sand and Hawkins, 1973). To ensure constant results, we allowed a delay time of 30 seconds from inserting the fish samples to data collection. For future applications with different species and size of fish, the Helmholtz resonance technique and swim bladder effect could be used to examine swim bladder behaviour, and possibly be able to identify different fish species based on their resonance property and ratio of swim bladder to total volume of the fish.

2.6.3. Precise fish volume estimation in both closed and open cavity resonators

From the tendency of decreased resonance frequency with increased volume of fish, a correlation was determined to predict the volume of fish using equation (1). Griffin et al., (2001) observed that resonators tend to deflect when sample volume measurement is conducted in a resonating cavity. Thus, a small change in the effective volume of the resonator occurs when sample measurement is in progress (Davies et al., 2010). This imprecision caused by wall losses in acoustic energy need to be compensated for precise estimation of sample volume (Harris, 1966). However, in the underwater Helmholtz resonance model developed for fish volume estimation, a rigid wall of the resonator is presumed. This led to higher frequencies observed in the simulation model compared to those observed in the experiment (Fig. 2.17 (a and b)).

(a) (b)

Fig. 2.17. When resonance occurs, pressure increase occurs in the cavity of the resonator hence (a) resonator walls deflect and (b) sample volume changes because of increased pressure.

Albeit, in actual experiment, when fish volume measurement was in progress, increased pressure in the elastic stainless-steel cavity of the resonator resulted to a small change in the volume of the resonator, V_r (See Fig. 2.16 (a)). Similarly, a small change in the volume of water V_w and volume of fish V_0 occurs as shown in Fig. 2.16 (b). This leads to small changes in the bulk modulus of the resonator, fish and water represented as K_r

(Pa), K_o (Pa) and K_w(Pa) respectively. The total pressure changes, ΔP (Pa) occurring in the cavity of the resonator can thus be represented as shown in Eq. (2.6).

$$\left\{\begin{array}{c} \Delta P = K_r \frac{\Delta V_r}{W} \\ \Delta P = K_o \frac{\Delta V_o}{W} \\ \Delta P = K_w \frac{\Delta V_w}{W} \\ \Delta P = K \frac{\Delta V_r + \Delta V_o + \Delta V_w}{W} \end{array}\right\} \tag{2. 6}$$

This means that the total volume of the cavity of the resonator is $W = V_r + V_o + V_w$ (mL). Hence the total bulk modulus in the resonator's cavity when fish is present is thus given as:

$$K = \frac{W}{\frac{V_r}{K_r} + \frac{V_o}{K_o} + \frac{V_w}{K_w}} \tag{2. 7}$$

However, the changes occurring in the volume of the resonator are much smaller than the actual volume of the resonator i.e. $0 \leq \Delta V_r \leq V_r \leq W$. If the changes in the wall of the resonator are minimal, the volume of the sample cavity can be represented as, $W = V_o + V_w$. Replacing the volume of water $V_w = W - V_o$ in the bulk modulus Eq. (2.7), and introducing a new variable representing the deflection of the resonator's wall $E_r = K_r/V_r$ (Pa), Eq. (2.7) can be represented as shown in Eq. (2.8).

$$K = \frac{W}{\frac{1}{E_r} + \frac{V_o}{K_o} + \frac{W - V_o}{K_w}} \tag{2. 8}$$

From the theory of Helmholtz resonance in water, when fish samples are inserted into the cavity, resonance frequency changes occur. From the frequency changes, the deflection of the resonator E_r (Pa) was expressed as shown in the Eq. (2.9) below.

$$E_r = \frac{K_w K_o \left\{1 - \left(\frac{f_o}{f}\right)^2\right\}}{V_o(K_o - K_w) - K_o W \left\{1 - \left(\frac{f_o}{f}\right)^2\right\}} \tag{2. 9}$$

The resonator deflection losses from Eq. (2.9) are plotted with increased volume of fish in both closed and open cavity resonators as shown in Fig. 2.18.

In the closed cavity resonator as the volume of fish increased, the deflection of the resonator decreased. This is because more fish samples were absorbing the resonance frequency leading to damping hence decreased pressure in the resonator's cavity. However, in the open cavity resonator, there were fluctuations in the resonator deflection due to the fluctuating high flow speed necessary to generate resonance. Furthermore, because of the increased stiffness caused by the opening on the side of the cavity, the increased pressure was easily lost through the opening on the side of the resonator's cavity. This led to reduced pressure compared to the closed cavity resonator, hence lesser resonator deflections values compared to those of the closed cavity resonator.

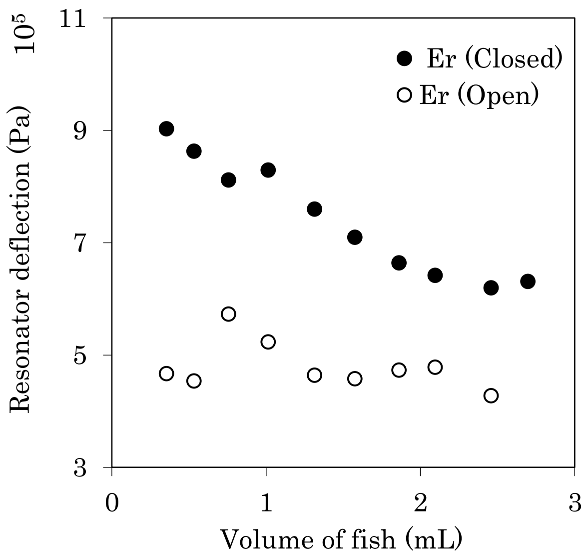

Fig. 2.18. Resonator's walls deflection with increased volume of fish in both closed and open cavity resonators.

To account for the deflection losses, an average value of 6.191×10^5 Pa and 4.601×10^5 Pa was obtained for the closed and open cavity resonator's respectively. Without compensating for the deflection losses, an underprediction occurs in both closed and open resonator cavities (See Fig. 2.19 (a and b)). However, by compensating for the deflection of the resonator's walls, as accounted for in Eq. (2.9) above, an improved model that can precisely estimate the volume V_o (mL) of the sampled fish, was obtained as shown in Eq. (2.10).

$$V_o = \frac{K_w K_o + E_r K_o W}{W(K_o - K_w)}\left\{1 - \left(\frac{f_0}{f}\right)^2\right\}W \qquad (2.10)$$

Using this improved model, a linear correlation between the predicted and the actual volume of fish in both the closed and open cavity resonator were plotted, as shown in Fig. 2.19 (a) and (b) respectively.

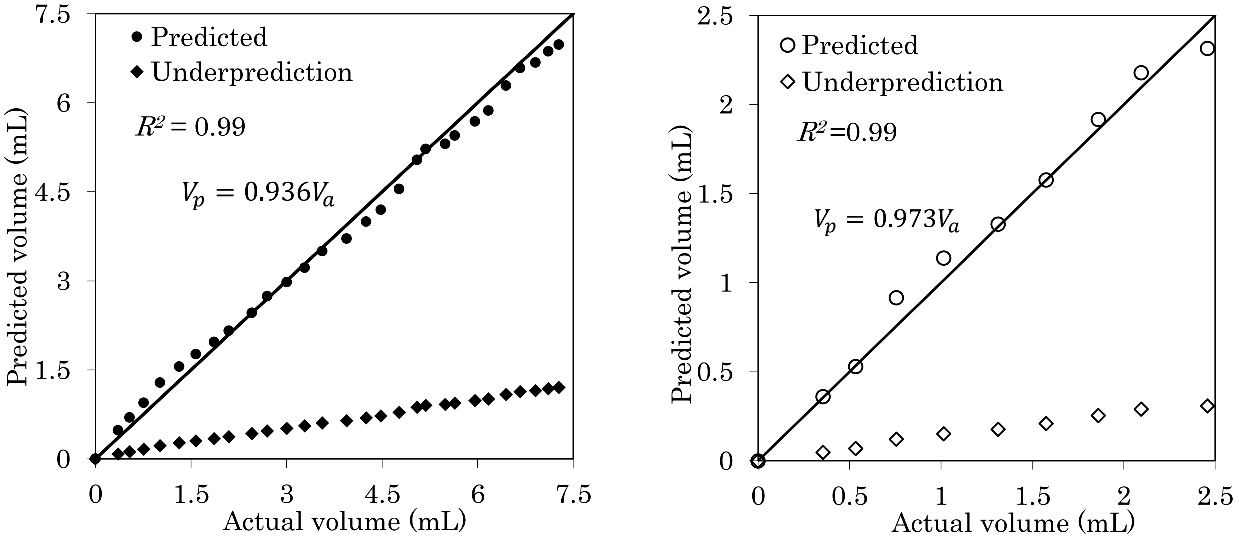

(a) (b)

Fig. 2.19. Predicted volume against actual volume of fish showing both underprediction and correct prediction in both (a) closed cavity and (b) open cavity resonators.

The proposed empirically developed model in conjunction with the fabricated underwater Helmholtz resonator could precisely estimate the volume of fish in both the closed and open cavity resonators (see Table 2.4).

Table 2.4 Linear regression model results for the measurement of Japanese rice fish in the resonator.

Resonator	Sample number	R^2	RMSE (mL)	Coefficients
Closed	28	0.994	0.104	0.936
Open	9	0.991	0.085	0.973

Moreover, in the future, the open cavity type resonator can be used as entry for fish and other aquatic products for automatic underwater volume estimation. However, design optimization would need to incorporate a higher cavity to sample volume ratio thus increasing the sensitivity of fish and other aquatic measurement.

2.7. Conclusion

Both the model simulations and the validation experiments demonstrate that open cavity resonators can be used to measure sample volume estimation with the same degree of accuracy as closed cavity resonators. Moreover, the open cavity resonators have less sudden jumps in resonance frequency, as well as fewer modes of vibration with flow variation. This leads to a wide range of flow velocities over which the volume of samples could be estimated. Unlike the open cavity resonators, flow variations with resonant frequencies will need to be analysed to determine the optimum flow for resonance generation in a closed cavity resonator. This is because they are characterized by jumps in frequencies, and increased modes of vibrations, which reduce the range of flow velocities over which the estimation of sample volume can be performed.

For future design optimization, a smaller cavity to sample volume ratio is preferred for samples denser than water. This is because the sensitivity of measurement increases with increased sample volume inside a given volume of a resonator's cavity. However, for samples less dense than water, a larger cavity to sample volume ratio is preferred. In comparison to the relative size of the resonator's cavity, small samples addition would lead to relatively large frequency changes. This is because of the ability of these samples to dampen the resonant frequency, hence reducing the sensitivity as sample volume increases. In the open cavity of the resonator, there was a high linear correlation between the proposed model's predicted volume and the actual volume of both less dense and denser samples. Precise, fast and non-invasive estimation of samples in water can be achieved by use of open cavity resonators. Moreover, this open cavity could allow sample insertion and, in the future, could potentially be used as an inlet for live aquatic products.

The mechanism for both closed and open type underwater Helmholtz resonators was investigated as an effective non-destructive method for estimating the volume of fish in water. In both closed and open cavity resonators, resonance frequency decreased with increased volume of fish. Damping occurs when resonance frequency is incident on the fish due to the viscous fish flesh and the elastic swim bladder of the fish. A closed cavity resonator is limited for practical applications as samples must be inserted into the cavity, the cavity locked, before measurement commences. However, in the open cavity resonator, samples can be measured without locking or closing the resonator's cavity. The opening on the cavity of the resonator increases the stiffness of the resonator's cavity, thus resulting in higher frequencies compared to those of a closed cavity type. The open cavity resonator has a viable future application in underwater automatic fish volume measurement where conditioned fish can pass through the resonator's opening for measurement.

References

Alexander, R.M., 1959. The physical properties of the swim bladder in intact cypriniforms. Journal of Experimental Biology, 36, 315–332.

Billon, A., Valeau, V., Sakout, A., 2005. Two feedback paths for a jet-slot oscillator. Journal of Fluids and Structures, 21, 121–132.

Brown, G.B., 1937a. The vortex motion causing edge tones. Proceedings of the Physical Society, 49, 493.

Brown, G.B., 1937b. The mechanism of edge-tone production. Proceedings of the Physical Society, 49, 508.

Cattafesta, L.N., Song, Q., Williams, D.R., Rowley, C.W., Alvi, F.S., 2008. Active control of flow-induced cavity oscillations. Progress in Aerospace Sciences, 44, 479–502.

Chanaud, R.C., 1994. Effects of geometry on the resonance frequency of Helmholtz resonators. Journal of Sound and Vibration, 178, 337–348.

Clay, C.S., Horne, J.K., 1994. Acoustic models of fish: The Atlantic cod (*Gadus morhua*). The Journal of the Acoustical Society of America, 96, 1661–1668.

Davies, C.E., Tallon, S.J., Webster, E.S., 2010. Applications of active acoustics in particle technology. Particuology, Special Issue in Honour of Professor Mooson Kwauk on his 90th Birthday 8, 568–571.

Deyu Li, Li Cheng, Ganghua Yu, 2007. Internal resistance optimization of a Helmholtz resonator in noise control of small enclosures. International Congress on Sound, CSV14.

Didenkulov, I., Martyanov, A.A., Pronchatov-Rubtsov, N., 2015. Interaction of acoustic waves with moving bubbles. Proceedings of Meetings on Acoustics, 24, 045005.

Diezma-Iglesias, B., Ruiz-Altisent, M., Barreiro, P., 2004. Detection of internal quality in seedless watermelon by acoustic impulse response. Biosystem Engineering, 88, 221–230.

Fine, M., Malloy, K., King, C., Mitchell, S., Cameron, T., 2001. Movement and sound generation by the toadfish swim bladder. Journal of Comparative Physiology [A], 187, 371–379.

Foote, K.G., 1980. Importance of the swim bladder in acoustic scattering by fish: A comparison of gadoid and mackerel target strengths. The Journal of the Acoustical Society of America, 67, 2084–2089.

Frinking, P.J.A., Jong, N. de, 1998. Acoustic modelling of shell-encapsulated gas bubbles. Ultrasound Medical Biology, 24, 523–533.

Glesser, M., Valeau, V., Sakout, A., 2008. Vortex sound in unconfined flows: Application to the coupling of a jet-slot oscillator with a resonator. Journal of Sound and Vibration, 314, 635–649.

Grassi, M., 2005. Do we hear size or sound? Balls dropped on plates. Perception and Psychophysics, 67, 274–284.

Griffin, S., Lane, S.A., Huybrechts, S., 2001. Coupled Helmholtz resonators for acoustic attenuation. Journal of Vibration and Acoustics, 123, 11.

Harris, C.M., 1966. Absorption of sound in air versus humidity and temperature. The Journal of the Acoustical Society of America, 40, 148–159.

Henriquez, T.A., Young, A.M., 1980. The Helmholtz resonator as a high-power deep-submergence source for frequencies below 500 Hz. The Journal of the Acoustical Society of America, 67, 1555–1558.

Iwamatsu, T., 2004. Stages of normal development in the medaka (*Oryzias latipes*). Mechanics of Development, Medaka, 121, 605–618.

Koju, V., Rowe, E., Robertson, W.M., 2014. Extraordinary acoustic transmission mediated by Helmholtz resonators. American Institute of Physics Advances, 4, 077132.

Kurdi, M.H., Duncan, G.S., Nudehi, S.S., 2014. Optimal design of a Helmholtz resonator with a flexible end plate. Journal of Vibration and Acoustics, 136, 031004.

Lo, A., Hovem, J.M., others, 1979. An experimental investigation of swim bladder resonance in fishes. The Journal of the Acoustical Society of America, 66, 850–854.

Love, R.H., 1978. Resonant acoustic scattering by swim bladder-bearing fish. The Journal of the Acoustical Society of America, 64, 571–580.

Ma, R., Slaboch, P.E., Morris, S.C., 2009. Fluid mechanics of the flow-excited Helmholtz resonator. Journal of Fluid Mechanics, 623, 1.

McCartney, B.S., Stubbs, A.R., 1971. Measurements of the acoustic target strengths of fish in dorsal aspect, including swim bladder resonance. Journal of Sound and Vibration, 15, 397–420.

Moloney, M.J., 2004. Quality factors and conductances in Helmholtz resonators. American Journal of Physics, 72, 1035.

Nakano, A., Torikata, Y., Yamashita, T., Sakamoto, T., Futaya, Y., Nishizu, T., 2005. Helmholtz resonance technique for measuring liquid volumes under micro-gravity conditions. Microgravity - Science and Technology, 17, 64–70.

Nariaki, H., 2001. COSMOS-V, an aerodynamic noise simulator. Toyota Centre, Research and Development Labs Inc. Technology. Journal of Research and Development Review, 36.

Nelson, P.A., Halliwell, N.A., Doak, P.E., 1983. Fluid dynamics of a flow excited resonance, part II: flow acoustic interaction. Journal of Sound and Vibration, 91, 375–402.

Neville, H.F., Thomas, D.R., 2010. The Physics of musical instruments, Second edition. ed. Springer New York.

Nishizu, T., Ikeda, Y., Manmoto, S., Umehara, T., Mizukami, T., 2001. Automatic, continuous food volume measurement with a Helmholtz resonator. Agricultural Engineering International: The CIGR Journal of Scientific Research and Development, FP01, 004 Vol. III.

Njane, S.N., Shinohara, Y., Kondo, N., Ogawa, Y., Suzuki, T., Nishizu, T., 2018. Improved underwater Helmholtz resonator with an open cavity for sample volume estimation. Computer and Electronics in Agriculture, 147, 18–26.

Petrie, A.M., Huntley, I.D., 1980. The acoustic output produced by a steady airflow through a corrugated duct. Journal of Sound and Vibration, 70, 1–9.

Pippard, A.B., 1989. The Physics of vibration, 1 and 2. Cambridge University Press, New York, United States of America.

Sand, O., Hawkins, A.D., 1973. Acoustic properties of the cod swim bladder. Journal of Experimental Biology, 58, 797–820.

Selamet, A., Lee, I., 2003. Helmholtz resonator with extended neck. The Journal of the Acoustical Society of America, 113, 1975–1985.

Shima, A., Mitani, H., 2004. Medaka as a research organism: past, present and future. Mechanics of Development, Medaka, 121, 599–604.

Wahlberg, M., Westerberg, H., 2003. Sounds produced by herring (*Clupea harengus*) bubble release. Aquatic Living Resources, 16, 271–275.

Wang, W.H., Dong, C., Shek, C.H., 2004. Bulk metallic glasses. Material Science and Engineering: R: Reports, 44, 45–89.

Webster, E.S., Davies, C.E., 2010. The use of Helmholtz resonance for measuring the volume of liquids and solids. Sensors, 10, 10663–10672.

Ziada, S., 2001. Interaction of a jet-slot oscillator with a deep cavity resonator and its control. Journal of Fluids and Structures, 15, 831–843.

Zoccola, P.J., 2004. Effect of opening obstructions on the flow-excited response of a Helmholtz resonator. Journal of Fluids and Structures, 19, 1005–1025.

Chapter III

Underwater Helmholtz resonator with double cavities for volumetric estimation of aquatic samples

Abstract

Non-destructive estimation of aquatic products' volume is important for efficient feed utilisation and for determining the appropriate time for landing. To enable this, we propose a double cavity underwater Helmholtz resonator for precise aquatic products' volume estimation. The fundamental principles were developed and the resonator consisting of the generating cavity and the sample cavity was designed and fabricated. By attaching an underwater speaker to the generating cavity, sweep sound was generated and captured using the speaker's impedance technique. Air, which is less dense than water, was inserted into the sample cavity to mimic aquatic samples of increasing volume. Resonance frequency decreased as air volume increased. A high linear correlation with an R^2 of 0.99 between the actual and predicted volume of air was obtained.

3.1. Introduction

Determining the volume of aquatic products underwater non-destructively, can be used to approximate the density of aquatic products; a useful parameter when sorting and grading (Chen and Sun, 1991; Sun et al., 2010). However, aquatic products vary in shape and size, which can differentially influence their growth as a result of feeding hierarchies and competition for feed (McCarthy et al., 1992). Not only is the cost of feed expensive, but intensive aquaculture systems generate waste from any excess feeds which accumulate at the bottom, forming sludge and enriched sediments that deprive fish of dissolved oxygen and may ultimately lead to the death of the fish (Yokoyama et al., 2009, 2006). Thus, it is paramount to estimate the size of these aquatic products in water. Fish position sampling analysed using a stereo camera (Shieh and Petrell, 1998) agrees well with physical sampling results, but these systems are expensive and cannot be used in murky water. While stereo-video systems can estimate the length, position and biomass of fish, as well as operate in areas with low visibility (Cappo et al., 2003), they are again expensive to install and need complicated calibration techniques. Therefore, there is a need for a fast, reliable, robust and non-invasive system that is not constrained by the above-mentioned limitations.

Recently, Helmholtz resonance techniques have potentially demonstrated rapid non-destructive estimation of the volume of products. The frequency generated by a Helmholtz resonator relies on the cavity-neck combination; with changes in this resonance frequency dependent upon cavity volume changes when a product is introduced into the cavity of the resonator. While Nishizu and Ikeda, (1995) could estimate the volume of grapes and apples with a coefficient of determination of 0.968, Webster and Davies, (2010) could precisely estimate the volume of water in a resonator with a high coefficient of determination of 0.99. However, because of the acoustic impedance between air and water, application of Helmholtz resonance for aquatic product volume estimation was paralysed. Njane et al., (2018) introduced the principles of underwater Helmholtz resonance technique for aquatic sample volume estimation using water reed, a flow-excited resonance. Water flowing at a specified velocity was directed to an edge on the top of the neck of a resonator by a nozzle, thereby generating resonance in the resonator's neck and cavity. However, this method is plagued by fluctuations in water velocity due to friction generated in the pipe as water is pumped from the tank to the resonator leading to fluctuating frequencies. Furthermore, although we could estimate the volume of fish in both resonators, the high water velocity for generating resonance may cause shear damage on the fish' body (Njane et al., 2019).

Alternatively, Helmholtz resonance can be generated by exciting a chirp wave (sweep sound) signal from a voice coil speaker to a sample cavity for volume estimation. Such a chirp wave signal has a higher acoustic density than white noise, thus a high signal to noise ratio (Nishizu et al., 2001). Unlike water reed technique where fluctuations in resonance frequency may occur due to unstable shear flow, resonance frequency generated by a chirp wave is very stable as the speaker can generate a similar sound without fluctuations. To generate resonance in water using the speaker's chirp wave signal, the sound signal would have to be sent from the air to the water. However, sending such a signal in water needs to be overcome the large acoustic impedance which is generated at the boundary of water and air (Chapman et al., 1992). Because of the difference in the density of air and water, and the large acoustic speed difference between the two mediums, the sound radiate from the speaker above the water surface is totally reflected and does not propagate into the water, hence no resonance occurs.

To overcome this limitation, we utilise a double cavity Helmholtz resonator, where an underwater speaker is attached onto a generating cavity for resonance generation and a sample cavity for aquatic product volume measurement. The double cavity Helmholtz resonator consists of two cavities connected by a neck as shown in Fig. 3.1 (a). The top cavity, referred to as the generating cavity, has a volume of W_1 (m^3) and is used for resonance generation. An underwater speaker is attached onto the generating cavity for exciting resonance frequency and for receiving the resonance frequency thus eliminating the need for a microphone. The lower cavity, referred to as the sample cavity, has a volume W_2 (m^3) where samples are inserted for measurement. The neck has a cross-sectional area S (m^2) and length l (m). The acoustical properties of this resonator can be considered equivalent to a mechanical vibration system (Nishizu et al., 2017) with one mass and two springs as portrayed in Fig. 3.1 (b). While the water column in the neck connecting the two cavities acts as the mass m (kg) ($m = \rho_w Sl$, where ρ_w (kg/m^3) is the density of water), the two cavities (generating cavity W_1 and the sample cavity W_2) provide the springiness k_1 and k_2. When the bulk of this water (with bulk modulus K_w (Pa)) in the neck pushes into the cavities, an increase in pressure (Pa) occurs inside the resonating cavities due to bulk strain. Because of the increased pressure in the resonator cavities, a resultant bulk modulus K_1 (Pa) and K_2 (Pa) occurs in the generating and sample cavities respectively, thus resulting in a resonance frequency f_o (Hz) as shown in the Eq. (3.1) below.

$$f_o = \frac{1}{2\pi}\sqrt{\frac{1}{\rho}\left(\frac{K_1}{W_1} + \frac{K_2}{W_2}\right)\frac{S}{l+l_e}} \tag{3. 1}$$

Moreover, consideration is given to the end effect of the resonator's neck $l_e = 0.85\ d$ (m), where d (m) is the diameter of the neck connecting the double cavity resonator (Alster, 1972; Kim et al., 2010; Selamet and Lee, 2003). When aquatic products, whose bulk modulus is K_o (Pa) and volume is V_o (mL), are inserted into the sample cavity, the effective volume of the cavity decreases. As a result, a proportionate change in resonance frequency occurs leading to a resultant frequency f (Hz), as shown in Eq. (3.2).

$$f = \frac{1}{2\pi}\sqrt{\frac{1}{\rho}\left(\frac{K_1}{W_1} + \frac{K_2}{W_2 - V_o}\right)\frac{S}{l+l_e}} \tag{3. 2}$$

By analysing the difference in resonance frequency before and after a sample is inserted into the sample cavity of the resonator, a model estimating the volume of aquatic samples can be utilised, as shown in Eq. (3.3).

$$V_o = \frac{K_o}{K_w - K_o}\left\{1 - \left(\frac{f_o}{f}\right)^2\right\}(W_1 + W_2) \tag{3. 3}$$

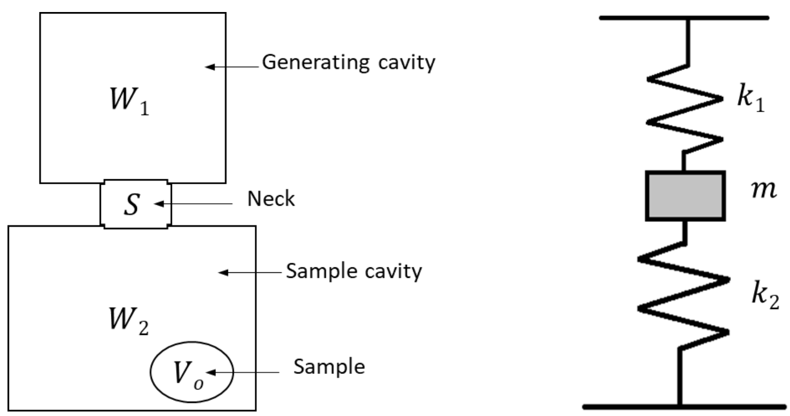

(a) (b)

Fig. 3.1. (a) Double cavity Helmholtz resonator consisting of generating and sample cavities connected by a neck (b) and Helmholtz resonance mechanism represented by mass (occurs in the neck) and two springs (generating and sample cavities).

We utilise these empirical models to design and fabricate a prototype double cavity Helmholtz resonator for aquatic sample volume estimation. However, from the empirical models Eq. (1) and (2), it can be clearly seen that apart from volume changes in the sample cavity, the resonance frequency will be influenced by the dimensions of the neck of the resonator. For optimal product volume estimation, we will investigate the effect of neck cross-sectional area and length change with resonance frequency, without changing the volume of the sample cavity of the resonator. As a proof of concept, a neck with a specified diameter and length will be utilised for optimal product volume estimation.

3.2. Materials and methodology

3.2.1. Material

Atmospheric air (at 20 °C) with a bulk modulus of 1.42×10^5 Pa (Ding et al., 2007) was utilised as a sample product for volume estimation. Since air bubbles, can acoustically model the behaviour of teleost fish (fish which possess swim bladder which contains gas inside) in water, the effect of air in the resonator can be used to model the effect of changes in resonance with fish volume changes that would be expected in an actual application. Air was injected into the sample cavity of the resonator by use of a gas syringe with a needle. To ensure accuracy, the gas syringe was filled with water up to the 0-mL mark before air was injected into the syringe. The injected air bubbles occupied a corner of the cavity and formed enlarged bubbles as more air was inserted into the resonator.

3.2.2. Devices

A double cavity Helmholtz resonator for product volume estimation was designed and fabricated from stainless steel material as shown in Fig. 3.2 (a). The resonator consists of two cylindrical cavities connected by a neck: The upper is the generating cavity and the lower is the sample cavity. A speaker was firmly fixed with screws to the top of the generating cavity. While the generating cavity had an internal volume of $W_1 = 4.715 \times 10^{-4}$ m^3 and the total bulk modulus inside the cavity was $K_1 = 1.71 \times 10^9$ Pa, the sample cavity had an internal volume of $W_2 = 1.645 \times 10^{-3}$ m^3 and a total bulk modulus of $K_2 = 1.94 \times 10^9$ Pa (without sample product) as shown in Fig. 3.2 (b). The sample cavity which had a lid with an opening, was connected to the generating cavity using a hollow neck. To optimise the resonator for optimal product volume estimation, we varied the internal diameter and the length of the neck without changing the volume of the cavities as shown in Table 3.1. A neck with a diameter of 20 mm and length 50 mm was utilised for precise estimation of air volume.

A UW30 Underwater loud speaker (Electro-Voice, U.S.A) was used to generate resonance. The speaker had a frequency response between 100-10000 Hz, a power handling of 30 W and an impedance of 8 ohms. To determine the frequency response of the speaker, a sinusoidal chip wave signal was applied. To maintain a constant current and maintain a proportionately equal voltage, a constant current amplifier (KU-6 AE-CA custom order, Kobayashi Instrument Co., Ltd., Japan) was utilised. An audio interface (Roland UA-101 USB, Roland, Japan) was utilized to amplify the signal and for connecting the amplifier to the computer. The audio interface has a sampling frequency of 48 kHz, and a signal to noise ratio of 107 dB and 101 dB for the output and input channels respectively.

Table 3.1 Varying neck lengths and diameter.

Neck parameter	**Neck diameter (mm)**	**Neck length (mm)**
Varying diameter	10	50
	20	50
	25	50
	30	50
Varying length	20	30
	20	40
	20	50
	20	70

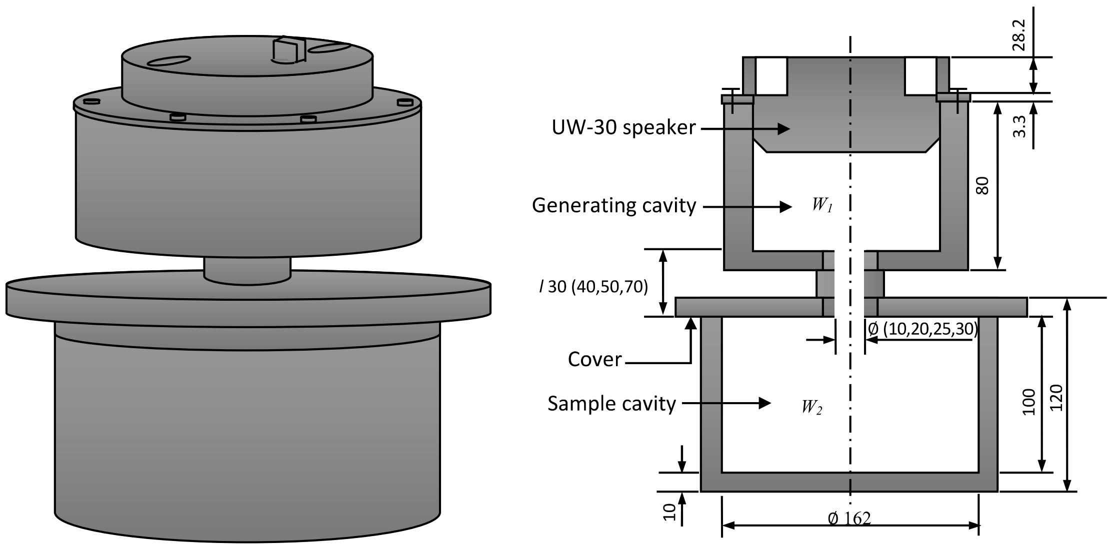

(a) (b)

Fig. 3.2. Helmholtz resonator consisting of (a) an underwater speaker attached onto a generating cavity and sample cavity connected by a neck (b) cross-sectional view of the double cavity Helmholtz resonator with measurements (dimensions in mm).

3.2.3. Methodology

The double cavity resonator with speaker connected on top of the generating cavity was set up inside a water tank with dimensions 1.45 m × 0.60 m × 0.60 m. Water was filled up to 0.5 m level from the bottom of the tank, as shown in Fig. 3.3 (a). The speaker was connected using a water proof cable to a constant current drive power amplifier, then to an audio device, which was externally connected to a computer via a USB audio interface. From the computer, a sinusoidal chirp wave signal was applied, and resonance frequency was recorded and analysed. To insert air bubbles into the sample cavity, the generating cavity was lifted together with the neck. A known amount of air was injected using a gas syringe with a needle through the hole on the top of the sample cavity cover as shown in Fig. 3.3 (b). The air bubbles accumulated at the bottom of the cover at a corner of the sample cavity. During the experiment, water in the tank was maintained at 20 °C to maintain a constant elastic limit of the stainless steel resonator (Upadhye and Agashe, 2016).

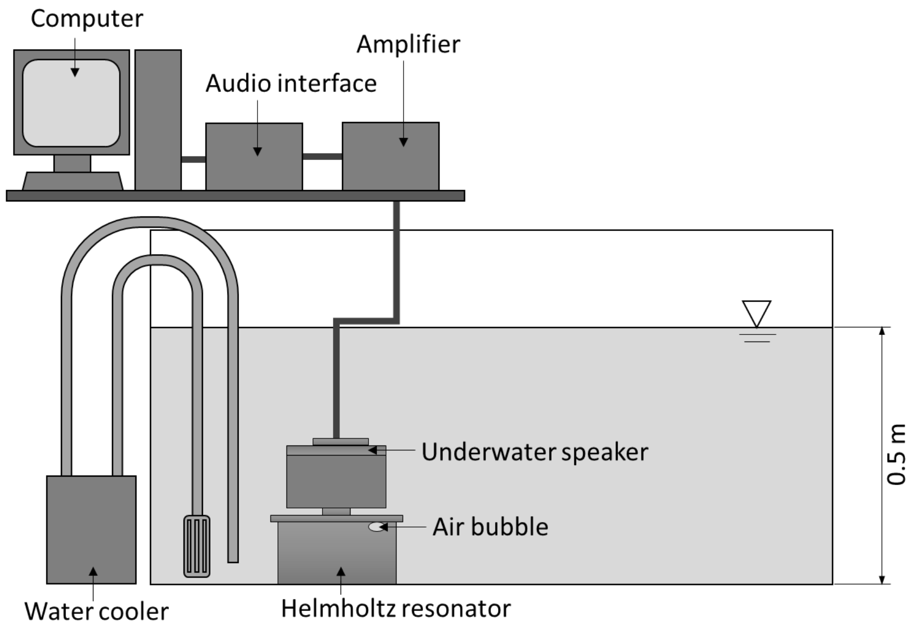

(a)

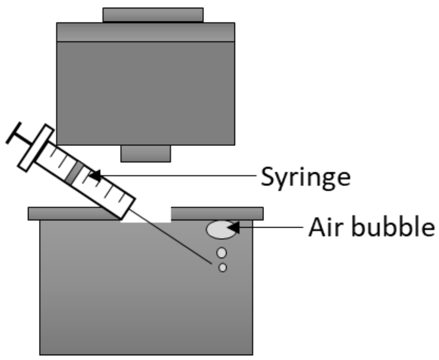

(b)

Fig. 3.3. Experimental set-up (a) in a water tank with a depth of 0.5 m, consisting of a double cavity Helmholtz resonator with speaker connected to an amplifier, audio interface and computer and (b) shows injection of air bubbles into the sample cavity.

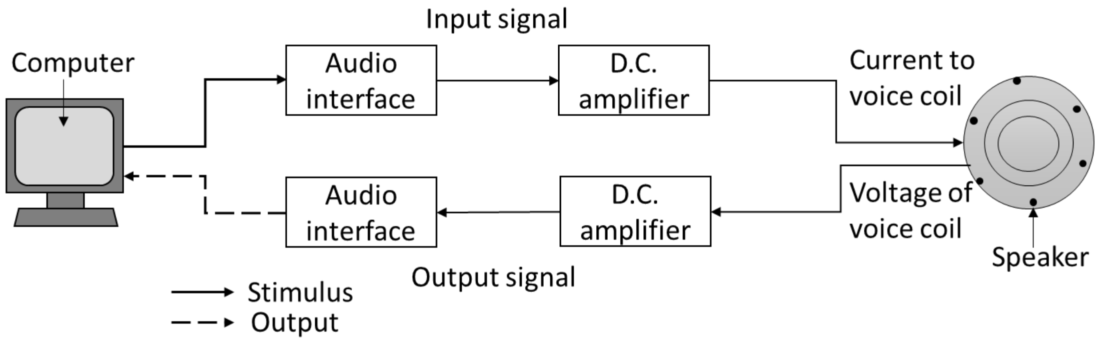

Fig. 3.4. Signal mechanism of the stimulus generated from the computer, through the audio interface, amplifier, speaker, resonator and then back to the computer for analysis.

The impedance of the voice coil was measured by applying a sinusoidal chirp wave signal from 5-3000 Hz with a sampling time of 20 seconds. Instead of directly measuring the electric impedance generated by the voice coil of the speaker, the voltage was measured as an estimate of the electric impedance of the voice coil. As the diaphragm of the membrane of the speaker vibrated, the signal was sent into the sample cavity which in turn, generated resonance as shown in Fig. 3.4. This resonance wave form was captured by the speaker. The obtained response waveform was then converted into a power spectrum by use of a Fast Fourier Transform algorithm using a volume spectrum analyser developed in the lab using Microsoft Foundation Class library, (MFC 6.0, Visual C++) (Njane et al., 2018). Smoothing was applied to the whole spectrum using Savitsky-Golay Filter (Savitzky and Golay, 1964). Furthermore, to identify the peaks clearly, a second order derivative was applied to the spectrum using OriginPro 8.0 software (OriginLab Corporation, Northampton, MA 01060 USA). The region of maximum peak occurrence was extracted for analysis.

3.3. Results and discussion

3.3.1. Resonance frequency change with increased volume of air

The spectrum obtained from the sinusoidal chirp wave resonance is shown in Fig. 3.5 (a). From the spectrum, two peaks could be identified. One of the peaks occurred at 2080.2 Hz as indicated in Fig. 3.5 (b). The peak had a higher amplitude and as air sample volume increased, the dominant peak did not shift. The high peak corresponds to the speaker resonance frequency that results from the thin membrane of the speaker, which vibrates in the enclosed casing of the underwater speaker. The enclosed casing of the speaker has a small volume thus the membrane of the speaker vibrates at a high frequency.

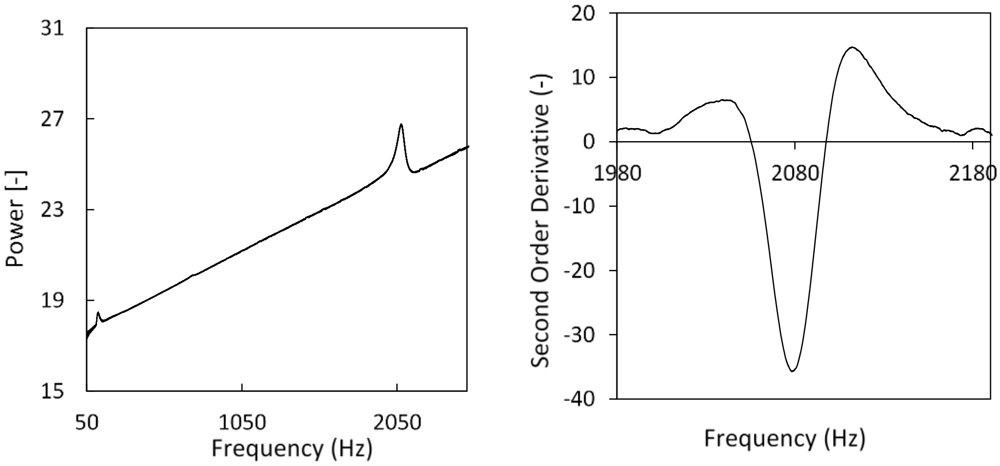

(a) (b)

Fig. 3.5. (a) Characteristic peaks appearing in the whole spectrum range (b) second order derivative of peak at 2080 Hz, suspected to be resonance frequency peak accruing from the vibration of the speaker's membrane in the casing of the speaker.

The other peak had a lower amplitude and a resonance frequency of 126.6 Hz was observed, as indicated in Fig. 3.6 (a). The intensity of this peak was low due to the larger sample cavity volume, which causes damping of the resonance frequency. As the volume of air samples increased, the peak shifted to lower frequencies. From the proposed theoretical model and the design specifications of the double cavity resonator, a resonance frequency of 141.5 Hz was predicted. The predicted value from the model is closer to the experimentally observed value of this second peak, hence providing assurance that it is associated with Helmholtz resonance frequency. By use of an empirical simulation model and experimental investigation, a graph depicting the relationship between resonance frequency and increasing volume of air was plotted, as shown in Fig. 3.6 (b).

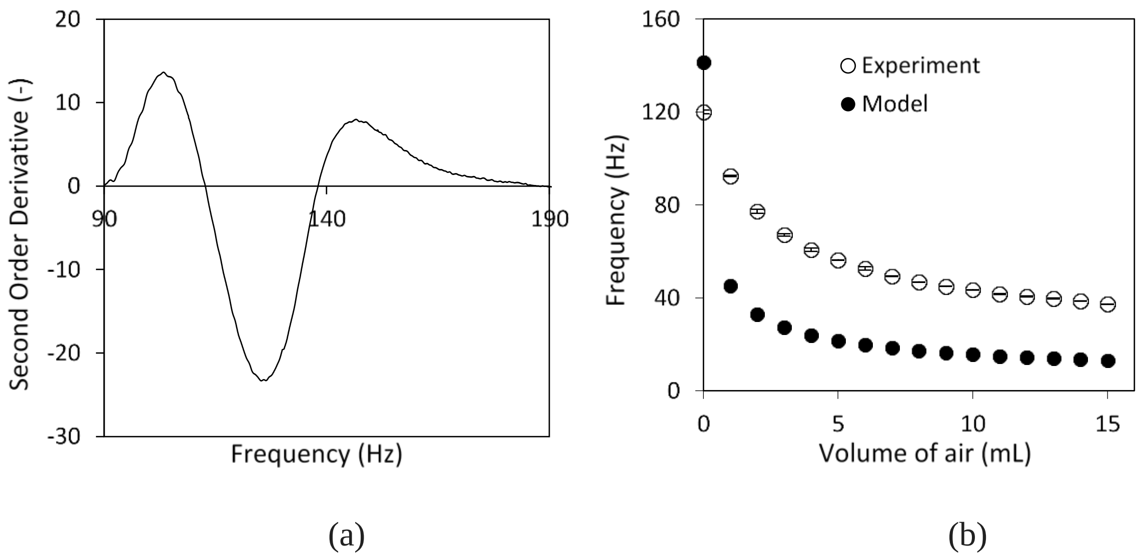

Fig. 3.6. (a) Second order derivative peak occurring at lower frequency of 126.6 Hz is suspected to be Helmholtz resonance frequency from the sample cavity and (b) resonance frequency decrease as volume of air increases, both empirically and by experimental validation.

When air, which is less dense than water (bulk modulus of air is 1.4×10^5 Pa while the bulk modulus of water is 2.1×10^9 Pa), was inserted into the sample cavity, the total bulk modulus inside the sample cavity decreased. As the volume of this air increased, more damping occurred leading to decreased resonance frequency, as shown in Fig. 3.6 (b). When sound strikes the air bubbles inside the sample cavity of the resonator, the bubbles, which are also a part of the rarefactions and compressions, result in resonance oscillation and damping. Thus, some of the energy from the incident sound waves is absorbed by the bubbles, some is scattered and some is converted to heat (Robert, 1975). This damping is caused by heat conduction radiated from the bubbles, and the viscosity of water surrounding the air bubble (Devin, 1959). Helmholtz resonance generated by the speaker impedance method had smaller error bars compared to the resonance frequency generated by the water reed method. The latter method is marred by larger error bars due unstable shear flow caused by fluctuating resonance frequency (Njane et al., 2018). Furthermore, samples can be measured with a higher sensitivity than with the water reed technique, where the high-water flow may eject air bubbles from the cavity and damage the fish *in situ* (Njane et al., 2019) thus limiting the measurement capacity of the resonator.

However, as shown in Fig. 3.6 (b), higher frequencies were predicted in the simulation model, unlike the experimental validation. While the empirical model assumes a rigid resonator wall, experimental validation has shown that occurrence of resonance leads to increased pressure in the sample cavity. As a result, deflection of the resonator walls occurs, leading to a small change in the volume of the cavity. As a result of the decreased cavity volume, lower frequencies were observed compared to the empirical model simulation.

A similar tendency for decrease in resonance frequency as fish volume increases can be predicted. This is because fish behave acoustically like air bubbles and most teleost fish have a swim bladder located between the alimentary canal and the kidney (Alexander, 1959). The swim bladder contains air and accounts for about 5-

10 % of the total fish volume (Love, 1978; Njane et al., 2019). Hence the resonator utilised, with a sample cavity volume of 1645 mL, has the potential to estimate total fish volume of between 150 to 300 mL. Although in our current experiment, a small cavity volume was utilised thus limiting the potential of fish volume that can measured, in future applications, a cavity to sample volume ratio of 5 to 10 would have a higher sensitivity for fish volume measurement. Furthermore, the larger the sample cavity, the lower the resonance frequency, hence an underwater speaker with a lower frequency range (less than 100 Hz) could be used; ideal for upscaling to larger fish volume estimation.

3.3.2. Prediction of sample volume

Using the results from the simulation of the empirical model Eq. (3.3), the actual versus predicted volume of air was plotted, as shown in Fig. 3.7. Predicted volume of air was lower than that experimentally observed with a high root mean square error (RMSE) of ± 5.454 mL. To improve the accuracy of the model, it is imperative to account for the losses that occur as a result of the resonator wall's deflection (Njane et al., 2018).

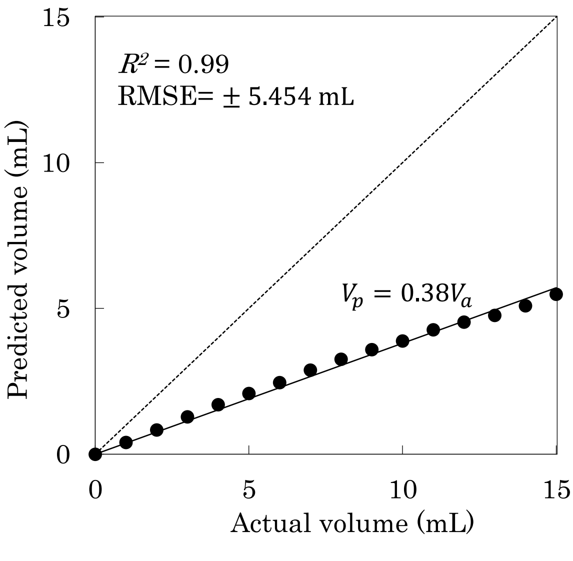

Fig. 3.7. Predicted versus actual volume of air showing underprediction because of uncorrected model.

As resonance occurred during sample volume estimation, pressure increased in the resonator's cavity. Since the walls of the resonator are not rigid, energy losses occurred due to the deflection of the wall of the resonator's cavity (Griffin et al., 2001). Webster and Davies (2010) reported that inaccuracies in sample volume prediction occur if loses are not accounted for. While in the generating cavity a small change in the volume of the resonator ΔV_{r1} (m^3) and in the volume of the water in the cavity ΔV_{w1} (m^3) occurs, a similar change in the volume of the sample cavity resonator ΔV_{r2} (m^3), volume of water ΔV_{w2} (m^3) and volume of the sample ΔV_o (mL) occurs as a result of the increased resultant pressure in the sample cavity as shown in Fig. 3.8.

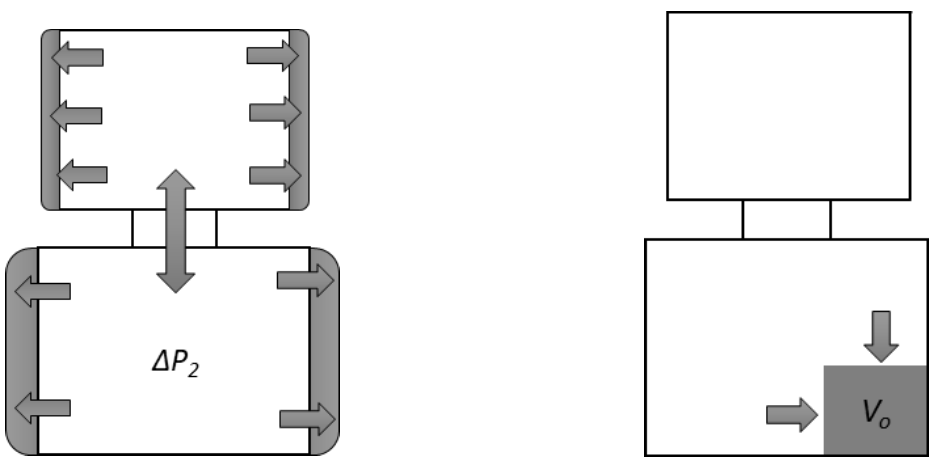

(a) (b)

Fig. 3.8. Pressure increase in the resonator cavity causes elastic walls to deflect (a) in both the generating cavity and sample cavity and (b) a small change in the volume of the sample occurs because of increased pressure in the sample cavity.

The resultant pressure changes that accrue in the sample cavity of the resonator when resonance occurs, are as shown in the Eq. (3.4) below. This is caused by the increased pressure in the walls of the resonator ΔP_{r2} (Pa), in the volume of water inside the sample cavity ΔP_{w2} (Pa) and on the sample product ΔP_0 (Pa). Thus, a resultant cumulative pressure ΔP_2 (Pa) can be derived as shown in Eq. (3.4).

$$\begin{aligned} \Delta P_{r2} &= K_{r2}\frac{\Delta W_{r2}}{W_2} \\ \Delta P_{w2} &= K_w\frac{\Delta V_{w2}}{V_{w2}} \\ \Delta P_o &= K_o\frac{\Delta V_o}{V_o} \\ \Delta P_2 = \Delta P_{r2} + \Delta P_{w2} + \Delta P_o &= K\frac{\Delta V_o + \Delta V_w + \Delta V_{r2}}{W_2} \end{aligned} \tag{3.4}$$

When there is no product in the sample cavity, the bulk modulus of the sample cavity is given as K_2 (Pa), as shown in Eq. (3.5) below.

$$K_2 = \frac{W_2}{\frac{W_2}{K_w}+\frac{1}{E_{r2}}} \tag{3.5}$$

By inserting aquatic products of volume V_o (mL) and bulk modulus K_o (Pa), resonance frequency shifts occur. This is because of the change in the bulk modulus when a product is inside the sample cavity, as shown in Eq. (3.6).

$$K_2 = \frac{W_2}{\frac{W_2-V_o}{K_w}+\frac{V_o}{K_o}+\frac{1}{E_{r2}}} \tag{3.6}$$

A new improved model, which accounts for the deflection of the resonator walls E_{r1} (Pa) and E_{r2} (Pa) in the generating cavity W_1 (m^3) and the sample cavity W_2 (m^3) respectively, was developed. The volume of the products can be estimated as shown below in Eq. (3.7).

$$V_o = \frac{K_o}{K_w-K_o}\left\{\frac{{f_o}^2}{\frac{E_{r1}}{E_{r1}W_1+K_w}(f^2-{f_o}^2)+\frac{E_{r2}}{E_{r2}W_2+K_w}f^2} - \frac{E_{r2}W_2+K_w}{E_{r2}}\right\} \tag{3.7}$$

The average deflection of the resonator in the sample cavity E_{r2} was 1.960×10^6 Pa. A correlation was made between the predicted and actual volume of air, as shown in the Fig. 3.9 and an improved prediction with a higher correlation accuracy was obtained.

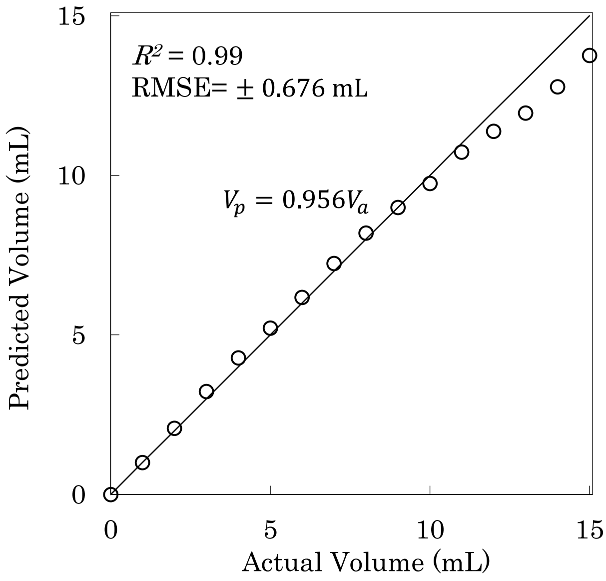

Fig. 3.9. Predicted versus actual volume of air in the corrected empirical model. High prediction is obtained with a lower RMSE (Root mean square error).

By use of the improved model that accounts for the losses on the wall of the resonator, a high linear correlation with an R^2 (R-squared) of 0.99 was obtained. However, as can be observed in Fig. 3.9, there was higher prediction of air volume between 1-10 mL, because of the lower cavity to sample volume ratio between 1645-164.5. However, with increased air volume in the sample cavity, the cavity to sample volume ratio further decreased to 109 resulting in underprediction thus, a higher RMSE of 0.676 mL. This is larger than the previously reported 0.02 mL (Njane et al., 2018), where the total volume of air measured was 0.5 mL in a sample cavity of 729 mL, thus a total cavity sample ratio of 1458. Increased sample volume results to decreased bulk modulus in the sample cavity leading to decreased sensitivity for volume estimation. For optimal product volume estimation, a larger cavity to sample volume ratio is recommended for higher sensitivity.

3.3.3. Effect of neck length and cross- sectional area on resonance frequency

The effect of increased neck length and cross-sectional area with resonance frequency was investigated, as shown below in Fig. 3.10.

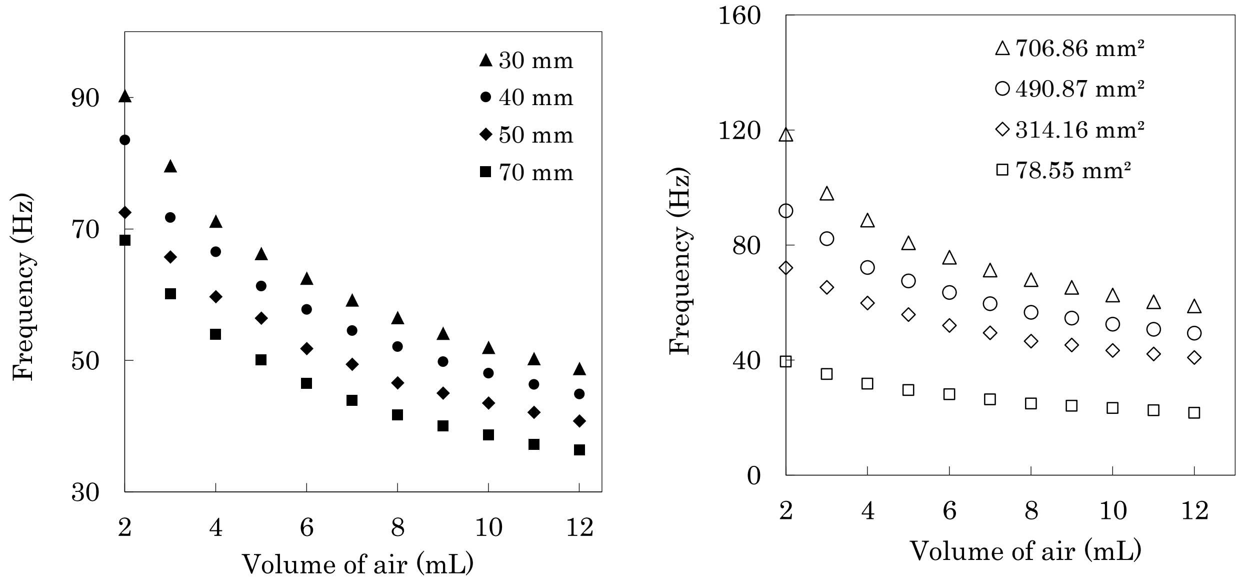

(a) (b)

Fig. 3.10. Frequency versus volume of air (a) as the neck length increases resonance frequency decreases and (b) as the cross-sectional area of the neck increases, resonance frequency increases.

As the length of the necks increased, resonance frequency decreased, as shown in Fig. 3.10 (a). By increasing the length of the neck of the resonator, the stiffness of the resonator decreases, thus resulting in more attenuation in such a resonator. Kang et al., (2008) reported that transmission losses increased hence more attenuation in an elongated neck of the resonator. Furthermore, Xu et al., (2010) observed that linearly increasing the length of the neck of a resonator results in a proportionate decrease in resonance frequency. Thus, shorter neck lengths would result in higher sensitivity due to the higher frequencies generated. Furthermore, less material is necessary to fabricate such a short neck. Altering the length of the neck connecting the two cavities is an effective way of manipulating the resonance frequency of the Helmholtz resonator without the need to change the volume of the cavity. As the cross-sectional area of the neck increased, resonance frequency increased as shown in Fig. 3.10 (b). Increasing the diameter of the neck leads to higher acoustic impedance coupled with decreased wavelength (Chanaud, 1994; Lee et al., 2004; Photiadis, 1991; Tang, 2005). This in turn leads to increased resonator stiffness resulting in higher frequencies.

Altering the dimensions of the neck is an effective means of controlling the resonance frequency without changing the volume of the cavity. From the result findings, a larger cross-sectional area in combination with a smaller neck length would achieve both economical and design optimization and utilisation characteristics for optimal product volume estimation. In addition, the compartmentalization of the top cavity and lower cavity improves the sound absorption capacity of the resonator (Tang et al., 2012). However, when up-scaling, larger sample cavities resonate at lower frequencies. In our current experiment, although a speaker with frequency range of 100 to10000 Hz was enough to generate resonance in the sample cavity, a speaker with a lower frequency range is paramount when generating resonance for sample volume estimation, in large tanks.

3.4. Conclusion

The functional design properties of an underwater double cavity Helmholtz resonator for precise aquatic products' volume estimation was proposed. To realise this, empirical models were developed and simulated, from which design and prototype of the resonator was developed and experimentally validated. For samples less dense than water, resonance frequency decreased as the sample volume increased. However, due to deflection of the resonator walls, lower frequencies were observed in the experimental validation. By accounting for these losses on the walls of the resonator, a high linear correlation between the predicted and the actual volume of samples was obtained. However, to improve sensitivity of measurement, a larger cavity to sample volume was proposed. Furthermore, by analysing the property of the neck connecting the two cavities, the resonance frequency property of such a resonator can be modified for optimal product volume estimation without altering the volume of the cavity. While a longer neck results to lower resonance frequency, a neck with a larger cross-sectional area results to increased resonance frequency due to increased resonator stiffness. A larger cavity to sample volume ratio with a short wide neck would be ideal for optimal product volume estimation in a double cavity Helmholtz resonator.

References

Alexander, R.M., 1959. The physical properties of the swim bladder in intact cypriniforms. Journal of Experimental Biology, 36, 315–332.

Alster, M., 1972. Improved calculation of resonant frequencies of Helmholtz resonators. Journal of Sound and Vibration, 24, 63–85.

Cappo, M., Harvey, E., Malcolm, H., Speare, P., others, 2003. Potential of video techniques to monitor diversity, abundance and size of fish in studies of marine protected areas. In: Proceedings of World Congress on Aquatic Protected Areas, Cairns, Australia, pp. 455–464.

Chanaud, R.C., 1994. Effects of geometry on the resonance frequency of Helmholtz resonators. Journal of Sound and Vibration 178, 337–348.

Chapman, D.M.F., Thomson, D.J., Ellis, D.D., 1992. Modelling air-to-water sound transmission using standard numerical codes of underwater acoustics. The Journal of the Acoustical Society of America, 91, 1904–1910.

Chen, P., Sun, Z., 1991. A review of non-destructive methods for quality evaluation and sorting of agricultural products. Journal of Agricultural Engineering Research 49, 85–98.

Devin, C.J., 1959. Survey of thermal, radiation, and viscous damping of pulsating air bubbles in water. The Journal of the Acoustical Society of America, 31, 1654–1667.

Ding, Y., Liu, Z., Qiu, C., Shi, J., 2007. Metamaterial with simultaneously negative bulk modulus and mass density. Physical Review Letters, 99, 093904-4.

Griffin, S., Lane, S.A., Huybrechts, S., 2001. Coupled Helmholtz resonators for acoustic attenuation. Journal of Vibration and Acoustics, 123, 11–17.

Kang, Z., Ji, Z., 2008. Acoustic length correction of duct extension into a cylindrical chamber. Journal of Sound and Vibration, 310, 782–791.

Kim, H.J., Cha, J.-P., Song, J.-K., Ko, Y.S., 2010. Geometric and number effect on damping capacity of Helmholtz resonators in a model chamber. Journal of Sound and Vibration, 329, 3266–3279.

Lee, J.W., Lee, J.M., Kim, S.H., 2004. Acoustical analysis of multiple cavities connected by necks in series with a consideration of evanescent waves. Journal of Sound and Vibration, 273, 515–542.

Love, R.H., 1978. Resonant acoustic scattering by swim bladder-bearing fish. The Journal of the Acoustical Society of America, 64, 571–580.

McCarthy, I.D., Carter, C.G., Houlihan, D.F., 1992. The effect of feeding hierarchy on individual variability in daily feeding of rainbow trout, *Oncorhynchus mykiss* (Walbaum). Journal of Fish Biology, 41, 257–263.

Nishizu, T., Ikeda, Y., 1995. Volume measuring system by acoustic method for agricultural products (Part 1) (in Japanese). Journal of Japanese Society of Agricultural Machinery and Food Engineers, 57 (5), 47–54.

Nishizu, T., Tomatsu, E., Katsuno, N., 2017. Airflow resistance measurement for a layer of granular material based on the Helmholtz resonance phenomenon. Bioscience, Biotechnology, and Biochemistry, 81, 823–830.

Njane, S.N., Shinohara, Y., Kondo, N., Ogawa, Y., Suzuki, T., Nishizu, T., 2019. Underwater fish volume estimation using closed and open cavity Helmholtz resonators. Engineering in Agriculture, Environment and Food, 12, 81–88.

Njane, S.N., Shinohara, Y., Kondo, N., Ogawa, Y., Suzuki, T., Nishizu, T., 2018. Improved underwater Helmholtz resonator with an open cavity for sample volume estimation. Computers and Electronics in Agriculture, 147, 18–26.

Photiadis, D.M., 1991. The effect of wall elasticity on the properties of a Helmholtz resonator. The Journal of the Acoustical Society of America, 90, 1188–1190.

Robert, J.U., 1967. Principles of underwater sound, First edition. McGraw-Hill, Inc., New York.

Savitzky, A., Golay, M.J.E., 1964. Smoothing and differentiation of data by simplified least squares procedures. Analytical Chemistry, 36, 1627–1639.

Selamet, A., Lee, I., 2003. Helmholtz resonator with extended neck. The Journal of the Acoustical Society of America 113, 1975–1985.

Shieh, A.C.R., Petrell, R.J., 1998. Measurement of fish size in Atlantic salmon (*Salmo salar*) cages using stereographic video techniques. Aquacultural Engineering, 17, 29–43.

Sun, T., Huang, K., Xu, H., Ying, Y., 2010. Research advances in nondestructive determination of internal quality in watermelon/melon: A review. Journal of Food Engineering, 100, 569–577.

Tang, S.K., 2005. On Helmholtz resonators with tapered necks. Journal of Sound and Vibration, 279, 1085–1096.

Tang, S.K., Ng, C.H., Lam, E.Y.L., 2012. Experimental investigation of the sound absorption performance of compartmented Helmholtz resonators. Applied Acoustics, 73, 969–976.

Upadhye, V., Agashe, S., 2016. Effect of temperature and pressure variations on the resonant frequency of piezoelectric material. Measurement and Control, 49, 286–292.

Webster, E.S., Davies, C.E., 2010. The use of Helmholtz resonance for measuring the volume of liquids and solids. Sensors, 10, 10663–10672.

Xu, M.B., Selamet, A., Kim, H., 2010. Dual Helmholtz resonator. Applied Acoustics, 71, 822–829.

Yokoyama, H., Abo, K., Ishihi, Y., 2006. Quantifying aquaculture-derived organic matter in the sediment in and around a coastal fish farm using stable carbon and nitrogen isotope ratios. Aquaculture, 254, 411–425.

Yokoyama, H., Takashi, T., Ishihi, Y., Abo, K., 2009. Effects of restricted feeding on growth of red sea bream and sedimentation of aquaculture wastes. Aquaculture, 286, 80–88.

Chapter IV

Improved double cavity Helmholtz resonator with acrylic sample cavity for precise fish volume estimation

Abstract

The precise estimation of fish volume is important for the monitoring fish growth. In this study, we fabricated and utilised an underwater double cavity Helmholtz resonator consisting of a generating cavity and a portable light-weight acrylic sample cavity for fish volume estimation. A sinusoidal chirp wave, with a frequency range of 100 - 500 Hz, was generated and captured using an underwater speaker attached to the generating cavity. As the cumulative volume of Japanese rice fish (*Oryzias latipes)* and Japanese dace fish (*Tribolodon hakonensis*) increased in the sample cavity, resonance frequency decreased. For both fish species, a high linear correlation with an R^2 (R-squared) of 0.99 between the actual and predicted volume was obtained.

4.1. Introduction

In precision aquaculture, the volume of fish is an essential parameter for monitoring the growth of fish in water. By determining the volume of the fish, the right population density of the fish can be determined (Minto et al., 2008) thus efficient feed management based on the growth and size of the fish, proper planning on landing and sale of fish can be carried out. To monitor and determine the size of the fish in off shore submerged sea cages, records of fork length and weight are taken aboard fishing vessels (Kennelly, 1995). In inland aquaculture tanks, the fish are drawn using a net, fork length and weight sampled as a representative of the fish *in situ*. However, this is not only laborious and time consuming since only a small representative can be sampled, but also sampling *ex situ* predisposes the fish to lack of oxygen and may die. Although SCUBA deep sea divers can visually inspect and sample the fish in water, their vision is not only limited to clear shallow water, but it is also very time consuming and hiring them is expensive (Pickering and Christie, 1981). Recently, there have been a number of advances in non-invasive (non-contact with the fish) techniques for underwater fish size estimation, such as using optical stereoscopy (Ruff et al., 1995; Strachan et al., 1990), machine vision (Hu et al., 2012) and stereo video techniques to survey fish abundance, length and weight (Cappo et al., 2003; Petrell et al., 1997). However, these optical methods are not only costly and time consuming, their practicability is limited especially in murky waters. Njane et al., (2018) reported that Helmholtz resonance by flow excited resonance could be used to estimate the volume of aquatic samples with different bulk modulus. Furthermore, fish volume could be accurately predicted in both a closed and open cavity Helmholtz resonator (Njane et al., (2019)). However, flow excited resonance is not only marred by flow fluctuations, thus inaccurate volume estimation, but also by the high flow velocities that could potentially damage fish tissue. This necessitates the need to generate underwater Helmholtz resonance, other than by flow excited resonance.

We have been developing an underwater double cavity Helmholtz resonance technique for aquatic sample volume estimation. In this system, a double cavity Helmholtz resonance system (consisting of a generating cavity, a neck and a sample cavity) is utilized, as shown in Fig. 4.1 (a). When resonance occurs, the mass of the water in the neck with a cross-sectional area S (m^2) and length l (m) connecting the two cavities oscillates as a result of the springiness provided by the generating cavity, W_1 (m^3) and the sample cavity, W_2 (m^3) filled with water, whose density is ρ (kg/m^3) and bulk modulus is K_w (Pa). When aquatic samples, whose volume is V_o (mL) and bulk modulus is K_o (Pa) are inserted into the sample cavity, resonance frequency changes from f_o (Hz) to f (Hz) due to the changes in the bulk modulus and volume of the cavity. For samples denser than water (such as glass balls), resonance frequency increases as the sample volume increases as shown in Fig. 4.1(b).

This is because their bulk modulus is greater than water, and as the volume of samples increase, the cavity volume decreases leading to increased resonance frequency. However, for samples less dense than water (air, fish), resonance frequency decreases as the sample volume increases as shown in Fig. 4.1 (b). This is because of the lower bulk modulus of these samples, resulting to a reduced bulk modulus in the sample cavity, thus causing decreased resonance frequency. Fish, similar to air bubbles, have a bulk modulus less than water, hence resonance frequency decreases as the volume of fish increases (Njane et al., 2019).

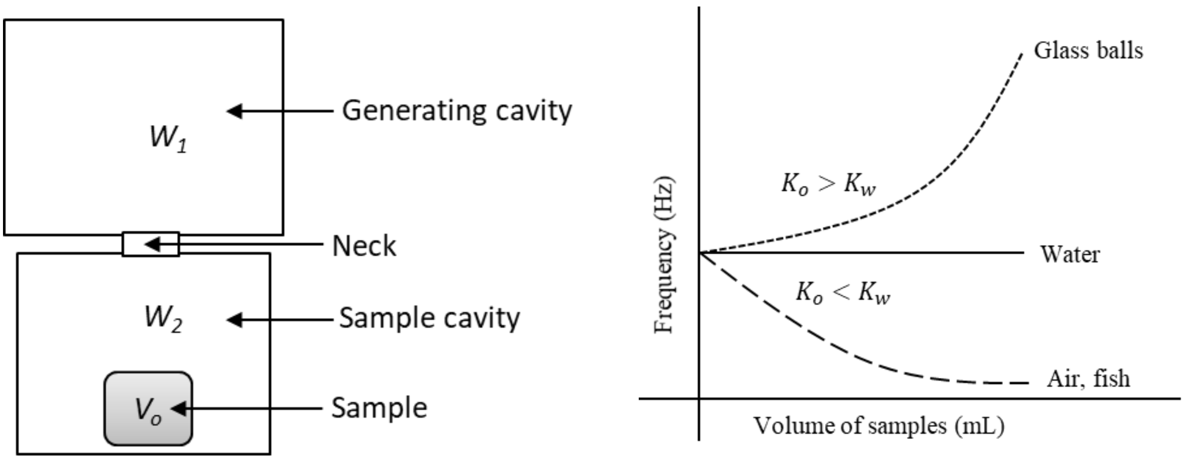

(a) (b)

Fig. 4.1. (a) Double cavity Helmholtz resonator consisting of a generating cavity and a sample cavity connected by a neck (b) resonance frequency against volume of samples, where resonance frequency increases with increased volume of denser samples and decreases with increased volume of less dense samples.

To precisely estimate the sample volume, it is essential to account for the losses that occur on the walls of the resonator due to increased pressure in the resonator cavities. To account for these deflection losses E_{r1} (Pa) and E_{r2} (Pa) are utilised for the generating and sample cavities respectively (Njane et al., 2018b). By analysing the difference in resonance frequency before f_0 (Hz) and after f (Hz) sample insertion into the sample cavity, the volume of samples V_o (mL) of whose bulk modulus is K_o (Pa), can be estimated using the model Eq. (4.1) below.

$$V_o = \frac{K_o}{K_w - K_o} \left\{ \frac{{f_o}^2}{\frac{E_{r1}}{E_{r1}W_1 + K_w}(f^2 - {f_o}^2) + \frac{E_{r2}}{E_{r2}W_2 + K_w} f2} - \frac{E_{r2}W_2 + K_w}{E_{r2}} \right\} \tag{4. 1}$$

However, to date, the volume of fish is yet to be estimated using a double cavity Helmholtz resonator. We hypothesis that utilising the speaker's impedance characteristics, we can generate sinusoidal chirp wave frequency and receive the resonance frequency from the sample cavity. By analysing the change in resonance frequency, the unknown volume of the fish can be derived. Fish behave acoustically like air bubbles, since the bulk modulus of fish is generally reported to be less than water (Njane et al., 2019). Experimental investigations have indicated that fish resonate when sound is incident (Lo et al., 1979; Sand and Hawkins, 1973), accruing from the resonance of the swim bladder, such as in gadoid and mackerel fish (Foote, 1980) whose swim bladder accounted for 90 - 95% of resonance. Therefore, utilising this acoustic property of fish, we hypothesize it can be utilised to develop an underwater Helmholtz resonator for fish volume estimation.

The objective of this research is to develop a portable underwater double cavity Helmholtz resonator for fish volume estimation. To do this, we fabricated a model concept of a double cavity Helmholtz resonator, consisting of a stainless-steel generating cavity for resonance generation and a clear acrylic sample cavity for in situ fish volume estimation. To generate resonance in water, a sinusoidal chirp wave signal was used to generate resonance frequency in the generating cavity, as this improves acoustic signal propagation (Johansson and Kleiner, 2001; Xu et al., 2010). As a proof of concept, fish samples were utilised, and their volume was estimated using the conventional displacement technique and compared with Helmholtz resonance technique. A calibration model developed from the precise estimation of fish volume using double cavity Helmholtz resonator has a vast application in, not only fish volume estimation, but also other aquatic organisms' volume measurement underwater.

4.2. Materials and methodology

4.2.1. Materials: Japanese rice fish and Japanese dace fish

Japanese rice fish (*Oryzias latipes*) commonly known as "medaka" were bought from Hamaichi bait manufacturing company in Wakayama, Japan as shown in Fig. 4.2 (a). The fish used were two months old after hatching. They were sorted, and 32 fish were used for volume measurement. The fish had an average fork length of 25 ± 5 mm and an average volume of 0.27 ± 0.15 mL. Because of their relatively smaller volume compared to the larger sample cavity volume, all the 32 Japanese rice fish, cumulatively could be inserted into the sample cavity of the resonator for volume estimation. To confirm the effect of larger fish on resonance frequency, Japanese dace fish (*Tribolodon hakonensis*) were purchased from Hamaichi Bait Manufacturing Company in Wakayama prefecture, Japan and 9 fish were utilised for measurement. The Japanese dace fish (locally known as "Ugui fish") which are fresh water fish were relatively larger and weighed about 14 ± 1.5 g and they were 10 months old as shown in Fig. 4.2 (b). The fish had an average fork length of 145 ± 20.5 mm. Their average volume measured by a water displacement method was 13.7 ± 2.5 mL.

(a) (b)

Fig. 4.2. Teleost fresh water fish (a) Japanese rice fish and (b) Japanese dace fish whose volume is measured.

4.2.2. Helmholtz resonator and supporting devices

The Helmholtz resonator utilised consisted of two cavities: A generating cavity and a sample cavity, as shown in Fig. 4.3. A cylindrical generating cavity was fabricated from stainless-steel and had an internal diameter of 126 mm, a height 34 mm and a volume of 471.45 mL. The acrylic sample cavity resonator had internal dimensions of 90 × 90× 85 mm and a cavity volume of 688.5 mL. Although in this set-up a small cavity volume has been adopted, implying that only small to medium fish sizes can be measured, in the future, upscaling such a sample cavity for targeted larger-sized fish volume measurement is also possible. The generating cavity was connected to the sample cavity through a neck of 25 mm long and 40 mm wide on the generating cavity and 60 mm wide on the top of the sampling cavity. The right side of the sample cavity had an inlet with a diameter of 60 mm where fish were inserted and was kept closed when sample volume measurement was ongoing. To generate the signal in water, a UW30 underwater speaker (Electro-Voice, U.S.A) with a frequency range of 100-10000 Hz was fixed onto the generating cavity. The speaker had an impedance of 8 ohms and a power handling capacity of 30 W and was connected to a constant current amplifier (KU-6 AE-CA Kobayashi Instrument Co., Ltd., custom order) for gain amplification. Furthermore, a Roland UA101 USB Audio (Roland Corporation, Shizuoka Japan) interface was connected to the amplifier and the computer. The audio interface device which functions as a stereo audio interface with a sampling frequency of 48 kHz and a signal processing specification of 24 bits, had a signal to noise ratio of 107 dB for the output and 101 dB for the input channel.

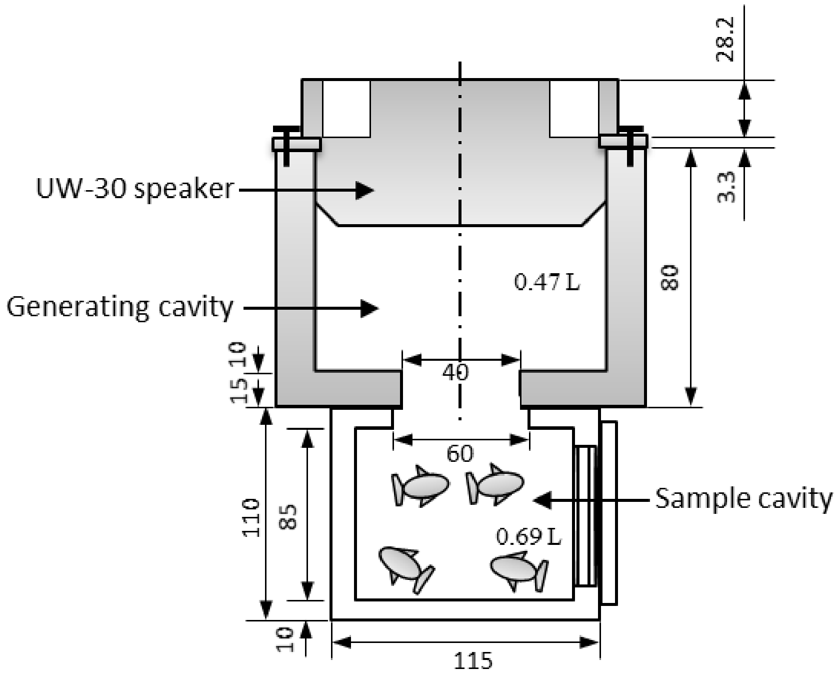

Fig. 4.3. Underwater double cavity Helmholtz resonator design specification consisting of the generating cavity connected to an underwater speaker and the sample cavity for fish volume measurement (dimensions in mm).

4.2.3. Methodology

The volume of both the Japanese rice fish and the Japanese dace fish were measured by water displacement as the actual volume of the fish. To estimate the volume of the fish using the Helmholtz resonance technique, the double cavity resonator was set up in a water tank, as shown in Fig. 4.4. The water in the tank was kept at 20 ℃ during the experiment, which was not only suitable for keeping the fish but also maintained the elasticity of the resonator's cavity (Upadhye and Agashe, 2016). The generating cavity with speaker firmly fixed on top was placed on top of the sample cavity and connected through an opening (neck) for resonance generation. With the sample cavity closed and no fish inserted, resonance frequency was excited, and the Helmholtz resonance frequency was measured as f (Hz). Fish with cumulative volume were inserted through the right side opening of the sample cavity, the opening was closed, and resonance frequency was generated to obtain the resonance frequency, f_o (Hz). Both the cumulative volume of Japanese dace fish and Japanese rice fish was measured separately. To confirm the effect of resonance frequency due to fish parts, 5 Japanese dace fish were killed by stabbing on a board, dissected and the fish meat, bones and the swim bladder were extracted from the fish body using a scalpel. In cumulative volume, the bones, fish meat and the swim bladder were inserted separately into the resonator's cavity and resonance frequency change measured. The swim bladder was cut in water and a beaker in water was placed on top to collect the gas extruded from the swim bladder. Using a graduated gas syringe, the gas was collected, and the volume was estimated using a gas syringe. An equal proportion of air was inserted into the resonator's cavity and the resonance frequency change with increasing volume of air was evaluated.

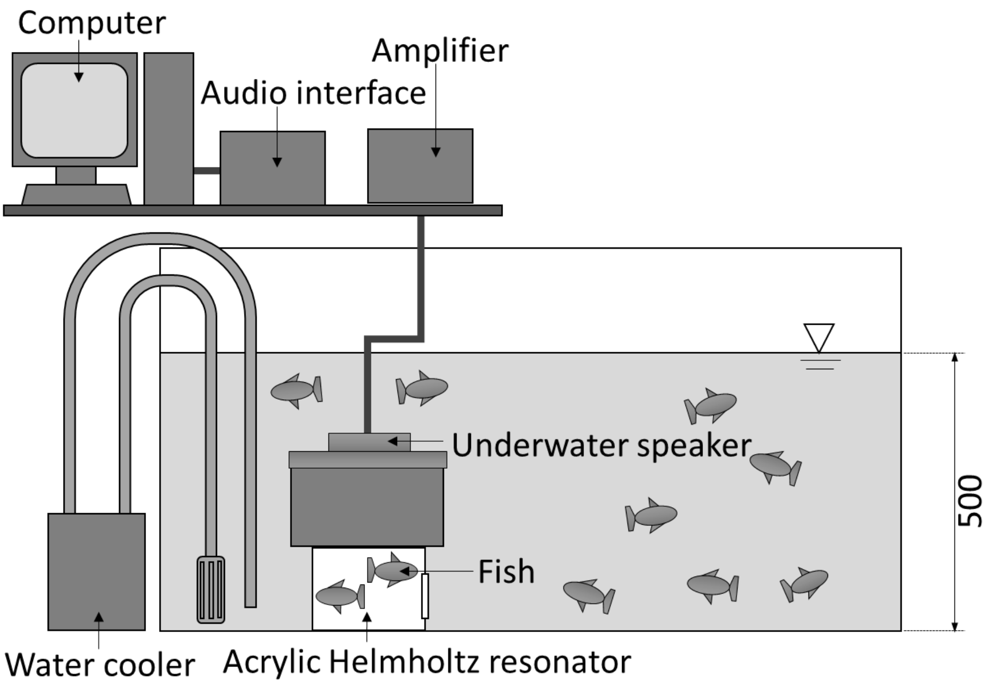

Fig. 4.4. Fish volume estimation in the acrylic Helmholtz resonator, and the generating cavity placed on top with a speaker fixed onto the generating cavity and submerged in a water tank (dimensions in mm).

To generate the resonance frequency, a sinusoidal chirp wave with a frequency range of 100-500 Hz was excited and captured by the underwater speaker, with a sampling time of 10 seconds. The diaphragm of the speaker's membrane was used to determine the frequency response of the speaker, thus acting as a transceiver (both transmitting and receiving the signal). The voltage was measured as an estimate of the electric impedance of the voice coil of the underwater speaker, since the direct current was proportional to the speaker's input voltage. Sound pressure changes inside the resonator's cavity resulted in the vibration of the speaker's diaphragm. This is the sum of the static impedance possessed by the voice coil and the dynamic impedance which comes from the vibration of the diaphragm of the speaker. When the speaker is attached to the resonator, the dynamic impedance generated by the speaker is proportional to the sound pressure that occurs inside the sample cavity of the resonator. By measuring this impedance, the resultant change in pressure in the resonator can be determined and thus a resonance frequency can be obtained, without the need to attach a hydrophone as the receptor of the signal. The obtained response waveform was converted into a power spectrum by use of a Fast Fourier Transform algorithm and the sampling frequency was set to 48 kHz. To transmit and analyse the signal, a volume spectrum analyser software developed using Microsoft Foundation Class library, MFC 6.0 using Visual C++, was utilised. The peak frequencies were captured and recorded and the spectrum obtained was smoothed using a Savitsky-Golay Function (Savitzky and Golay, 1964). Two dominant peaks were observed, as shown in Fig. 4.5 (a).

One of the peaks occurred at about 142 Hz. This peak which had higher intensity resulted from the resonance in the generating cavity of the resonator. Furthermore, with increased volume of fish in the sample cavity, the peak remained constant since there were no samples in the generating cavity.

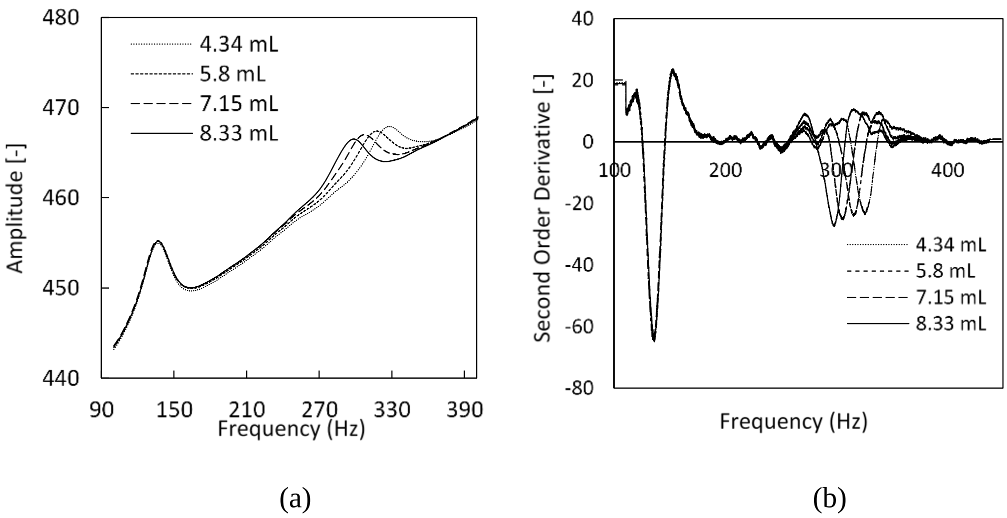

Fig. 4.5. Spectrum of resonance frequency (a) amplitude with resonance frequency and two peaks appear at 142 Hz and about 270-350 Hz and (b) after second order derivative, while the peak at lower frequency of 142 Hz with high amplitude has no shift in resonance frequency, the lower amplitude peak which has a higher frequency, shifts from 318-298 Hz with increased volume of fish from 4.34 - 8.33 mL.

However, the other peak had a lower amplitude and a resonance frequency range of 270-350 Hz, occurred. This peak had a lower amplitude because of the larger volume of the sample cavity thus resulting in damping of the frequency. Furthermore, as the volume of the fish increased, the resonance frequency shifted as shown in Fig. 4.5 (a). To quantify the peak frequency shift, a second order derivative was applied to the spectrum using OriginPro 8.0 software (OriginLab Corporation, Northampton, MA 01060 USA) and a shift in resonance frequency was observed, as shown in Fig. 4.5 (b). The peak frequencies were plotted against the cumulative volume of fish and a comparison was made between the empirical model simulation and the experimental validation.

When Helmholtz resonance occurs in the sample cavity, damping occurs because of the presence of fish in the sample cavity. To understand the resonance property of the fish, the acoustic property was investigated as a lead to decipher the damping effect of the acoustic signal on the fish. By modelling the fish and the swim bladder as a sphere, the acoustic scattering of the swim bladder causes damping of the resonance frequency. The acoustic scattering cross section, σ_s (m^2) is given by:

$$\sigma_s = \frac{4\pi R_2^2}{\left(1-\frac{\omega_o^2}{\omega^2}\right)^2 + \delta_T^2} \tag{4. 2}$$

Where the damping δ_T of the swim bladder and the resonance frequency of the fish is represented as ω_o (Hz), the radius of the fish is R_2 (mm) and the resonance frequency of the cavity is represented as ω (Hz). By inclusion of the tension of the swim bladder membrane σ_{bl} into the equation, then the resonance frequency is expressed as:

$$\omega_o = \frac{1}{R_2}\left(\frac{3\gamma P_o + (3\gamma - 1)\frac{2\sigma_{bl}}{R_1} + 4\mu DE}{E\rho_l}\right)^{\frac{1}{2}} \tag{4. 3}$$

The parameters E and D are given as $E = [4\mu + (2\mu + 3\lambda_T)e^3]/(6\mu + 3\lambda_T)$ and $D = [(2\mu + 3\lambda_T)/(6\mu + 3\lambda_T)] \times (1 - e^3)$. Where P_o (Pa) is the hydrostatic pressure, γ is the ratio of specific heats of air inside the swim bladder, ρ_l (kg/m^3) is the density of water. μ (N/m^2) and λ_T are Lame constants while e is the ratio of the radius of the swim bladder to the radius of the fish i.e. $e = R_1/R_2$. The total damping factor at resonance is given as δ_T. While the surface tension of the swim bladder and the liquid viscosity may both affect the low-frequency scattering from the swim bladder fish, other more relevant factors, such as the flesh of the fish and the swim bladder wall, affect the resonance frequency. We will therefore utilise the resonance property of the fish, as a lead on precise fish volume estimation in order to determine the scattering cross section using the models developed by Ye and Farmer (1994).

4.3. Results and discussion

4.3.1. Increased fish volume with resonance frequency

The characteristic property of resonance frequency change with increased volume of both fish species using the derived empirical simulation and experimental validation were obtained, as shown in Fig. 4.6. As the volume of Japanese rice fish increased, resonance frequency decreased as indicated in Fig. 4.6 (a). Lo, (1979) attributed, such a decrease in resonance frequency, to be caused by the viscosity of the fish. Love, (1978) demonstrated that most teleosts have a swim bladder that causes damping of resonance frequency. Furthermore, Chapman et al., (1966) observed that swim bladders are responsible for the resonance and reverberation in bathypelagic fishes.

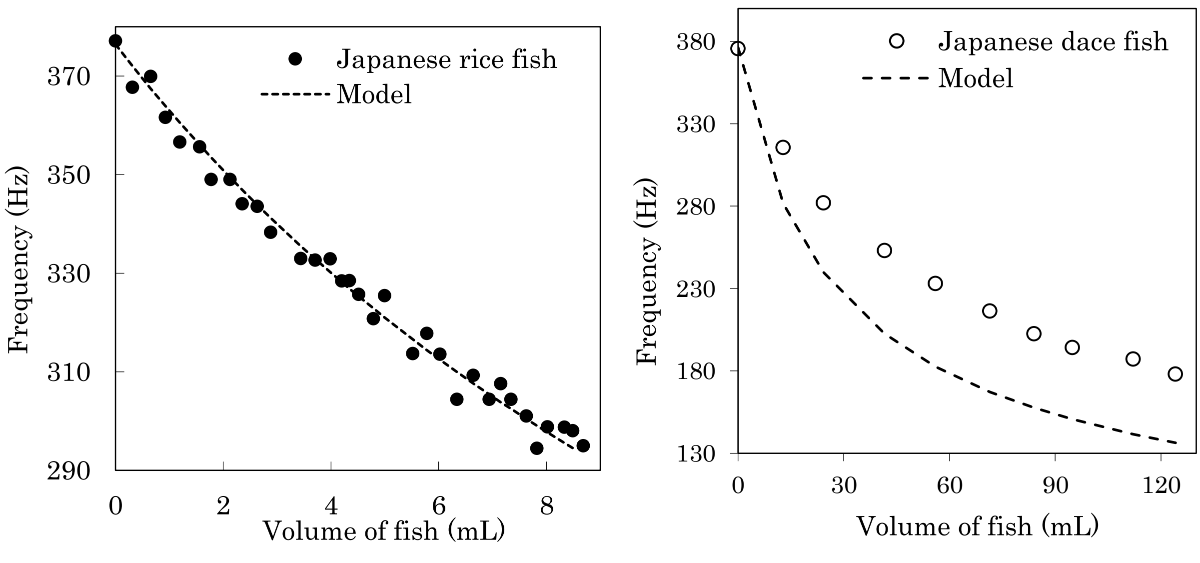

(a) (b)

Fig. 4.6. Empirical simulation and experimental validation showing decreased resonance frequency as the volume of (a) Japanese rice fish and (b) Japanese dace fish increased in the sample cavity.

Njane et al., (2019) using flow-excited could estimate the volume of both individual and total volume of fish. From our results, although a high sensitivity for total fish volume measurement could be achieved, there was a lower sensitivity when individual fish volume was measured. This is because of the higher cavity volume compared to the smaller fish samples utilised. For future application, a cavity to sample volume ratio of less than 2295 would be ideal for achieving high sensitivity for both individual and total fish volume measurement. However, unlike Njane et al., (2019), the experimental observations fitted with the derived empirical simulation model. This is because when determining the bulk modulus of the fish, the model assumed the ratio of the swim bladder to the total volume of the fish is 9.473%, similar to previously measured Japanese rice fish (Njane et al., 2019). Fish volume estimation using the speaker impedance technique offers non-invasive, rapid and precise fish volume measurement. Unlike the flow-excited resonance, where fluctuations of resonance frequencies occur, and fish may be damaged by the high-water flow.

Similarly, as the volume of Japanese dace fish increased, resonance frequency decreased as shown in Fig. 4.6 (b). The Japanese dace fish investigated, like most teleosts possess a swim bladder located between the alimentary canal and the kidney of the fish (Alexander, 1959), which is used to maintain buoyancy and can detect sound pressure changes inside the water (Wahlberg and Westerberg, 2003). Most teleosts, resonate when sound is incident (Fine et al., 2001), which also causes damping of the resonance frequency. Due to the larger volume of the Japanese dace fish, there was a lower cavity to sample volume ratio, thus resulting in higher sensitivity for individual fish volume measurement (cavity to sample volume ratio of 36.8). Thus, the Helmholtz resonator cavity volume was ideal in estimating individual fish volume with a higher sensitivity.

However, as shown in Fig. 4.6 (b), the empirical model simulation tendency was lower than the experimental validation tendency when Japanese dace fish volume was measured. This is because of the variation in the ratio of the swim bladder to the total volume of fish. The simulation model assumes that the ratio of the swim bladder to the total volume of the fish is 9.473, similar to previous findings of the Japanese rice fish (Njane et al., 2019). Swim bladder varies in position, size and this affects the total bulk modulus of the fish. Thus, it is paramount to investigate the ratio of the swim bladder volume to the total volume of fish for precise fish volume estimation. Furthermore, the swim bladder may not be solely responsible for damping of the resonance frequency. It is therefore imperative to investigate the effect of other fish parts on the resonance frequency to fit the model.

4.3.2. Resonance from swim bladder, fish meat and bones

To confirm the effect of the damping of resonance frequency of the intact fish measured in situ, the effect of resonance frequency changes with the cumulative volume of extracted fresh fish bones, fish meat, swim bladder and air extracted from 5 Japanese dace fish were investigated, as shown in Fig. 4.7. As the volume of extracted fresh fish meat and bones increased, resonance frequency gradually decreased as indicated in Fig. 4.7 (a). However, there was more damping of the resonance frequencies with the freshly extracted meat compared to the freshly cut fish bones. This is because the bones are stiffer than the fish meat, hence a higher resonance frequency. Research has shown that unlike the fish bones, fish meat resembles soft rubber and hence can be modelled as a viscous fluid, since fish meat consists of 80% water and about 15-20 % protein and lipid contents, which varies based on fish species (Love, 1978). The meat and the bones, as well as other parts of the fish, vibrate at a similar amplitude to the surrounding water particles (Sand and Hawkins, 1973). Ye and Farmer (1994), noted that tissue elasticity increases resonance frequency. Most of the fish tissues and parts also lead to damping when resonance frequency is incident, thus the swim bladder is not sole contributor.

As the volume of the extracted swim bladder increased, resonance frequency decreased, as shown in Fig. 4.7 (b). The sound pressure incident on the fish, sets the swim bladder into motion, because of the high compressibility of the gas in the swim bladder, relative to the surrounding water and tissues (Rogers et al., 1988). Furthermore, the swim bladder contains gas inside for maintaining hydrostatic pressure and also leads to damping of the resonance frequency (Love, 1978). This results in the swim bladder higher damping (lowering) resonance frequencies compared to intact fish. However, air bubbles dampened even more than a swim bladder of equal volume. This is because there was higher tension on the walls of the swim bladder compared to the walls surrounding the air bubbles, thus increased stiffness of the swim bladder compared to air bubbles.

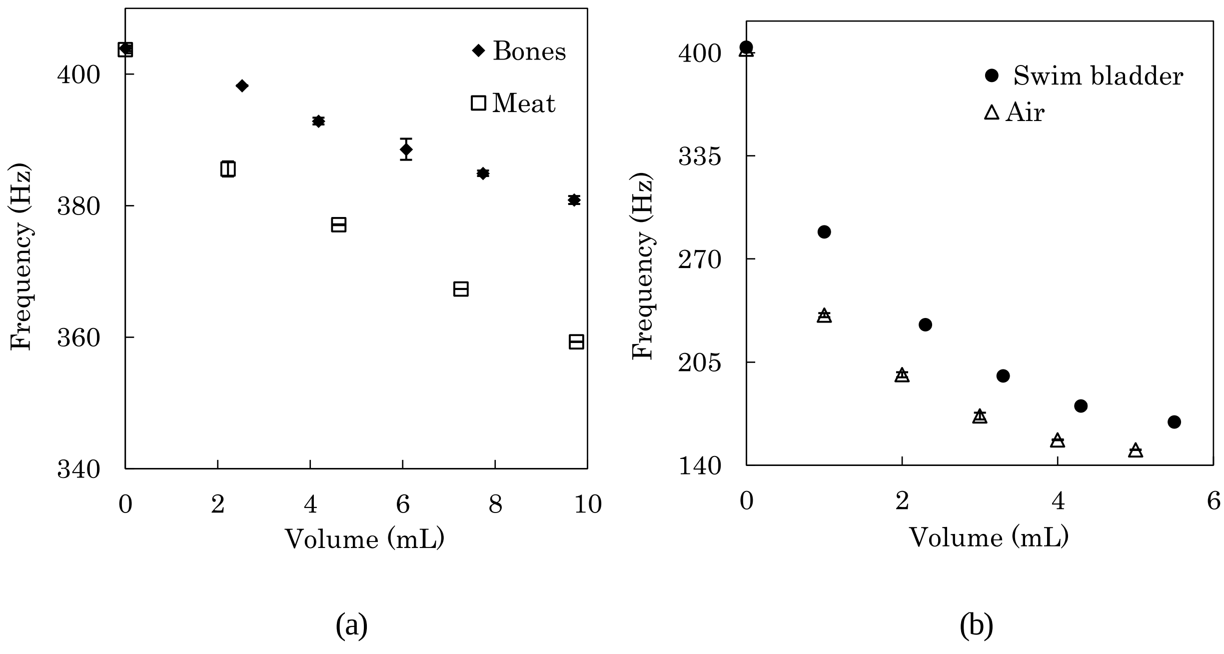

Fig. 4.7. Resonance frequency decrease with increased volume of (a) fresh bones and fish meat and (b) swim bladder and air.

Studies have shown that the acoustic property of fish is like that of an air bubbles, and that oxygen and nitrogen constitute most of the gas inside the swim bladder of most fish (Foote, 1980). Although the acoustic pressure of the swim bladder of the fish, is similar to an air bubble, and was distributed at all points in the swim bladder, the shape of the extracted swim bladder was different from the shape formed by increased air bubbles trapped at the wall of the resonator (Fine et al., 2001).This might lead to differences in static pressure between the gas bubbles and the swim bladder, hence less dampened frequencies observed in the swim bladder compared to air bubbles. Only hydrostatic pressure is significant in causing a change in the volume of the swim bladder during fast and steady displacements (Taylor et al., 2010). However, in the future it will also be necessary to evaluate the movements that might be caused by the localized excitation of sonic muscles in some fish (Fine et al., 2001).

As the volume of the extracted air increased, resonance frequency decreased as shown in Fig. 4.7 (b). This is because the bulk modulus of air is less than that of water (bulk modulus of air is 1.4×10^5 Pa. while the bulk modulus of water is 2.1×10^9 Pa.). By exposing the air bubbles to sound pressure, the bubble pulsates and with increased volume of the gas, a loss of energy in the resonance frequency occurs, leading to damping of the resonance frequency (Sand and Hawkins, 1973). The proportionate volume of air in the swim bladder to the total volume of the fish is used to evaluate the bulk modulus property of the fish. After extracting the air from the swim bladder, the average volume of the swim bladder V_s (mL) to the total volume of the fish, V_f (mL) was 7.90 % in Japanese dace fish (Fig. 4.8) and for the Japanese rice fish a proportion of about 9.67% was reported by Njane et al., (2018b).

Since the average value of the bulk modulus of fish meat is 2.5×10^9 Pa and the bulk modulus of air is 1.42 $\times 10^5$ Pa, by utilising the proportionate volume of air in the swim bladder volume compared to the total fish volume, the bulk modulus of the fish can thus be given as, $K_{fish} = \frac{1}{\frac{1-V_r}{K_{meat}}+\frac{V_r}{K_{air}}}$.

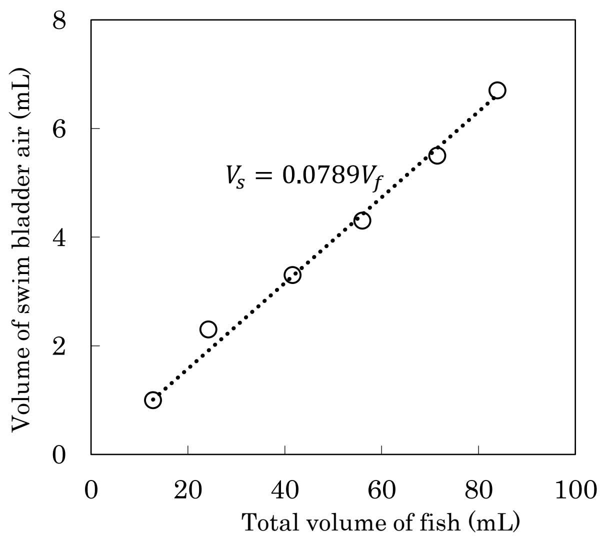

Fig. 4.8. Proportionate volume of air extracted from the swim bladder compared to the total volume of fish in Japanese dace fish.

From this model, the bulk modulus of the Japanese dace fish and Japanese rice fish is given as 1.75×10^6 Pa and 1.55×10^6 Pa respectively. By assuming that the swim bladder is spherical with a radius R_1 (m) and is surrounded by an inelastic fish flesh of radius R_2 (m), the ratio of the radius of the swim bladder to the radius of the fish is given as, $e = R_1/R_2$: 0.476 for the Japanese dace fish and 0.455 for the Japanese rice fish.

To determine the acoustical scattering around the fish, using the Eq. (4.2), we assume that the longitudinal stress is much smaller compared to the shear modulus i.e. $\lambda_T \ll \mu$, the parameters $E = (4 + e^3)/6$ and $D = (1 - e^3)/3$. This makes $E = 0.684$ and $D = 0.297$ for Japanese dace fish and $E = 0.682$ and $D = 0.302$ for Japanese rice fish. We assume that the shear modulus of Japanese dace fish is similar to that of Oscar fish, as described by Thomas et al., (1996) , i.e. $\mu \approx 10^5$ N/m^2. The surface tension of the swim bladder wall σ_{bl} is about 2 N/m. The ratio of the specific heat of air in the swim bladder γ is 1.01. The density of water ρ_l is 1000 kg/m^3 and the hydrostatic pressure P_o is 10^5 N/m^2. Substituting these values into the equation above, the resonance frequency is 277.03 Hz for Japanese dace fish and 291.854 Hz for Japanese rice fish. From this value, we now calculate the damping factor at resonance due to the inelasticity of the fish flesh $\delta_f = 0.013$ in both fish. With assumption that $\mu_2 \approx 0.2$ and that our isonifying frequency from the Helmholtz resonator ω is 375 Hz. From references, the total damping coefficient due to thermal conductivity δ_{th}, radiation δ_r and shear viscosity δ_v is 0.03. Therefore, the total damping factor δ_T is 0.043. We then calculate the Q factor which is $Q = \frac{1}{\delta_T} = 23.25$, as shown in Table 4.1.

Table 4.1 Fish acoustic property and damping factor

Fish property	*Symbol*	*Japanese dace fish*	*Japanese rice fish*
Bulk modulus of fish	K_f	1.75×10^6 Pa	1.443×10^6 Pa
Acoustical scattering	σ_s	3170.475 mm^2	1021.045 mm^2
Resonance frequency	ω_o	277.03 Hz	291.854 Hz
Radius of fish	R_2	15 mm	3.57 mm
Radius of swim bladder	R_1	6.48 mm	1.625 mm
Ratio of Radius	e	0.476	0.455
Tension of swim bladder walls	σ_{bl}	2 N/m	2 N/m
Longitudinal and shear stress constants	E	0.684	0.682
Longitudinal and shear stress constants	D	0.297	0.302
Shear modulus of fish	μ	10^5 N/m^2	10^5 N/m^2
Fish flesh inelasticity damping	δ_f	0.013	0.013
Total damping factor	δ_T	0.043	0.043
Q factor	Q	23.25	23.25

4.3.3. Precise fish volume prediction and estimation

Because of resonance occurring in the sample cavity, pressure changes occurred in the sample cavity. The pressure changes in the sample cavity led to the deflection of the resonator walls, which are accounted for as

E_{r2} (Pa) in Eq. (4.1). In order to precisely estimate the volume to fish, we need to account for the deflection changes of the resonator's wall as a result of increased pressure in the resonator's cavity (Griffin et al., 2001). From the empirical model Eq. 4.1, the deflection of the resonator's wall E_{r2} (Pa) with increased volume of fish samples was evaluated, as shown in Fig. 4.9.

With initial increase in the volume of Japanese rice fish, a high deflection of the resonator i.e., E_{r2} of 2.61×10^5 Pa was obtained as shown in Fig. 4.9 (a). This deflection was caused by sudden changes in the stiffness of the resonator's wall because of increased pressure when a single fish was inserted into the resonator's cavity. However, with increased cumulative volume of the Japanese rice fish in the sample cavity, a constant pressure change resulted in a relatively constant deflection of the resonator's wall leading to an average E_{r2} value of 1.20×10^5 Pa. During the measurement of Japanese dace fish, a similar increased resonator deflection value was obtained with initial input of fish into the resonator's cavity (Fig. 4.9 (b)).

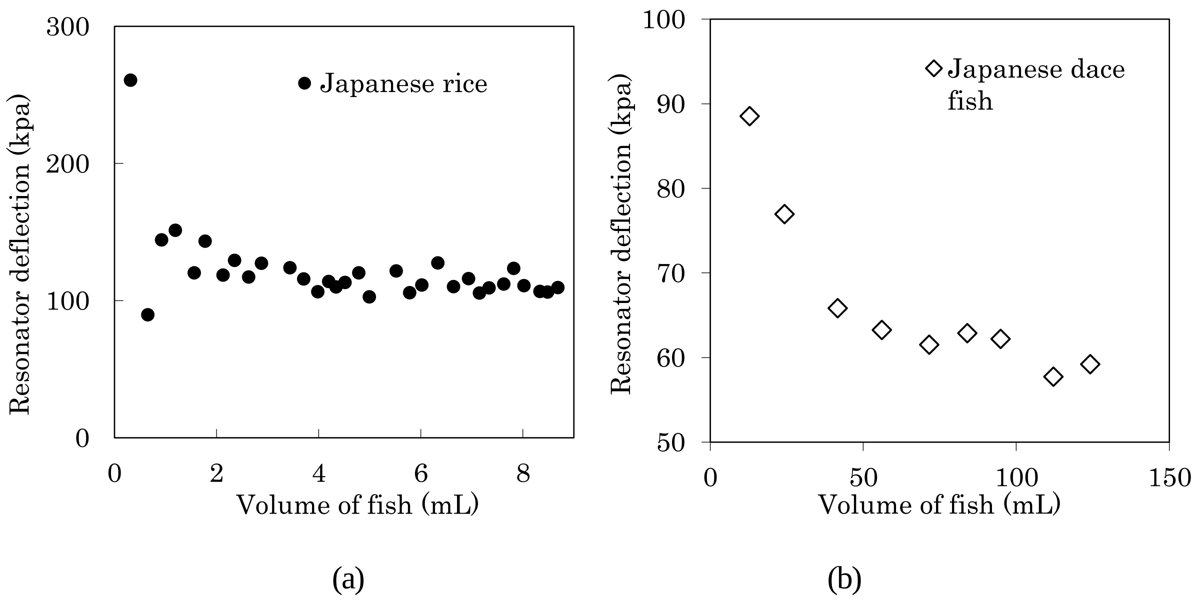

Fig. 4.9. Resonator's deflection values E_{r2} (Pa) with increased volume of (a) Japanese rice fish and (b) Japanese dace fish in the acrylic sample cavity of the resonator.

However, with increased fish volume inside the resonator's cavity, this value decreased and a stable value of about 6.18×10^4 Pa was observed. By compensating the resonator's deflection changes E_{r2} (Pa), the volume of the fish measured in situ can be precisely estimated (Njane et al., 2019). A correlation was made between the predicted volume of fish V_p (mL) and the actual volume of fish V_a (mL) for both Japanese rice fish and Japanese dace fish, as shown in Fig. 4.10 (a) and (b) respectively.

A high linear correlation between predicted and actual volume of Japanese rice fish was obtained. However, a smaller cavity to sample volume ratio would be preferred to increase the sensitivity of the measurement. Similarly, a high linear correlation between predicted and actual volume of Japanese dace fish was obtained. The proposed resonator's cavity was enough with high sensitivity for measurement of the Japanese dace fish.

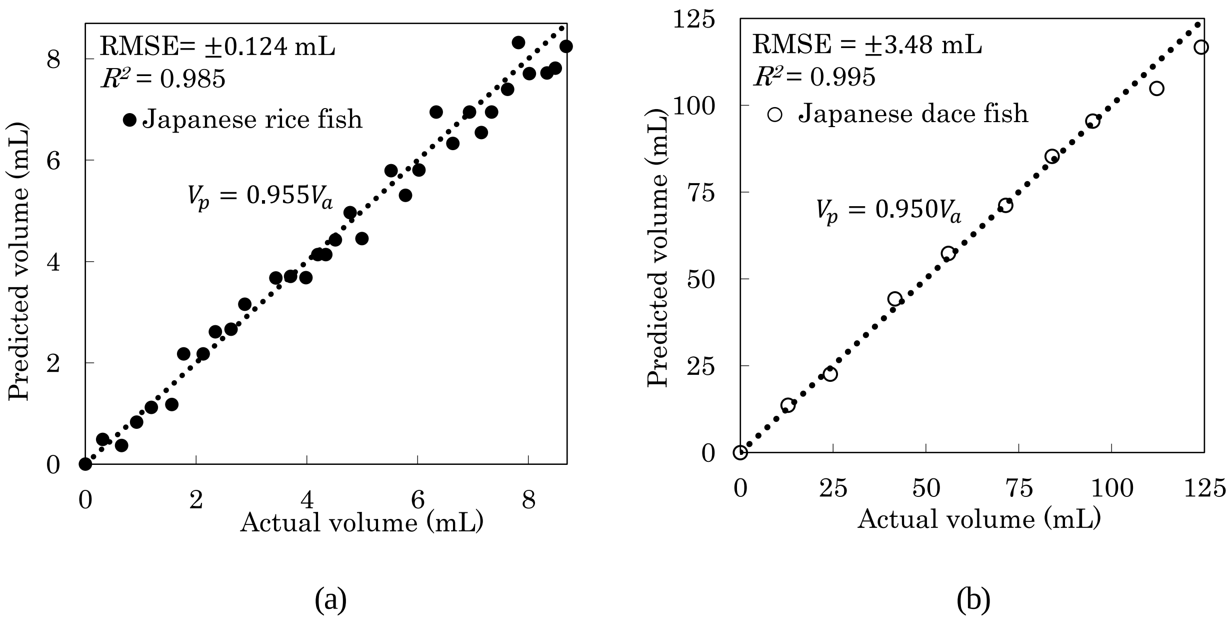

Fig. 4.10. Predicted volume vs actual volume of (a) Japanese dace and (b) Japanese rice fish in a double cavity Helmholtz resonator.

4.4. Conclusion

An underwater fish volume estimation system using a double cavity Helmholtz resonator was developed. A prototype of the double cavity resonator consisting of a speaker fixed onto a stainless-steel generating cavity and a clear acrylic sample cavity where fish volume was estimated was fabricated and utilised. A chirp wave signal generated from the speaker's impedance generated a resonance frequency as a result of the vibration of the membrane of the speaker, emanating from the resonance of the sample cavity. As the volume of the sample fish increased, resonance frequency decreased. This is because of the presence of the swim bladder in the intact fish. Further investigations revealed that other fish parts, such as the meat and the bones also contribute to the total damping of the resonance frequency. A high linear correlation between the actual and predicted volume of the fish measured in situ was obtained. For resonator optimisation and increased sensitivity, a lower cavity to sample volume ratio would be preferred for measuring small fish. Thus, an underwater double cavity Helmholtz resonator has potential to precisely estimate the volume of fish and other aquatic species in situ.

References

Alexander, R.M., 1959. The physical properties of the swim bladder in intact cypriniforms. Journal of Experimental Biology, 36, 315–332.

Cappo, M., Harvey, E., Malcolm, H., Speare, P., others, 2003. Potential of video techniques to monitor diversity, abundance and size of fish in studies of marine protected areas. In: Proceedings of World Congress on Aquatic Protected Areas, Cairns, Australia, pp. 455–464.

Chapman, R.P., Marshall, J.R., 1966. Reverberation from deep scattering layers in the Western North Atlantic. The Journal of the Acoustical Society of America, 40, 405–411.

Fine, M., Malloy, K., King, C., Mitchell, S., Cameron, T., 2001. Movement and sound generation by the toadfish swim bladder. Journal of Comparative Physiology A: Sensory, Neural, and Behavioural Physiology, 187, 371–379.

Foote, K.G., 1980. Importance of the swim bladder in acoustic scattering by fish: A comparison of gadoid and mackerel target strengths. The Journal of the Acoustical Society of America, 67, 2084–2089.

Griffin, S., Lane, S.A., Huybrechts, S., 2001. Coupled Helmholtz resonators for acoustic attenuation. Journal of Vibration and Acoustics, 123, 11.

Hu, J., Li, D., Duan, Q., Han, Y., Chen, G., Si, X., 2012. Fish species classification by colour, texture and multi-class support vector machine using computer vision. Computers and Electronics in Agriculture, 88, 133–140.

Johansson, T.A., Kleiner, M., 2001. Theory and experiments on the coupling of two Helmholtz resonators. The Journal of the Acoustical Society of America, 110, 1315–1328.

Kennelly, S.J., 1995. The issue of bycatch in Australia's demersal trawl fisheries. Reviews in Fish Biology and Fisheries, 5, 213–234.

Lewis, T.N., Rogers, P.H., 1996. The vibrational response of single-chambered fish swim bladders to low-frequency sound. ICES Journal of Marine Sciences, 53, 285–287.

Lo, A., Hovem, J.M., others, 1979. An experimental investigation of swim bladder resonance in fishes. The Journal of the Acoustical Society of America, 66, 850–854.

Love, R.H., 1978. Resonant acoustic scattering by swim bladder-bearing fish. The Journal of the Acoustical Society of America, 64, 571–580.

Minto, C., Myers, R.A., Blanchard, W., 2008. Survival variability and population density in fish populations. Nature, 452, 344.

Njane, S.N., Shinohara, Y., Kondo, N., Ogawa, Y., Suzuki, T., Nishizu, T., 2019. Underwater fish volume estimation using closed and open cavity Helmholtz resonators. Engineering in Agriculture, Environment and Food, 12, 81–88.

Njane, S.N., Shinohara, Y., Kondo, N., Ogawa, Y., Suzuki, T., Nishizu, T., 2018. Improved underwater Helmholtz resonator with an open cavity for sample volume estimation. Computers and Electronics in Agriculture, 147, 18–26.

Petrell, R.J., Shi, X., Ward, R.K., Naiberg, A., Savage, C.R., 1997. Determining fish size and swimming speed in cages and tanks using simple video techniques. Aquacultural Engineering, 16, 63–84.

Pickering, A.D., Christie, P., 1981. Changes in the concentrations of plasma cortisol and thyroxine during sexual maturation of the hatchery-reared brown trout, (*Salmo trutta* (L.)) General and Comparative Endocrinology, 44, 487–496.

Rogers, P.H., Popper, A.N., Hastings, M.C., Saidel, W.M., 1988. Processing of acoustic signals in the auditory system of bony fish. The Journal of the Acoustical Society of America, 83, 338–349.

Ruff, B.P., Marchant, J.A., Frost, A.R., 1995. Fish sizing and monitoring using a stereo image analysis system applied to fish farming. Aquacultural Engineering, 14, 155–173.

Sand, O., Hawkins, A.D., 1973. Acoustic properties of the cod swim bladder. Journal of Experimental Biology, 58, 797–820.

Savitzky, A., Golay, M.J.E., 1964. Smoothing and differentiation of data by simplified least squares procedures. Analytical Chemistry, 36, 1627–1639.

Strachan, N.J.C., Nesvadba, P., Allen, A.R., 1990. Fish species recognition by shape analysis of images. Pattern Recognition, 23, 539–544.

Taylor, G.K., Holbrook, R.I., de Perera, T.B., 2010. Fractional rate of change of swim-bladder volume is reliably related to absolute depth during vertical displacements in teleost fish. Journal of the Royal Society Interface, 7, 1379–1382.

Upadhye, V., Agashe, S., 2016. Effect of temperature and pressure variations on the resonant frequency of piezoelectric material. Measurement and Control, 49, 286–292.

Wahlberg, M., Westerberg, H., 2003. Sounds produced by herring (*Clupea harengus*) bubble release. Aquatic. Living Resources, 16, 271–275.

Xu, M.B., Selamet, A., Kim, H., 2010. Dual Helmholtz resonator. Applied Acoustics 71, 822–829.

Ye, Z., Farmer, D.M., 1994. Acoustic scattering from swim-bladder fish at low frequencies. The Journal of the Acoustical Society of America, 96, 951–956.

Chapter V

Fish volume estimation in an open aquatic tank using Helmholtz resonator

Abstract

The precise estimation of total fish volume in inland aquaculture is important for ensuring proper feed utilisation and monitoring growth and development of fish, in preparation for landing. Until today, sampling of fish size has been done manually, a process which is not only tedious but could result in fish death when measured, *ex situ*. We introduce, for the first time a non-invasive (non-contact) Helmholtz resonance technique for total fish volume estimation in land-based aquarium tanks. To do this, a speaker was fixed onto a generating cavity and the set were connected onto the side of an aquatic tank on the land. A chirp wave signal (100-500 Hz) was excited from the speaker leading to resonance occurrence in the aquatic tank. The resonated sound was captured by a hydrophone, and a correlation between the resonance frequency and the volume of fish in the tank was plotted. As the volume of the model fish, Japanese dace fish (*Tribolon hakonensis*), increased the resonance frequency decreased. The model fish, like other teleost fish, have a swim bladder that resonates when sound is incident on them leading to damping of the resonance sound. Furthermore, such teleost fish, which possess a swim bladder, have a bulk modulus lower than that of water, resulting in decreased resonance frequency as total fish volume increases. A linear coefficient of R^2 of 0.98 between the actual and predicted volume of the fish was obtained.

5.1. Introduction

Knowing the volume of fish in inland aquaculture facilities is critical for determining stocking density of fish, monitoring the growth of the fish and for determining the appropriate time for landing. Ellis et al., (2002) found that when trout were stocked at high densities, not only was the food intake of the individual fish reduced, but also the growth rate was reduced (Papoutsoglou et al., 1987), thus leading to a lower feed conversion efficiency (Logan and Johnston, 1992), degraded water quality and an increased fish mortality rate. Thus, by determining the size of the fish and adjusting feed management based on that, efficient feeding can be carried out which reduces the cost of production and minimizes detrimental environmental effects caused by excessive feeding and overstocking.

Hitherto, fish size estimation has solely been done based on farmer experience and the history of stocking similar fish, or ultimately manually sub-sampling fish size. When manually sampled, length measurements are taken from tail to head and the weight of the fish is recorded as representative of the *in-situ* fish population. However, manually sampling is not only tedious and predisposes the fish to diseases, it is also difficult to sample bottom feeders in deep tanks. Recently, the use of non-invasive techniques (without contact) such as Charge coupled cameras (CCD), image processing algorithms (Zion et al., 1999), stereo imagery (Williams et al., 2016) and video imagery (Shafait et al., 2017) have been used to successful discriminate between fish species and estimate their length in a fish tank. However, these techniques are limited by not only the high cost of such cameras and complicated algorithms, but also by the low contrast between the fish and the background due to deteriorating water quality, which results in increased opaqueness, thus ultimately resulting in low image quality. Acoustic non-invasive techniques have also viable applications owing to the fast speed of sound in water, robustness of utilisation - irrespective of the water quality, and the acoustic reverberation property of fish in water (Chapman and Marshall, 1966). Although echo sounders have been utilised to estimate the number density of fish in the acoustic beam (MacLennan, 1990), they can only be used for fish that are sparsely distributed (low density) due to overlapping echoes from adjacent or individual fish.

Recently, a Helmholtz resonance technique has been successful used to estimate fish underwater. Njane et al., (2018) found that in experiments establishing the principles of the technique that difference in density between samples and water resulted in resonance frequency increased as the volume of denser samples (such as glass balls) increased, while resonance frequency decreased as the volume of samples less dense than water (such as air bubbles or fish) increased. Fish that contain a swim bladder behave acoustically like an air bubble; thus Helmholtz resonance generated by water flow-excited resonance could be used to estimate the cumulative volume of Japanese rice fish (*Oryzias latipes*) in both closed and open cavity resonators (Njane et al., 2019). However, flow-excited resonance requires high-water velocity that not only leads to non-uniform flows that lead to fluctuations in resonance frequency but could also potentially damage the fish in the tank.

To our knowledge, this research introduces for the very first time, a Helmholtz resonance mechanism where fish volume can be estimated non-invasively (without contact or using water flow) in an open aquarium tank. To do this, we utilised a double-cavity-based Helmholtz resonator where a generating cavity, which has speaker attached to it for resonance generation, is attached to the side of an aquatic tank (sample cavity) where total fish volume was measured *in situ*. A prototype of the double-cavity based aquatic tank resonator is shown below in Fig. 5.1 (a). The double-cavity based resonator system can be considered as a one mass, two spring system, as shown in Fig. 5.1 (b). When resonance occurs, the mass of water, *m* (kg) at the neck oscillates due to the springiness k_1 and k_2 provided by the generating and sample cavities, respectively. When there is no fish inside the sample cavity, the resonant frequency, f_o (Hz) is given as shown in the Eq. (5.1). below.

$$f_o = \frac{1}{2\pi}\sqrt{\frac{1}{\rho} \times \left(\frac{K_1}{W_1} + \frac{K_2}{W_2}\right) \times \frac{S}{l}} \tag{5. 1}$$

While the bulk modulus in the generating cavity is derived as K_1 (Pa) and the volume of the cavity as W_1 (mL), the bulk modulus of the sample cavity and the total volume of the sample cavity are derived as K_2 (Pa) and

W_2 (mL) respectively. When fish whose unknown total volume, V_o (mL) are present in the sample cavity, the resultant resonance frequency f (Hz) can be obtained as shown in the Eq. (5.2) below.

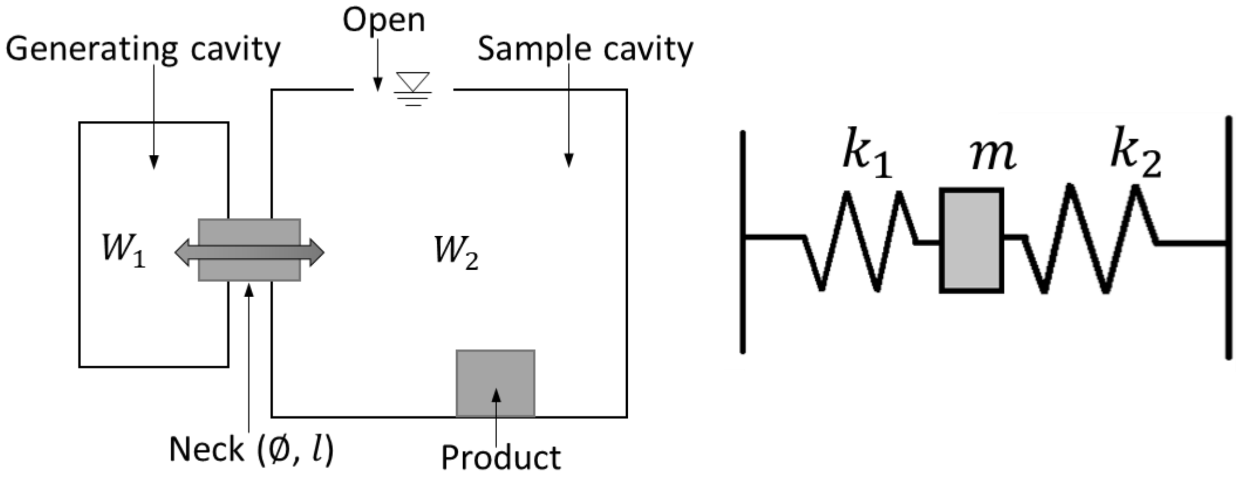

(a) (b)

Fig. 5.1. Double cavity-based resonator prototype (a) with generating cavity and sample cavity (b) considered as mass with two springs.

$$f = \frac{1}{2\pi}\sqrt{\frac{1}{\rho} \times \left(\frac{K_1}{W_1} + \frac{K_2}{W_2 - V_o}\right) \times \frac{S}{l}} \tag{5.2}$$

However, when deriving these principles, it is important to account for the losses that occur due to the deflection of the wall of the resonator, E_r (Pa) as a result of increased pressure in the cavities when resonance occurs (Njane et al., 2018). Therefore, considering these losses in both the generating cavity E_{r1} (Pa) and the sample cavity E_{r2} (Pa), the total volume of fish V_o (mL) can be derived as:

$$V = \frac{K_o}{K_w - K_o} \left\{ \frac{f_o2}{\frac{E_{r1}}{E_{r1}W_1 + K_w}(f2 - f_o2) + \frac{E_{r2}}{E_{r2}W_2 + K_w} f2} - \frac{E_{r2}W_2 + K_w}{E_{r2}} \right\} \tag{5.3}$$

In this research, we developed empirical models for a double-cavity-based inland aquatic resonator for precise fish volume estimation. As proof of concept, a resonator consisting of a generating cavity was designed, fabricated and attached to a sample cavity (tank) to measure fish volume. The results obtained from this were compared with those from a conventional displacement technique. Furthermore, to understand the resonance properties of an aquarium tank, open at the top, we varied the diameter of the opening and investigated changes in resonance frequency properties with reference to increased sample volume.

5.2. Materials and methodology

5.2.1. Materials: Japanese dace fish and air

13 Japanese dace fish (*Tribolodon hakonensis*), were purchased from Hamaichi Bait Manufacturing Company in Wakayama prefecture, Japan for volume measurement. The Japanese dace fish (locally known as "Ugui fish") are fresh water fish. Their average mass was 14 ± 1.5 g and had an average volume of 13.7 ± 2.5 mL. They were 10 months old at time of purchase from the from hatchery and had an average fork length of 145 ± 20.5 mm. Air, with a bulk modulus of 1.4×10^5 Pa (20 °C, 1 atm.) was utilised as a representative of sample that is less dense than water. Air bubbles are also known to behave acoustically like fish since they resonate when there is an incident resonant sound.

5.2.2. Double cavity-based Helmholtz resonator for aquatic tank

A double-cavity-based resonator prototype consisting of an underwater speaker, generating cavity and sample cavity was designed and prototyped, as shown in Fig. 5.2 (a). The underwater speaker was firmly fixed onto the generating cavity whose dimensions were; diameter of 126 mm, height 34 mm and a volume capacity of 471.45 mL. An acrylic neck with a diameter 30 mm and length 30 mm was used to connect the generating cavity to the sample cavity, and a net was used to prevent the fish from entering the generating cavity. The acrylic sample cavity had external dimensions 200 × 200 × 200 mm and a wall thickness of 15 mm, thus capacity of 4.913 L. The sample cavity was open at the top, with an opening diameter of 80 mm where fish were inserted for measurement. A cap with an opening in it was used to close the opening at the top of the sample cavity, as shown in Fig. 5.2 (b). The diameter of the opening of the cap was varied from 15 to 23 mm.

An AQH-020 (Aqua Sound Inc. Kobe, Japan) hydrophone was used to capture the resonated sound from the inside of the sample cavity of the resonator. The hydrophone knob had a diameter 30 mm and length 60 mm and was connected to the Aqua feeler SH20K System Intec (Aqua Sound Inc. Kobe, Japan), for gain amplification. A Roland UA101 Audio (Roland Corporation, Shizuoka Japan) interface device was connected to the computer through the USB. The device which functions as a stereo audio interface with a sampling frequency of 48 kHz and a signal processing specification of 24 bits had a signal to noise ratio of 107 dB for the output and 101 dB for the input channel. A constant current amplifier (KU-6 AE-CA, Kobayashi Instrument Co., Ltd., custom order) was utilised for controlling the attenuation level of the speaker.

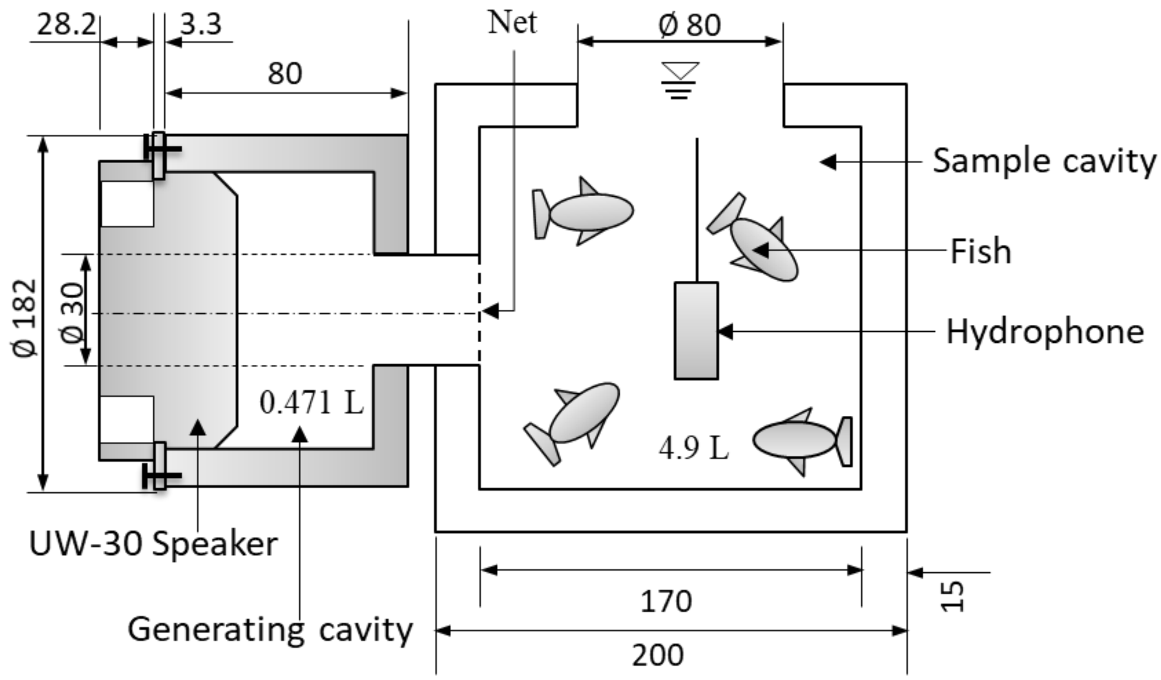

(a)

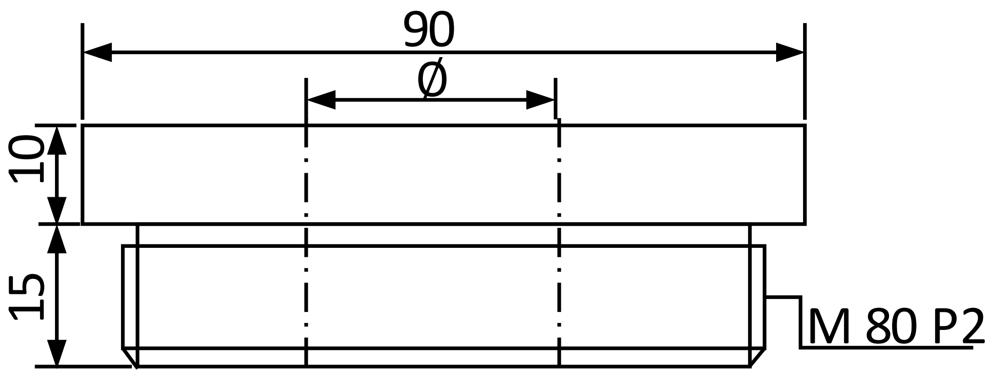

(b)

Fig. 5.2. Double cavity-based resonator design prototype consisting of the generating cavity with a speaker connected to it and the water filled sample cavity with fish and the (b) cap used to close the resonator top opening to vary the diameter : 15, 17, 19, 21, 23 and 70 mm (all dimensions in mm).

5.2.3. Methodology

The stainless-steel generating cavity with an underwater speaker fixed onto it, was connected to the acrylic sample cavity. The sample cavity was filled with water which had been pre-cooled at an average temperature of 20 ± 2 °C and the speaker and hydrophone were connected to the amplifier, audio interface and the computer, as shown below in Fig. 5.3. A chirp wave signal in the range 5-400 Hz exited the generating cavity at a sampling time of 10 seconds through the neck connecting the two cavities into the sample cavity (aquatic tank). As a result, resonance occurred in the sample cavity and the signal was captured by the hydrophone. The signal from the hydrophone was amplified using the Aqua feeler amplifier and the signal was sent to the sound device and finally recorded by the computer as shown in Fig. 5.4. Fish with known volume were inserted cumulatively into the sample cavity and for each successive addition of fish into the sample cavity, the resonance frequency change was recorded.

To analyse the effect of swim bladder resonance, 4 sample fish were killed by stabbing on a board and the swim bladders extracted. The intact inflated swim bladder with gas still in it were inserted into the sample cavity in cumulative volume, and the effect of resonance frequency with increased volume of swim bladder was analysed. After measurement, the swim bladders were cut in the water under a beaker and the gas extruded from the swim bladder was extracted from the beaker using a gas syringe and the volume measured. Similarly, atmospheric air, similar to the volume of air extracted from the swim bladder of the fish, was injected into the sample cavity using a gas syringe in cumulative steps and the effect on resonance frequency recorded. The resonated sound, which was in the time domain, was converted to the frequency domain using a Fast Fourier Transform algorithm in the volume spectra analyser developed in the lab using Microsoft Foundation Class library, (MFC 6.0, Visual C++) (Njane et al., 2018). The spectrum was smoothed using Savitsky-Golay with

OriginPro 8.0 software (OriginLab Corporation, Northampton, MA 01060 USA) and the region of maximum peak occurrence was utilised to extract the resonance frequency. The relationship between resonance frequency change and cumulative volume added was plotted.

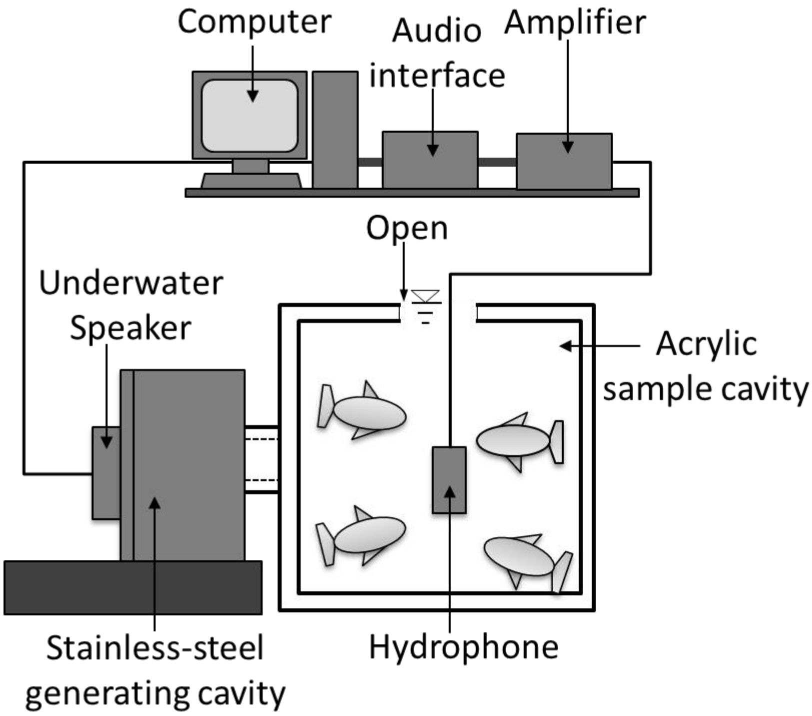

Fig. 5.3. Experimental set-up for fish volume estimation in the acrylic sample cavity of the Helmholtz resonator, and the generating cavity placed by the side of the fish tank.

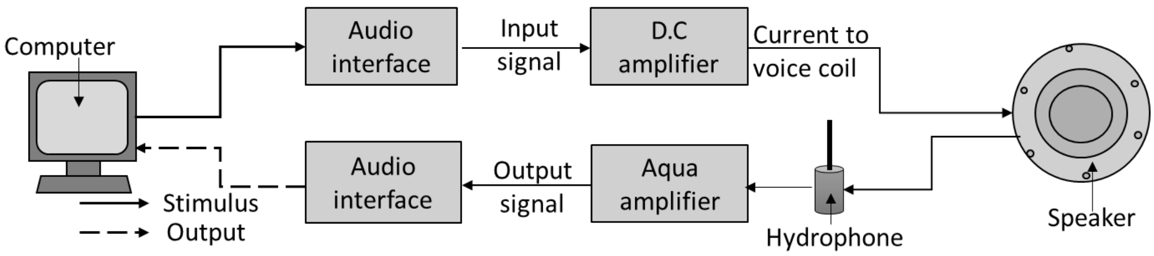

Fig. 5.4. Chirp wave signal generated from computer to speaker and the resonated sound captured by the hydrophone to the computer for analysis.

5.3. Results and discussion

5.3.1. Resonance frequency tendency with cumulative fish volume

Resonance frequency spectra changed with increased volume of fish as shown in Fig. 5.5 (a). As the volume of fish increased, resonance frequency decreased, and the amplitude of the resultant spectrum also decreased, as shown in Fig. 5.5 (b). The damping in resonance frequency is associated with the presence of the intact swim bladder in the fish (Fine et al., 2016).

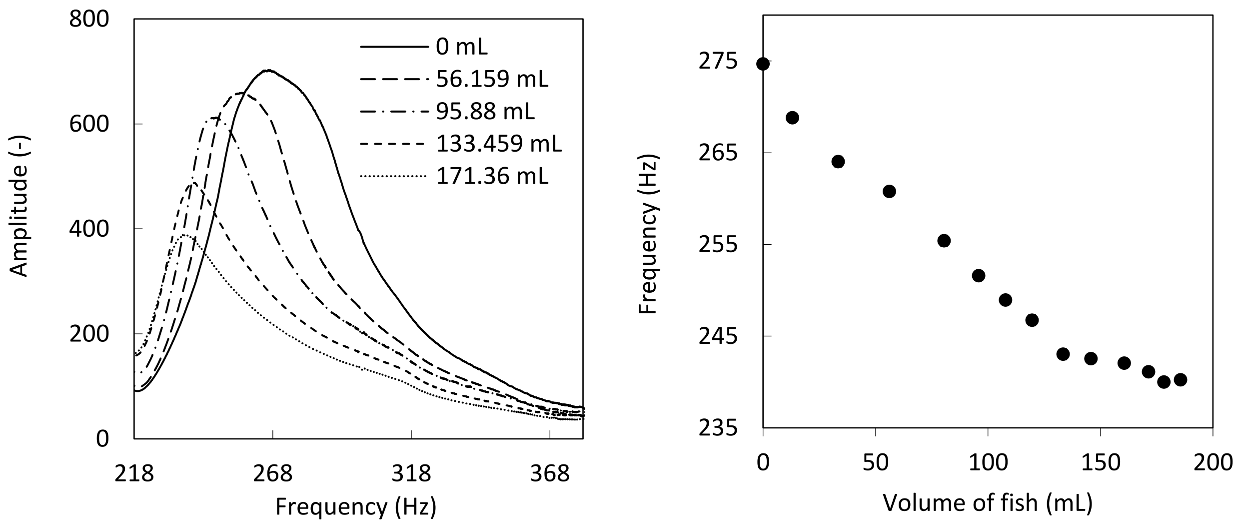

(a) (b)

Fig. 5.5. As the volume of fish increased (a) resonance frequency decreased and amplitude decreased from the spectrum data (b) resonance frequency decreased as fish volume increased until about 133 mL where sensitivity of measurement was lower with increasing fish volume.

Swim bladders, in teleost fishes, are gas filled organs that not only provide fish with buoyancy, but can also detect sound and hydrostatic pressure at different depths (Taylor et al., 2010). They are also known to resonate sound when communicating with other fish (Whitehead and Blaxter, 1989). The walls of the swim bladder are elastic, while the meat and organs surrounding the swim bladder are modelled as a viscous shell. Normally, fish flesh is assumed to resemble soft rubber, hence the fish flesh and the swim bladder wall increase the stiffness of the fish, thus leading to damping of the resonance frequency (Love, 1978). The viscous property of the fish as a result of the viscous fish flesh (Raveau and Feuillade, 2016) and intact swim bladder of the fish result in reduced bulk modulus of the fish, thus leading to damping of resonance frequency.

As cumulative fish volume increased in the sample cavity, the resonance frequency decreased relatively linearly up until 133 mL, where after the intensity of resonance frequency change declined as indicated in Fig. 5. 5 (b). Due to increases in fish volume in the cavity, the effective volume of the sample cavity decreased. The reduced sensitivity of resonance frequency changes at higher fish volumes resulted from increased resonator stiffness. The sample cavity utilised had an internal capacity of 4.913 L and fish volume up until 133 mL of could be estimated with high sensitivity. To maintain measurement sensitivity for larger sample volumes in the future, a larger tank (sample cavity) to fish volume ratio would be desirable.

5.3.2. Swim bladder and air volume measurement

To understand the cause of damping and resonance frequency decreases with increased volume of fish, the extracted swim bladders with their gas intact were inserted into the sample cavity in cumulative volumes and the resonance frequency changes with increased volume of the swim bladders were plotted, as shown in Fig. 5.6 (a). As the volume of the swim bladder increased, resonance frequency decreased, and as did the resultant amplitude as shown in Fig. 5.6 (b). This result is similar to that observed as fish volume increased. However, compared to the fish, there was more damping of the resonance frequency. This is thought to be due to the thin membrane on the surface of the swim bladder, compared to the fish flesh and bones in the fish, thus making the fish stiffer compared to the swim bladder. Similarly, as the volume of air increased in the sample cavity, resonance frequency decreased as shown in Fig. 5.6 (b). However, compared to the air, there were higher resonance frequencies as the volume of the swim bladder increased as shown in Fig. 5.6 (b). This was due to thin elastic layer on the surface of then swim bladder resulted in increased stiffness compared to the thin layer of the air bubbles in water.

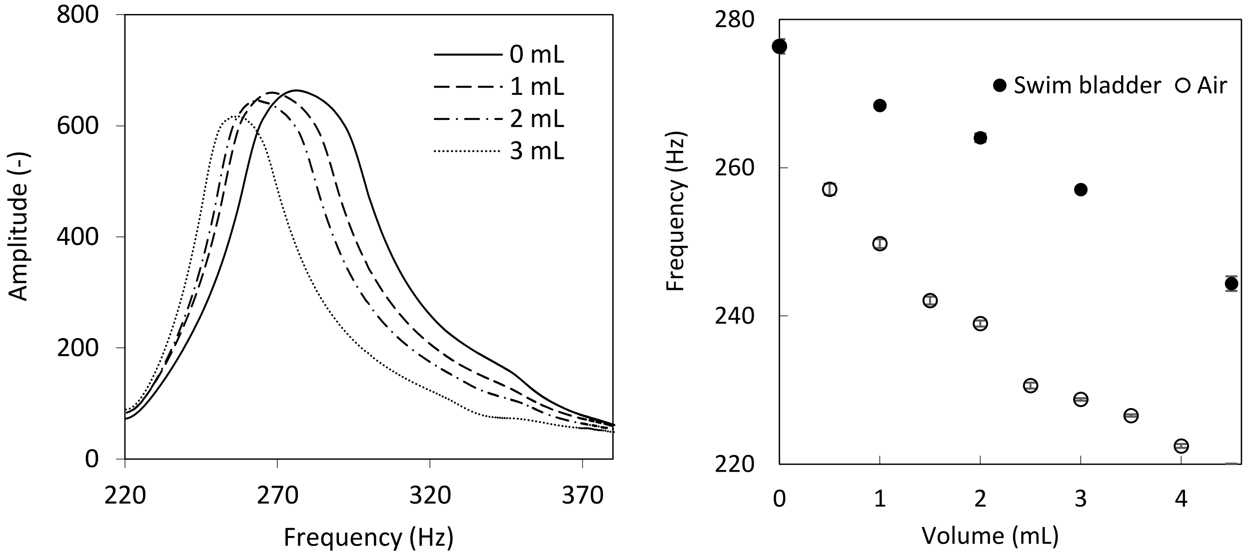

(a) (b)

Fig. 5.6. (a) Spectral property of increased volume of swim bladder with resonance frequency and amplitude (b) comparison between air and swim bladder volume with resonance frequency.

Air, similar to the gas present inside the swim bladder, has a lower bulk modulus than water (bulk modulus of air, $K_{air} = 1.4 \times 10^5$ Pa while that of water, is, $K_{water} = 2.2 \times 10^9$ Pa). According to underwater Helmholtz resonance principle, resonance frequency decreases as the volume of samples less dense than water increases. Dedenkulo at al., (2015) observed that larger bubbles resulted to increased sensitivity of measurement leading to reduced acoustic radiation force and hence large frequency changes. Similarly to fish and swim bladder, when sound is incident air bubbles, scattering occurs as a result of the quick change in the acoustical impedance at the spherical interface between air and water (Feuillade and Werby, 1994). When modelling the effect fish resonance, similar to the air bubble and swim bladder, effect of the swim bladder wall causes the resonance frequency to decrease and the peak amplitude is reduced. By exposing the air bubble to sound pressure of varying frequency, the air bubble tends to pulsate because of the damping effect leading to loss of energy as the air bubble pulsates (Sand and Hawkins, 1973). These losses in energy are attributed to occur because of either re-radiation, thermal effects or the viscous property of such an air bubble in water. Studies have shown that the elasticity of the air bubble shell and the viscosity of the air inside the shell of the air bubble, result to damping of the resonance (Feuillade and Nero, 1998; Love, 1978). Similar to swim bladder in fish, air bubbles in water tend to form varied shapes such as spherical or prolate spheroids, whose shape of the air bubble may cause a shift in resonance frequency (Feuillade and Werby, 1994).

5.3.3. Fish volume prediction and estimation

Because of resonance occurrence, pressure increases occur in the sample cavity. This leads to deflection of the resonator walls leading to small changes in the volume of the sample cavity. To precisely estimate the volume of samples in such an aquatic tank, we need to account for these losses as the model assumes a rigid resonator wall. By compensating for these losses, the accuracy of the model is improved and samples' volume can be estimated (Njane et al., 2018). The deflection in the sample cavity of the resonator's walls are accounted for as E_{r2} (Pa) and Fig. 5.7 (a) and (b) show the resonator's deflection with increased volume of both air and fish respectively. When air volume was increased from 0.2 m to 0.4 mL a sudden drop in resonator deflection was observed. The sudden increased air volume leads to more damping hence reduced resonance frequency and decreased amplitude. As a result, the total bulk modulus of the sample cavity decreases hence making the resonator wall less rigid, thus resulting in a drop in the resonator wall's deflection. However, when successive cumulative air volume is added into the resonator's cavity, the deflection of the resonator walls occurs gradually as most of the sound energy is damped by the air bubbles and hence reduced pressure changes. An average deflection of the resonator's cavity, E_{r2} of 8 $\times 10^5$ Pa was obtained when air bubbles were present in the resonator's cavity.

However, with increased volume of fish in the resonator's cavity, there was an initial gradual increase in the resonator's deflection followed by a gradual decrease as shown in Fig. 5. 7 (b). With the initial increase of fish samples into the sample cavity, the effective volume of the sample cavity was reduced due to the volume occupied by the fish in the sample cavity. This resulted in increased pressure in the sample cavity thus making the walls of the resonator stiffer. As a result, there was increased resonator deflection with increased volume of fish. However, with more fish samples in the resonator, the sensitivity of the resonator decreases, and the walls of the resonator tends to be less stiff leading to decreased deflection of the resonator walls. An average E_{r2} value of 2.6 $\times 10^3$ Pa was obtained and was much lesser than that of air bubbles. This is because unlike air bubbles, which mainly consist of air and a thin membrane enclosing the air bubble, the fish also consist of a more elastic swim bladder, fish muscle and bones that increase the stiffness of the fish thus a higher bulk modulus leading to a reduced resonator's deflection.

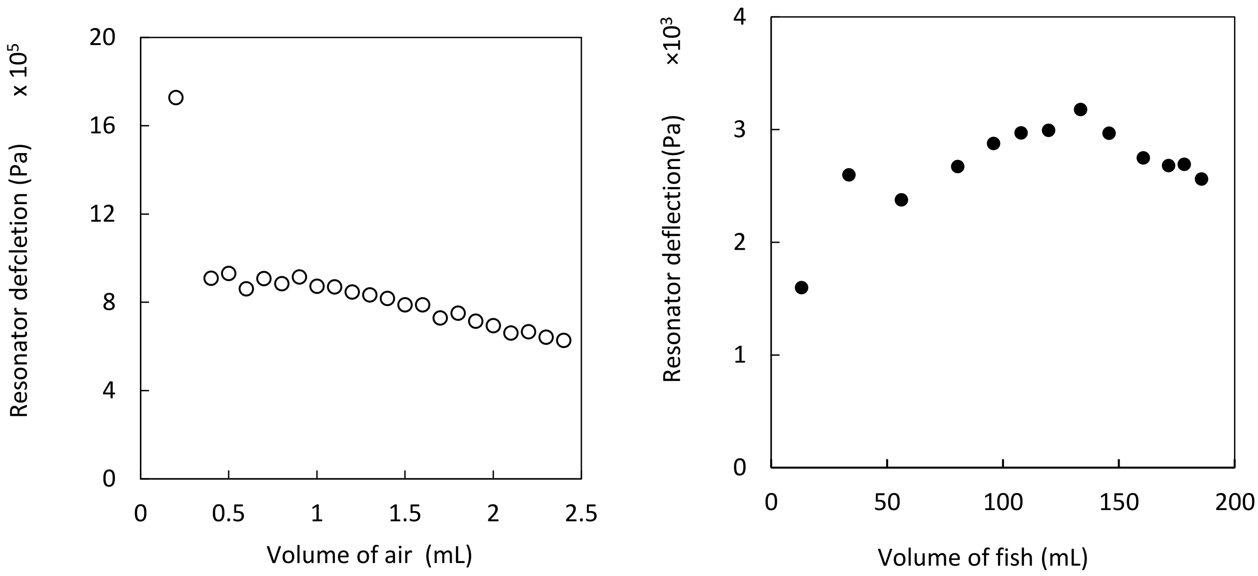

(a) (b)

Fig. 5.7. Sample cavity deflection (a) with increased volume of air and (b) with increased volume of fish.

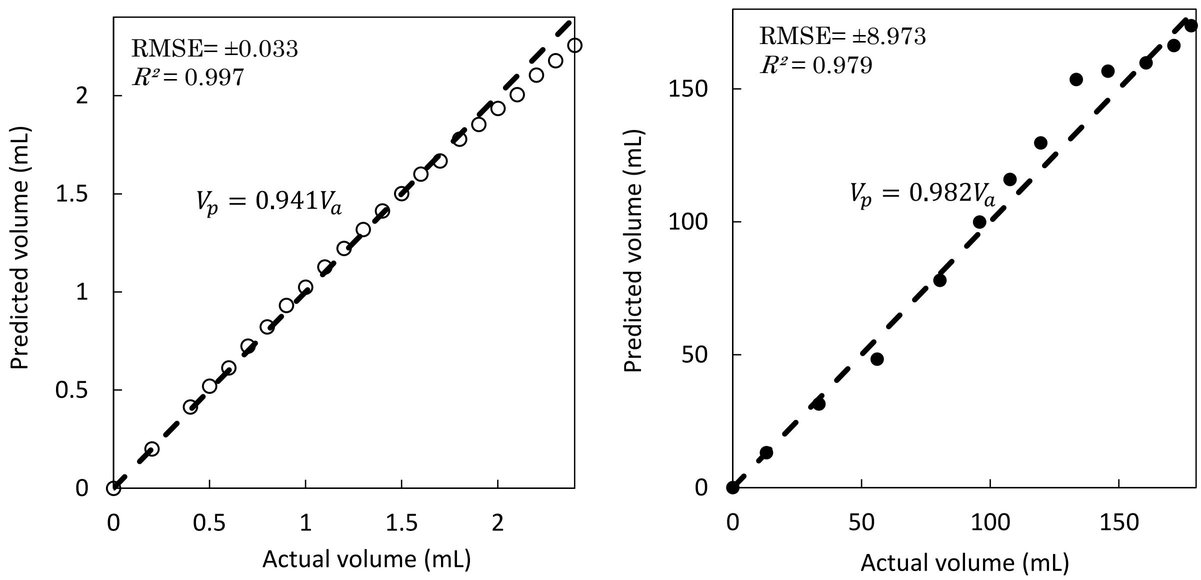

(a) (b)

Fig. 5.8. Predicted volume and the actual volume of (a) air and (b) fish using Helmholtz resonance technique.

By accounting for the deflection losses on the walls of the resonator, the volume of air and fish can be predicted as shown below in Fig. 5.8 (a) and (b) respectively. The linear regression model results between the actual and the predicted volume of both air and fish were as shown in Table. 5.1. In both the air bubbles and the fish, a high linear correlation between the actual and the predicted volume was obtained.

Table 5.1 Linear regression model results of closed cavity resonator.

Fish	R^2	RMSE (mL)	Coefficients
Air bubbles	0.997	± 0.033	0.941
Japanese dace fish	0.979	± 8.973	0.982

However, to improve the model, a higher cavity to sample volume ratio would not only increase the number of samples to be estimated but would also result to a higher sensitivity for resonance frequency change hence increased precision.

5.3.4. Top of the cavity diameter variation with resonance frequency

The effect of the changing the dimeter of the opening on the top of the resonator with resonance frequency change was investigated as shown below in Fig. 5.9. As the diameter of the opening increased from 15 to 23 mm the resonance frequency increased as shown in Fig. 5.9 (a). For every 1 mm change in the diameter of the opening results a 1 Hz change in resonance frequency was observed. The acoustic pressure accumulating in the sample cavity is lost through the wide opening on the top of the resonator. This decreases the damping of the resonator leading to decreased amplitude and increased resonance frequency. Cai et al., (2017) showed that altering the dimensions of such openings is an effective way of controlling the resonance frequency without modifying the cavity volume. Similar to the empirical model derivations and the Helmholtz resonance principles, as the volume of air increased, resonance frequency decreased in all openings as shown in Fig. 5.9 (b). Air, which is less dense than water has a bulk modulus less than water, leading to decreased resonance frequency with increased volume of air. Similar to our findings, Chanaud (1994) observed that as the orifice area of Helmholtz resonator increased, resonance frequency increased. In the future, although a wider opening of the resonator would be preferred for larger fish insertion, a trade-off must be made more energy is lost leading to peaks with low amplitude.

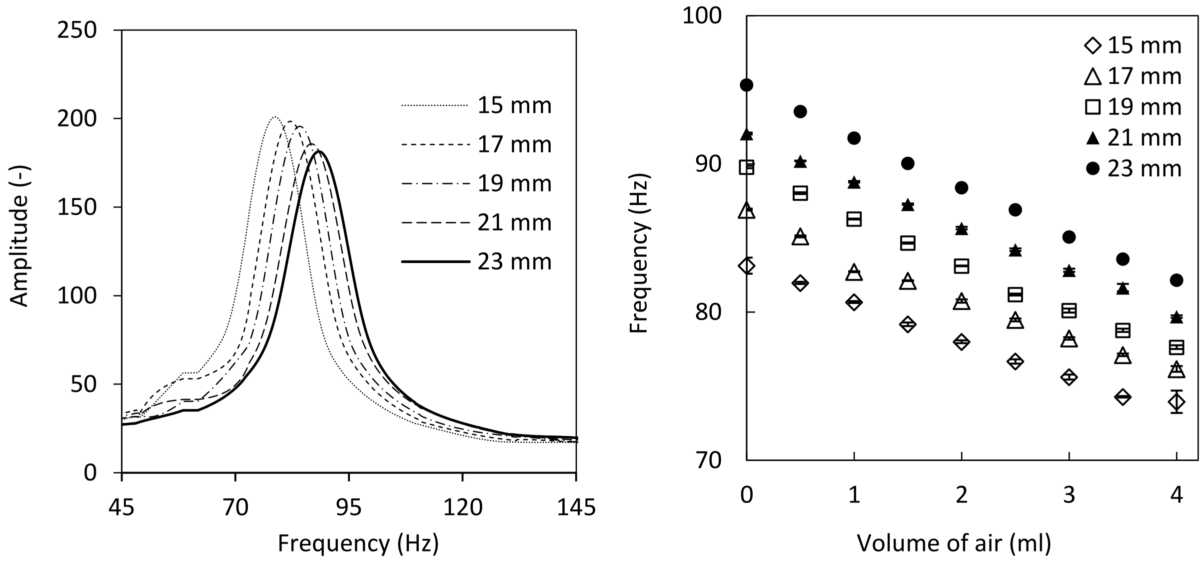

(a) (b)

Fig. 5.9. Varying diameter of the opening (a) resonance frequency increased while amplitude decreased (b) while resonance frequency increased with increased diameter of the opening, in all openings, resonance frequency decreased with increased volume of air.

5.4. Conclusion

A double-cavity-based Helmholtz resonator for inland aquatic tanks was proposed and prototyped. The resonator consisted of a speaker-attached generating cavity that was connected to the side of an aquarium tank for total fish volume measurement. A chirp wave signal was generated, resonance occurred in the sample cavity and the resonated sound was captured by a hydrophone inserted into the sample cavity. As the volume of fish increased, resonance frequency decreased due to the presence of swim bladder intact the fish. A high linear correlation between the actual and the predicted volume of fish was obtained. However, due to decreased effectively volume of the sample cavity, a lower sensitivity was obtained for larger fish volume. Although, in this research an acrylic type sample cavity with a capacity of 4.913 L could precisely estimate the total volume of about 133 mL, in the future, a larger cavity to sample volume ratio would increase the sensitivity for more fish volume to be estimated. Furthermore, the effect of the opening on top of the aquarium cavity was investigated. As the diameter of the opening increased, resonance frequency increased due to increased cavity stiffness. The use of double-cavity based resonators for open aquatic tank has potential for precise fish volume estimation.

References

Cai, C., Mak, C.-M., Shi, X., 2017. An extended neck versus a spiral neck of the Helmholtz resonator. Applied Acoustics, 115, 74–80.

Chanaud, R.C., 1994. Effects of geometry on the resonance frequency of Helmholtz resonators. Journal of Sound Vibration, 178, 337–348.

Chapman, R.P., Marshall, J.R., 1966. Reverberation from deep scattering layers in the Western North Atlantic. The Journal of the Acoustical Society of America, 40, 405–411.

Didenkulov, I., Martyanov, A.A., Pronchatov-Rubtsov, N., 2015. Interaction of acoustic waves with moving bubbles. Proceedings Meeting on Acoustics, 24, 045005.

Ellis, T., North, B., Scott, A.P., Bromage, N. R., Porter, M., Gadd, D., 2002. The relationships between stocking density and welfare in farmed rainbow trout. Journal of Fish Biology, 61, 493–531.

Feuillade, C., Nero, R.W., 1998. A viscous-elastic swim bladder model for describing enhanced-frequency resonance scattering from fish. The Journal of the Acoustical Society of America, 103, 3245–3255.

Feuillade, C., Werby, M.F., 1994. Resonances of deformed gas bubbles in liquids. The Journal of the Acoustical Society of America, 96, 3684–3692.

Fine, M.L., King, T.L., Ali, H., Sidker, N., Cameron, T.M., 2016. Wall structure and material properties cause viscous damping of swim bladder sounds in the oyster toadfish (*Opsanus tau*). Proceedings of the Royal Society of Biology, 283, 20161094.

Logan, S.H., Johnston, W.E., 1992. Economics of commercial trout production. Aquaculture, The Rainbow Trout, 100, 25–46.

Love, R.H., 1978. Resonant acoustic scattering by swim bladder-bearing fish. The Journal of the Acoustical Society of America, 64, 571–580.

MacLennan, D.N., 1990. Acoustical measurement of fish abundance. The Journal of the Acoustical Society of America., 87, 1–15.

Njane, S.N., Shinohara, Y., Kondo, N., Ogawa, Y., Suzuki, T., Nishizu, T., 2019. Underwater fish volume estimation using closed and open cavity Helmholtz resonators. Journal of Engineering in Agriculture Environment and Food, 12, 81–88.

Njane, S.N., Shinohara, Y., Kondo, N., Ogawa, Y., Suzuki, T., Nishizu, T., 2018. Improved underwater Helmholtz resonator with an open cavity for sample volume estimation. Journal of Computer and Electronics in Agriculture, 147, 18–26.

Papoutsoglou, S.E., Papaparaskeva-Papoutsoglou, E., Alexis, M.N., 1987. Effect of density on growth rate and production of rainbow trout (*Salmo gairdneri* Rich.) over a full rearing period. Aquaculture, 66, 9–17.

Raveau, M., Feuillade, C., 2016. Resonance scattering by fish schools: A comparison of two models. Journal of the Acoustical Society of America, 139, 163–175.

Sand, O., Hawkins, A.D., 1973. Acoustic properties of the cod swim bladder. Journal of Experiment Biology, 58, 797–820.

Shafait, F., Harvey, E.S., Shortis, M.R., Mian, A., Ravanbakhsh, M., Seager, J.W., Culverhouse, P.F., Cline, D.E., Edgington, D.R., 2017. Towards automating underwater measurement of fish length: A comparison of semi-automatic and manual stereo–video measurements. ICES J. Marine Science, 74, 1690–1701.

Taylor, G.K., Holbrook, R.I., de Perera, T.B., 2010. Fractional rate of change of swim-bladder volume is reliably related to absolute depth during vertical displacements in teleost fish. Journal of the Royal Society Interface, 7, 1379–1382.

Whitehead, P.J.P., Blaxter, J.H.S., 1989. Swim bladder form in clupeoid fishes. Zool. Journal of the Linnean Society, 97, 299–372.

Williams, K., Lauffenburger, N., Chuang, M.-C., Hwang, J.-N., Towler, R., 2016. Automated measurements of fish within a trawl using stereo images from a Camera-Trawl device (CamTrawl). Methods in Oceanography. Special section on Novel instrumentation in Oceanography: a dedication to Rob Pinkel, 17, 138–152.

Zion, B., Shklyar, A., Karplus, I., 1999. Sorting fish by computer vision. Journal of Computer and Electronics in Agriculture, 23, 175–187.

Chapter VI

Conclusion and future plan

6.1. All conclusion

The precise estimation of the volume of fish using underwater Helmholtz resonator in an open cavity resonator was established. Such an open cavity can improve the limitations of a closed cavity resonator as samples have to be inserted and the resonator closed before measurement commences. However, in an open cavity resonator samples volume can be measured without the need to close the cavity of the resonator and could act as inlet for fish in the future. Firstly, a water reed technique where water flowing through the nozzle was directed to an edge attached on the neck of both the closed and open cavity resonators for resonance generation. Unlike the closed cavity resonator which was marred by jumps in resonance frequency and high modes of vibration leading to less range of resonance frequency generation, open cavity resonator had less jumps in resonance frequency coupled with fewer mode of vibration hence a wide range of flow velocities could be utilised for resonance generation, when flow was varied on both resonators. An optimised flow speed of 4 L/min and 14 L/min was utilised for the closed and open cavity respectively. Both the simulation of the empirical models and experimental validation demonstrated that the open cavity resonators could measure aquatic samples with the same degree as the closed cavity resonator. As the volume of glass balls, a representative of denser samples increased, resonance frequency increased in both closed and open cavity resonators. As the volume of air (less dens than water) increased, resonance frequency decreased. Similar to air, as the volume of Japanese rice fish (*Oryzias latipes*) increased, resonance frequency decreased in both closed and open cavity resonators and a high linear correlation with an R^2 of 0.99 could be obtained in both resonators between the actual and predicted volume of fish. Furthermore, higher resonance frequencies were observed in the open cavity resonator due to increased cavity stiffness because of energy loss through the open holes. However, the closed cavity resonator was limited as samples had to be inserted and resonator closed for measurement to commence. However, the open cavity resonator could overcome the limitations of a closed cavity since samples could be measured without the need to close or lock the cavity. Furthermore, such an improved open cavity can be utilised for future automatic sample volume estimation. However, water reed technique, was marred by water fluctuations thus leading to fluctuating frequencies. Furthermore, such a technique could damage the fish muscle especially where high flows are utilised in open resonator cavities.

To overcome this limitation, Helmholtz resonance generation using speaker's impedance technique was proposed and utilised for aquatic sample volume estimation. Empirical models indicated that the double cavity resonator acts as mass with two springs leading to resonance occurring in the sample cavity. As a proof of concept, a cylindrical stainless-steel double cavity resonator consisting of a generating cavity and a sample cavity connected by a neck was designed and fabricated. A chirp wave (sweep frequency) signal generated by an underwater speaker attached onto the generating cavity was excited and by measuring the impedance of the speaker because of vibration of the diaphragm on the membrane of the speaker, resonance frequency was obtained. To develop the model and validate experimentally, air bubbles, which have acoustic properties similar to fish, were inserted into the sample cavity and as the volume of air increased resonance frequency decreased, similar to the empirical model simulation. A high linear correlation between the actual and predicted volume of air with an R^2 of 0.99 was obtained between the actual and predicted volume of air. To optimise the resonator for higher sensitivity, the neck length and cross-sectional area were varied. Not only did a neck with a large cross-sectional area and a shorter neck length have higher sensitivity due to higher frequency, but also it is economical in the reduction of the material used to fabricate such necks. However, utilising a stainless-steel sample cavity is expensive to fabricate and for actual utilisation.

As an improvement of the double cavity Helmholtz resonator, an acrylic sample cavity was utilised for fish volume estimation. The acrylic cavity was not only light and cheaper to fabricate, a step closer to commercialisation and practicability, but also by directly placing the generating cavity on top of the sample cavity resulted in higher frequency and increased sensitivity for measurement. As the volume of both Japanese dace fish (*Tribolodon hakonensis*) with average volume of 13.7 ± 2.5 mL and Japanese rice fish (*Oryzias latipes*) with an average volume of 0.27 ± 0.15 mL increased, resonance frequency decreased. This was attributed to the presence of gas in the swim bladder intact the teleost fishes. Furthermore, it was also observed that resonance was also contributed by other parts of the fish such as the fish bones and fish flesh. Not only were the fish parameters important in the precise estimation of fish volume, but also accounting for the losses because of the deflection on the walls of the resonator resulted in higher estimation accuracies. Both the Japanese dace fish and the Japanese rice fish could be precisely estimated with a high accuracy and a linear coefficient of R^2 of 0.995 and 0.985 respectively, between the actual and predicted volume of both fishes was obtained.

The precise estimation of total fish volume in inland aquatic tanks using Helmholtz resonator was established. A generating cavity filled with water and connected to a speaker was attached onto the side of a 4.91 L acrylic tank, which was open on top using a neck. A chirp wave signal, generated from the speaker, was sent from the generating cavity to the sample cavity. To capture the resonated sound, a hydrophone was inserted into the open tank and as the volume of the Japanese dace fish (*Tribolodon hakonensis*) increased, resonance frequency decreased, and amplitude also decreased. The swim bladder present in the fish not only lead to resonance thus reduced frequency, but also such swim bladder lead to damping of sound leading to reduced amplitude. Furthermore, as a lead on optimisation of such open tanks, the effect of increased cross-sectional area with resonance frequency was investigated. As the cross-sectional area increased, resonance frequency increased. However, since for resonance occurrence, increased pressure from the cavity walls is vital, increasing the opening hole size of such resonators leads to increased pressure losses and energy losses. This results in decreased amplitude thus low resonance peaks. We propose an allowance between the cavity wall and hole opening to limit the energy loss leading to increased resonance in such open cavities.

6.2. Research contribution and expected outcome

The use of underwater Helmholtz resonator is not only fast and precise but could also be cost friendly considering the high cost of excessive feed utilized. In Japan, similar to worldwide trend, the growth of aquaculture has been increasing unlike the wild capture fisheries. The development of this technique has a niche market in Japan where fresh water fishes such as eels are reared by approximately 3000 farmers in 5000 ponds and marine aquaculture is practised by approximately 15,000 farmers with 300,000 cages and 100 buildings. With the development of IoT infrastructure, this technique can be utilised and spread to the world where aquaculture production is at 100 million tonnes/year (that is, 80 times that of Japan), which produces about 1.3 million tonnes/year. Furthermore, this technique has attracted the attention of several companies who regularly visit our lab where we hold discussions on possible commercialisation. If the utilization of Helmholtz resonator for instantaneous and frequent monitoring of cultured fish growth is successful, then there is a possibility to develop optimal feeding plans based on each species growth model and their optimal landing plan too. By measuring the volume of fish, the quality of the fish can be controlled through effective feeding thus ensuring high quality fish meat, as the demand is rapidly increasing. Furthermore, this can subsequently help in the early detection of any abnormalities in the water or the prevalence of a disease and hence mitigation. Subsequently, each fish has unique acoustic characteristics, leading to specific resonance frequency tendencies.

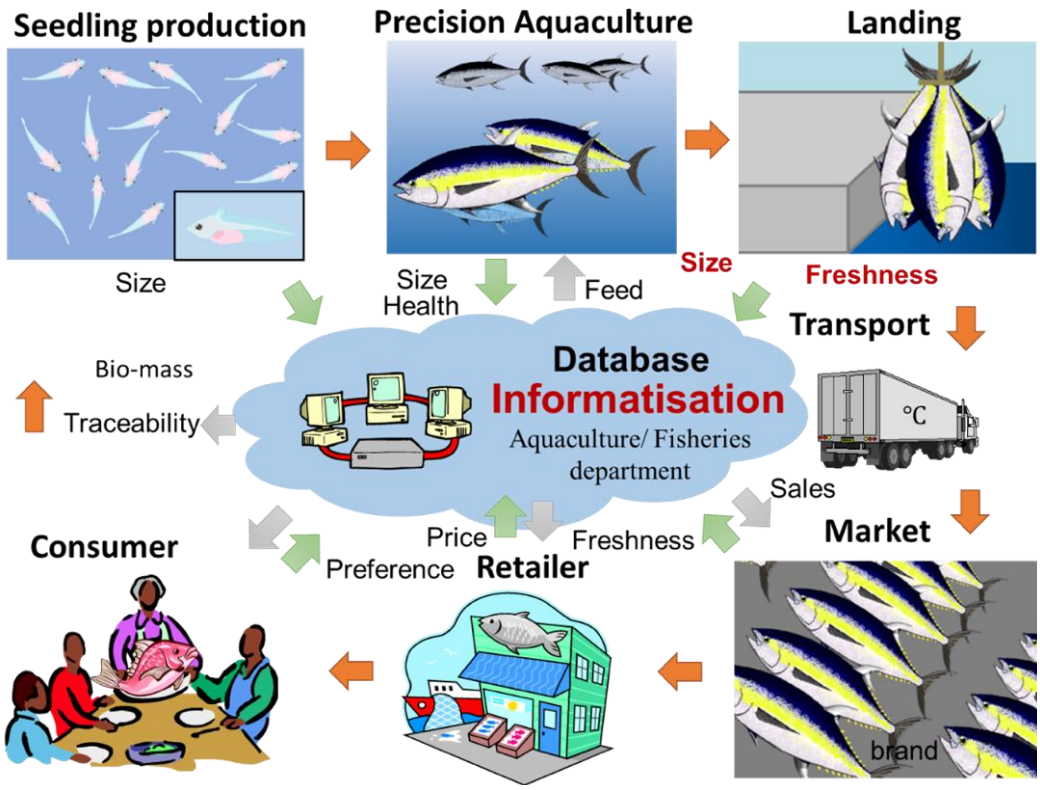

Fig. 6.1. Informatisation of fisheries and aquaculture by developing a database with information about the fish from seedling, to maturity, landing, marketing and to consumer and back.

While some fish such as the flounder have a very small air bladder, most teleost have a swim bladder that accounts to 5-10 % of the fish total volume. The swim bladder, a hydrostatic organ that controls the position of fish in water is also a resonant feature that pulsates when resonance frequency is incident. Therefore, by determining the resonance frequency property of each fish, thus determining their volume and their growth models, we can develop a database for these fishes hence achieve optimal feeding of each fish. This database consisting of various fishes will be key in the development of precision aquaculture and smart aquaculture thus achieving the informatisation of aquaculture as shown in Fig. 6.1.

Furthermore, the determination of the volume of fish in the offshore cages can be recorded in the database and in conjunction with GIS (Geographical Information Systems) information, the relationship between certain fish species and their environmental conditions can be determined. It is also expected that this technology will also contribute to the understanding of global warming, thus mitigating climate change.

6.3. Future plan

6.3.1. Simulation of actual practical application for total fish volume estimation in tanks

Although we could develop a technique to estimate the volume of fish in inland aquatic tanks, the size of such a tank was limited to 4.91 L. For actual application and realisation of commercialisation, larger tanks or cages are utilised in the rearing of inland aquatic species such as Japanese eel-fish, yellowtail and other fish species as well (Fig. 6.2).

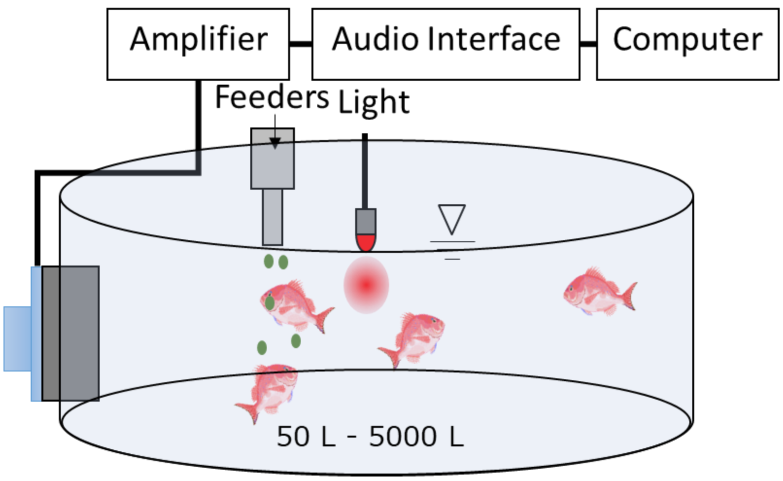

Fig. 6.2. Illustration of the upscaled inland tank for total fish volume estimation. The generating cavity with speaker attached to it is placed on the side of the aquatic tank where total fish volume is measured.

Thus, it is paramount to upscale the resonator in the actual application size for fish volume estimation. To do this, step-wise upscaling is necessary to determine the relationship between tank size and the fish size for optimum sensitivity. Firstly, it is imperative to simulate the empirical models and optimise the tank size for specific fish total volume target. Initially preliminary results indicate that the larger the tank size, the lower the frequency. However, the effect of lower amplitude and lower peak is also expected due to lower resonance occurrence in large tanks from the experiments. Therefore, the step-wise upscaling of Helmholtz resonators for practical application is paramount. Firstly, we will confirm the mechanism of resonance occurrence in these tanks by understanding the relationship between frequency and volume of the tanks. From the resonance occurrence, we will determine the optimum cavity to fish volume ratio for highly sensitive measurement.

To upscale, we began by first simulating the effect of larger tank volume from 10, 20 up to 50 L as shown in Fig. 6.3 (a).

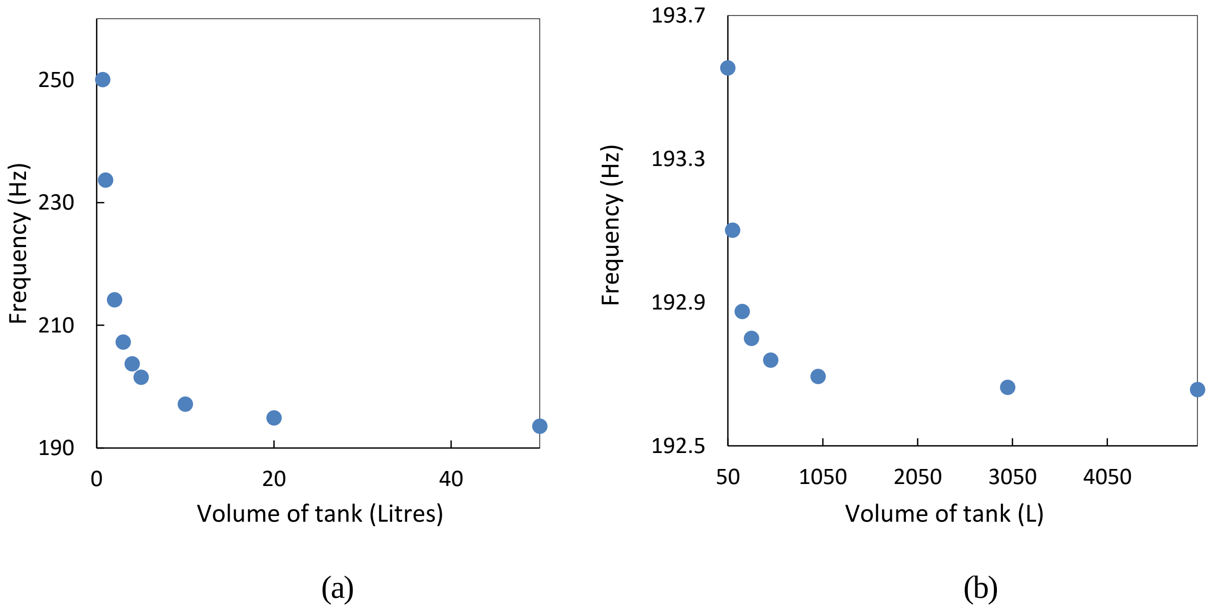

Fig. 6.3. Simulation of frequency against the volume of tank (a) from 0.68 -50 L and (b) from 50-5000 L tanks.

There was a rapid drop in resonance frequency from 250 – 197.13 Hz when the volume of the tank increased from 1 L to 10 L, after which a gradual drop in resonance frequency occurred until a volume of 50 L. With increased volume of the tank i.e. from 50 L to 1000L tank, rapid drop in resonance frequency from 193.55 Hz to 192.7 Hz was observed as shown in Fig. 6.3 (b). However, such a change in resonance frequency was smaller in comparison with the proportionate change in the volume of the tank. Larger tank volume ranging from 1000 L to 5000L, depicted a gradual decrease in resonance frequency, as shown in Fig. 6.3 (b).

Similarly, the effect of increased volume of fish in the different tank volume was simulated as shown in Fig. 6.4. It can be clearly observed that as the volume of the tank increased, resonance frequency decreased with increased volume of fish. Furthermore, the sensitivity of measurement of total fish volume decreased with increased volume of tank volume. For larger tank volume, a larger fish volume is necessary for highly sensitive measurements. However, the deflection of the resonator and the material of the resonating tank may influence these frequencies tendencies hence in the future, comparison of simulation with experimental results through step-wise upscaling is paramount for optimised fish volume measurement.

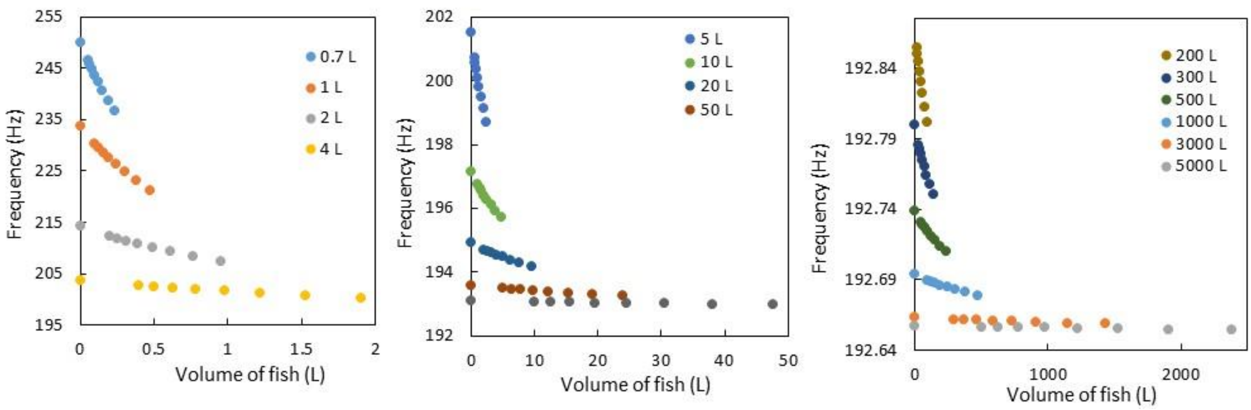

Fig. 6.4. Resonance frequency change with increased volume of fish in varying tank volume from 0.7- 5000 L.

6.3.2. Future actual experimental set up for larger fish volume estimation – a case study of yellow tail

To demonstrate the set-up for future inland aquaculture measurements, a 1000 L tank was set-up for yellowtail fish volume measurement as shown in Fig. 6.5 (a). The objective of the experiment was to measure the volume of citrus peel-mixed fed yellow tail fish volume at Ehime fisheries research centre. This is because in Ehime, the growing of citrus is very popular and lately there has been a surge in the mixing of fish feed with citrus peels for yellowtail fish in aquaculture. Such feeding is done in the last two weeks before landing the fish and as a result, citrus flavour can be tasted when the raw fish is eaten as "sashimi" or "sushi", compared to the normal fed fish. Yellow tail fish was landed from the cages and inserted into the experimental set-up shown in Fig. 6.5 (a). The length and weight of the citrus fed fish was measured in comparison to the normal fed-fish as shown in Fig. 6.5 (b). However, it should be noted that only the citrus-fed fish was measured since it was alive. The normal fed fish was already dead thus volume was not measured and only the weight and length were recorded.

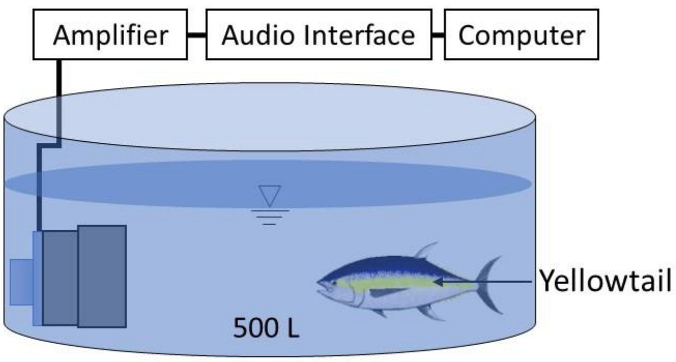

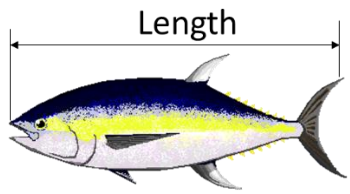

Parameter	Normal-fed	Citrus-fed
Weight (Kg)	5.5	9.055
Length (mm)	607.2	760
Location	Farmer	Ehime Fish. R.C

(a) (b)

Fig. 6.5. Experimental set-up for the yellowtail fish measurement (a) in a 1000 L tank, half-filled with water and (b) the specifications of the citrus-fed yellow tail fish compared to the normal fed fish.

The fish was landed from the cages nearby where they were kept and fed usually for 2 years. After landing the fish was placed inside a half-filled in the 1000 L tank (thus total water volume was approximately 500 L) as shown in Fig. 6.6. The generating cavity was set-up facing eastwards inside the tank as shown in Fig. 6.5 (a) and a sinusoidal chirp wave was generated and captured suing the speaker impedance technique (Fig. 6.7).

Fig. 6.6. Experimental demonstration for yellow tail fish volume measurement. Where: 1 is the cages where yellow tail fish are kept. 2 shows filling up of the 1000 L tank half with sea water. 3 experimental measurement in progress. 4 shows the fish with less movement in the water thus enabling measurement. 5 the fish was killed by stabbing and swim bladder was observed in 6.

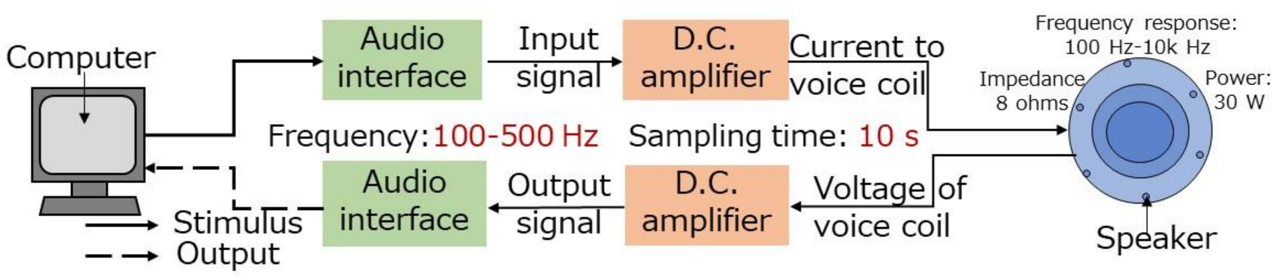

Fig. 6.7. Speaker impedance technique for generating sinusoidal chirp wave and capturing resonance frequency.

A shift in resonance frequency was observed after the yellowtail fish was inserted into the tank as shown in Fig. 6.8 (a). A decrease in the peak amplitude also was observed when the fish was placed inside the tank.

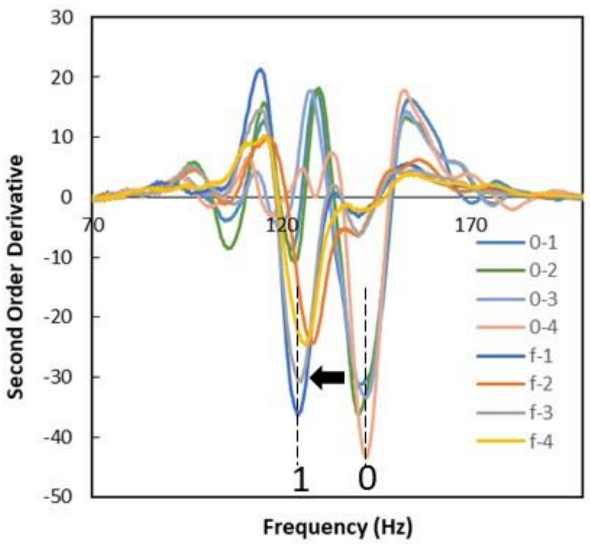

(a)

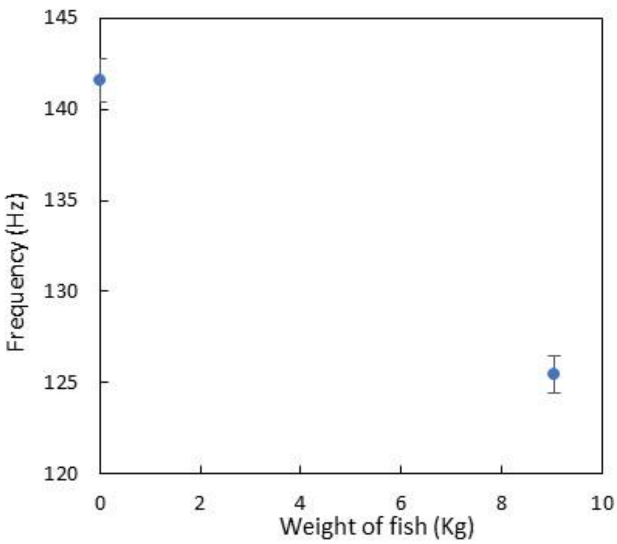

(b)

Fig. 6.8. Spectral property before -0 and after fish was inserted into the tank-1 (a) frequency shifted and amplitude decreased (b) resonance frequency decreased when the fish was inserted into the tank.

As a result of the change in the bulk modulus in the tank when the fish was inserted, resonance frequency shifted and decreased from 143 Hz to 125 Hz when a 9 kg yellowtail fish was measured as shown in Fig. 6.8 (b). This was due to the presence of the air in the swim bladder of the yellowtail fish, thus resulting in decreased bulk modulus of the fish. For samples less dense than water, such as air or fish, as the volume of the fish increases in the tank, the resonance frequency decreases. Furthermore, such a swim bladder which has air leads to damping of the acoustic signal thus leading to amplitude decreases. In the future, more fish volume is necessary to determine the limit of sensitivity of measurement in such large tanks.

Another important factor is the material selection of the resonator. Lately, aqua culturalists and fish farmers have been using softer tank materials such as tarpaulin. This is cost friendly to the farmers and easy to repair and maintain. However, utilization of such softer materials as Helmholtz resonators would attenuate all the sound leading to low resonance occurrence. Therefore, we aim to reinforce the inner lining of softer tanks with thin sheets made from acrylic.

Another important factor is the specification of the speaker for resonance frequency generation. From the empirical model simulations, the larger the tank volume, the lower resonance frequency. Although in the current experiments, the speaker with frequency sensitivity range of 100 Hz- 10 kHz was utilised, in the future speaker with much lower sensitivity (less than 100 Hz) would be ideal for generating resonance in large tanks.

6.3.3. Open duct-type resonators for future underwater sorting and sizing of fish

Another important factor is sizing and sorting underwater. Normally landed fish vary in size due to the variation in feeding patterns, even in fish of similar species. Until today, farmers must harvest all their fish include the smaller ones and they cannot return the smaller fish back to the water as they normally die a short while after landing. It is thus necessary to sort the fish underwater before harvesting to ensure the smaller-sized fish can still grow and be harvested later. Furthermore, such an underwater sorting system can be used when transferring fish to other cages and determine their size hence help in stock taking. In the future, feeding patterns based on size differentiation are also possible. Therefore, an underwater Helmholtz resonator with an open duct would provide the potential for underwater sizing and sorting of fish.

To do this it is important to optimise the hole size for fish volume measurement. For open duct-type resonators, the larger the hole size, the higher the frequency. However, since resonance is based on vibration of cavity walls, increasing the hole size leads to energy losses through the opening. This intern leads to reduced resonance and hence lower amplitude. It is thus important to analyse the optimum hole size for considerable resonance and optimised amplitude for fish volume estimation.

The conditioning of fish to pass through the opening whilst measuring the volume of the fish could be optimised for sizing and sorting of fish underwater. Fish can learn to associate feeding with certain sound frequencies (below 1000 Hz), therefore by conditioning the fish to pass through the orifice, we can also estimate the fish volume, while ensuring optimum feed utilisation. In the future, sound can be generated, and as the fish passes through the hole from one tank (resting tank) to the feeding tank, their volume can be measured as shown in Fig. 6.9, thus enabling real-time sorting and size estimation.

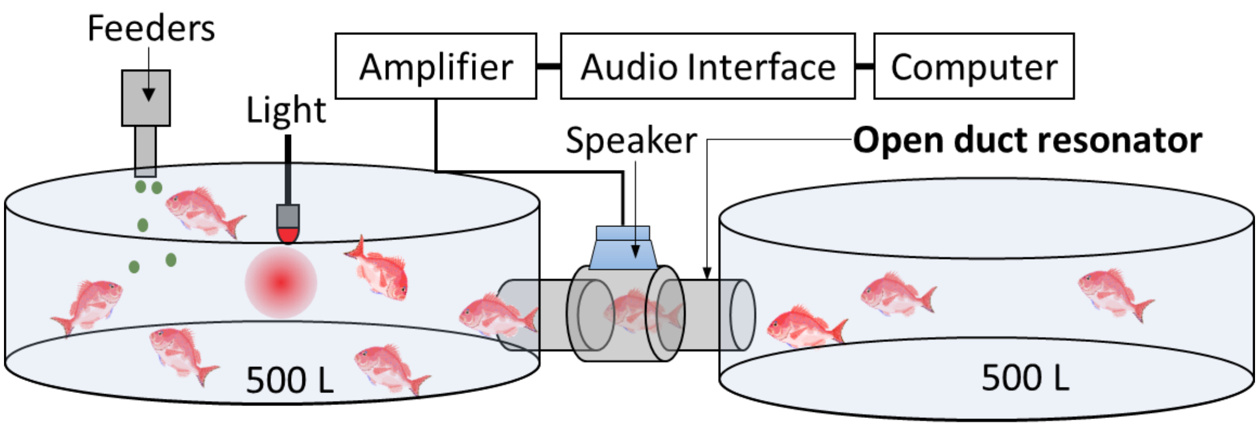

Fig. 6.9. Two tanks connected by an open-duct type resonator that enables underwater sizing and sorting of fish. Feeding can also be used as the reward for fish when conditioning to pass through the open-duct hole.

6.3.4. Effects of precision farming based on volume estimation on meat quality

Furthermore, not only does effective feeding affect the size of the fish (volume) but also the quality of the fish. Consumers not only prefer fresh fish but also tender with high lipid content. Lipids are known to be energy reserves, thus regulate body density and can be utilized as a potential indicator for size, growth and development thus enabling farmers to sort, size and sale their fish. Furthermore, lipids distribution and quantity affect the taste and fish oil containing omega-3 polyunsaturated fatty acids (PUFA's), has vast health benefits. In the future, the effect of controlled feeding on the volume of the fish will be important in monitoring the volume of fish to ensure high quality fish production. Continuously monitoring and estimating the volume of fish using underwater Helmholtz resonator would thus be correlated with the feeding pattern and ultimately the quality of the fish.

Acknowledgement

This study was supported by the funds from JSPS KAKENHI Grant number [15K14834] from the Ministry of Education, Culture, Sports, Science and Technology. Furthermore, the upscaling of the research to larger resonators was supported by the GAP Fund, Grant number [207010] that has helped propel thus research.

I would like to express my utmost sincere gratitude to Professor Naoshi Kondo of the Laboratory of Bio-Sensing Engineering for the opportunity to research on precise fish volume estimation using underwater Helmholtz resonance, a topic I explored since my master's degree. I am grateful that he welcomed me to Japan and to the lab of Bio-Sensing Engineering, Kyoto University where the environment was conducive for my study. We would also like to thank the associate Professor Yuichi Ogawa and the assistant professor Tetsuhito Suzuki for immense advice and support during the study. I would also like to recognize the overwhelming support from Professor Takahisa Nishizu from Gifu university for the much helpful discussions during the period of the study. We also acknowledge Professor T. Shiigi from National fisheries university for helpful advice while conducting experiments. We are indebted to Fukushin-denki company for the valuable advice and support to make the Helmholtz resonator devices and to Kyoto Prefecture, Fisheries Department for lending us some of the devices to conduct experiments. We are also thankful to Professor Garry Piller from the Graduate School of Agriculture for always proof reading our manuscripts. I would like to specially thank the MEXT (Ministry of Education, Culture, Sports, Science and Technology) for the 5-year scholarship awarded during my study, from master's degree to PhD degree.

This research would not have been possible if it were not for the unwavering support of my colleague Kohei Ogata, and the entire sound team members. Furthermore, I am very grateful for the support and helpful advice I got from the lab members during the lab seminars and presentations.

We cannot forget the effort and the sacrifice made by my family in Kenya, led by my mum and the entire Njane family for the daily prayers and support during my stay here in Japan. I am forever grateful for your support and prayers.

Lastly, I would also like to specially thank the Sugino family which has been a dear family to me during my stay here in Kyoto. Their warmth, love and overwhelming support has enabled me to stay here in Kyoto comfortably and propel my research with an intangible great understanding of the Japanese culture and norms.

Njane Stephen Njehia

June 2019.

List of publications

Peer reviewed journal

1. **S. N. Njane**, Y. Shinohara, N. Kondo, Y. Ogawa, T. Suzuki and T. Nishizu, "Underwater fish volume estimation using closed and open cavity Helmholtz resonators" Engineering in Agriculture, Environment and Food, 12 (1) 81-88, January 2019.
2. **S. N. Njane**, Y. Shinohara, N. Kondo, Y. Ogawa, T. Suzuki and T. Nishizu, "Improved underwater Helmholtz resonator with an open cavity for sample volume estimation" Journal of Computers and Electronics in Agriculture, 147, 18-26, April 2018.
3. **S. N. Njane,** Y. Ogawa, T. Suzuki, K. Ogata, Y. Shinohara, T. Kawamura, T. Nishizu and N. Kondo, "Underwater resonator with double cavities for volumetric estimation of aquatic samples" Journal of Japanese Society of Agricultural Machinery and Food Engineers 81 (4) (*in press*)**.**
4. **S. N. Njane,** Y. Ogawa, K. Ogata, T. Suzuki, T. Kawamura, T. Nishizu and N. Kondo, "Precise fish volume estimation using underwater double cavity Helmholtz resonator" Journal of Japanese Society of Agricultural Machinery and Food Engineers (*under review*).
5. **S. N. Njane,** K. Ogata, N. Kondo, Y. Ogawa, T. Suzuki, T. Nishizu, "Fish volume estimation in an open aquarium tank using Helmholtz resonator" (under *preparation for submission*).

Proceedings

1. **Stephen N. Njane**, K. Ogata, N. Kondo, Y. Ogawa and T. Suzuki, "Precision Aquaculture: Fish volume estimation in a double cavity Helmholtz resonator". In Proceedings of the Asian Aquaculture: Bangkok, Thailand, December 2018; p 44.
2. **Njane Stephen**, Kohei Ogata, Tetsuhito Suzuki, Yuichi Ogawa, Naoshi Kondo, "Precision aquaculture for fish volume estimation".77th Joint Conference on Environmental Engineering in Agriculture: Ehime, Japan, September 2018; p 26.
3. **Njane Stephen**, Kohei Ogata, Naoshi Kondo, Yuichi Ogawa, Tetsuhito Suzuki, Harshana Habaragamuwa. "Underwater volume of samples estimation in a closed type Helmholtz resonator using impedance method". In Proceedings of the 76th annual meeting for the Japanese Society of Machinery and Food Engineers; JSAM: Tokyo, Japan, September 2017; p 103.
4. **Stephen N. Njane**, Naoshi Kondo, Yuichi Ogawa, Tetsuhito Suzuki, Habaragamuwa Harshana, "Underwater Fish Volume Estimation Using an Open Helmholtz Resonator". In proceedings of the World Aquaculture: Cape Town, South Africa, June 2017; p 16.
5. **S. N. Njane,** N. Kondo, Y. Ogawa, T. Suzuki, Shusaku Nakajima, "Underwater fish volume estimation using an open Helmholtz resonator". In Proceedings of the 75th annual meeting for the Japanese Society of Machinery and Food Engineers; JSAM: Kyoto, Japan, May 2016; p 228.
6. **Njane Stephen**, Kondo Naoshi, Ogawa Yuichi, Imai Kouki, Suzuki Tetsuhito, "Underwater Helmholtz resonance variation with temperature, salinity and flow speed". Proceedings of the 134th Regular Meeting, Kansai Brach of the Japanese Society of Machinery and Food Engineers; JSAM: Shiga, Japan, October 2015; p 98.

7. Q. Liao, T. Suzuki, Y. Shirataki, **S. Njane**, M. Kuramoto, N. Kondo, "Study on fluorescence compounds in Japanese dace fish (*Tribolodon hakonensis*) eye fluid" In proceedings of CIGR-AgENG Conference: Aarhus, Denmark, June 2016; pp1-7.

List of Patents

1. **Njane Stephen Njehia,** 近藤　直、小川　雄一、鈴木 哲仁、緒方　康平、 "インピーダンス法を用いた体積測定用ヘルムホルツ共鳴器　（京大整理番号：6252）

   発明の名称　：体積計測装置および体積計測方法

   出願番号　　：2018-167565

   出願日　　　：2018/09/07

List of awards

1. 緒方康平 , **Njane Stephen Njehia**，斎藤嘉人，西津貴久，鈴木哲仁，小川雄一，近藤直, " 水中ヘルムホルツ共鳴を用いた豆腐の力学的特性の評価" 農業食料工学会 関西支部 第139 回例会 **(Best student presentation award)**.

Appendix

Support information and experimental results

Design specification of the double cavity stainless steel resonator and UW 30 Speaker

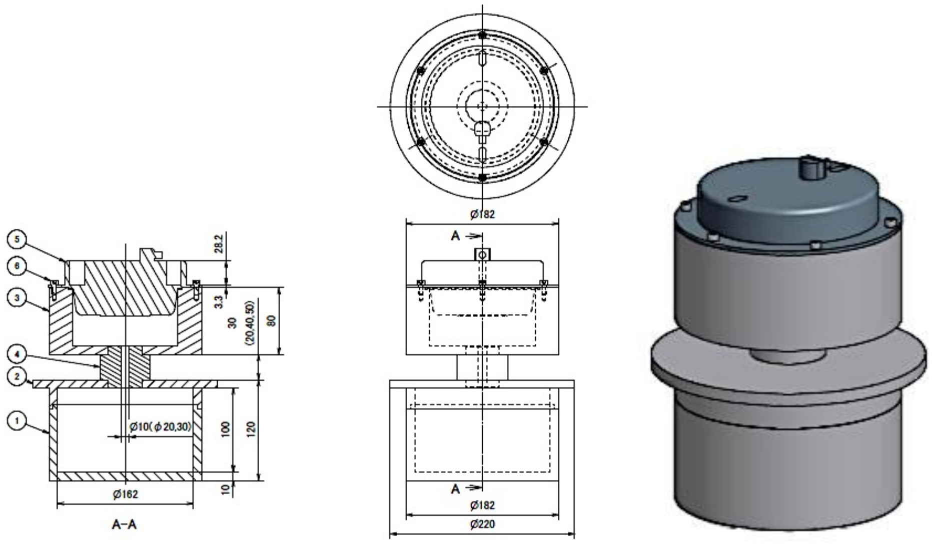

(a)

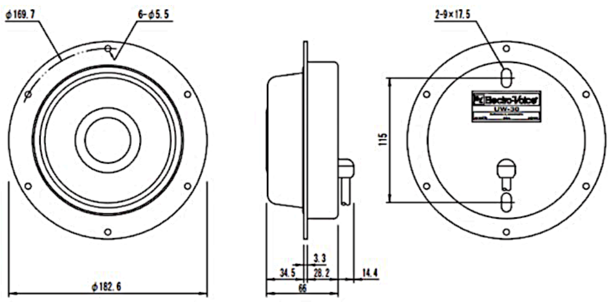

(b)

Fig. A. Diagram of stainless-steel double cavity Helmholtz resonator with speaker attached on the top cavity (generating cavity) while the lower cavity (sample cavity) is for sample volume estimation with dimensions in mm. (b) The cross-sectional diagram of the UW30 speaker with both front view and side view with dimensions in mm.

Variation of the UW-Speaker with depth in presence or absence of resonator

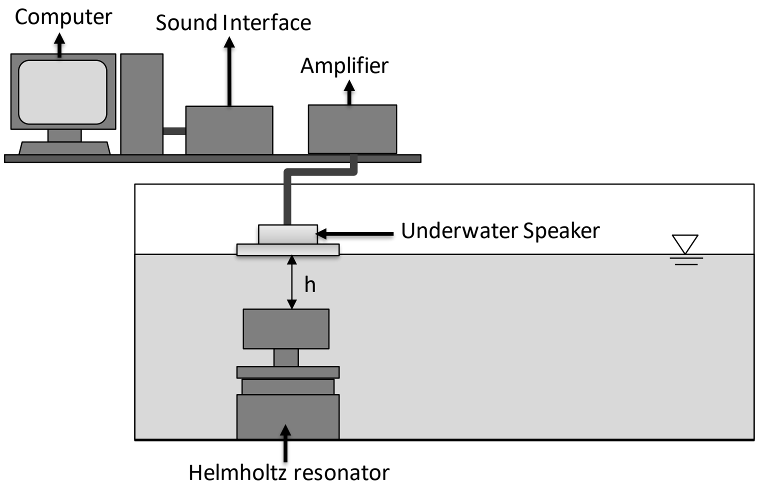

(a)

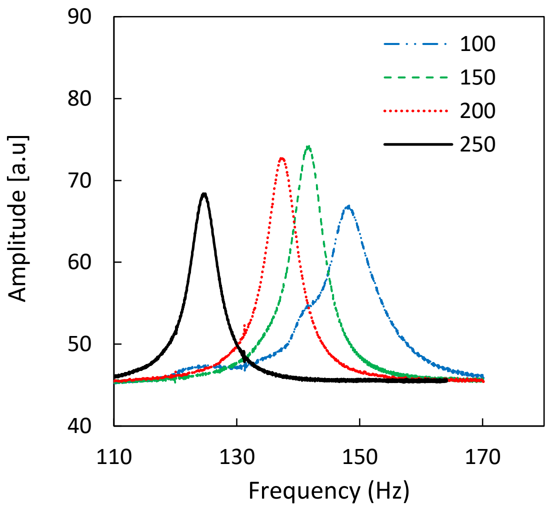

(b)

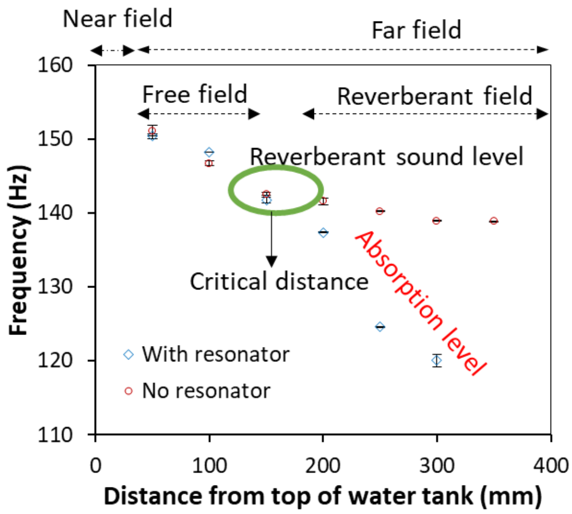

(c)

Fig. B. Set up showing the effect of (a) varying the depth of speaker in the tank, with or without the resonator underneath, in a tank of 500 mm depth. Peak amplitudes and shift of resonant frequency (b) when underwater speaker, UW30 was lowered into the water tank and the effect of resonance frequency with depth was analysed. (c) Resonance frequency vs distance with depth of the tank, from the top of water tank with or without a resonator was analysed.

Double cavity-based open Helmholtz resonator: Stainless-steel sample cavity with open necks on the side: Neck length and diameter variation with resonance frequency

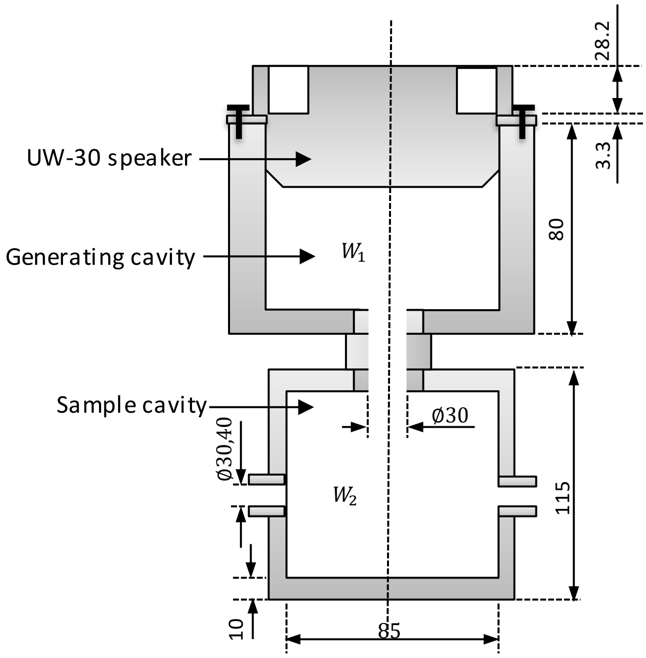

(a)

Diameter (mm)	Length (mm)
30	70
30	100
40	70
40	100

(b)

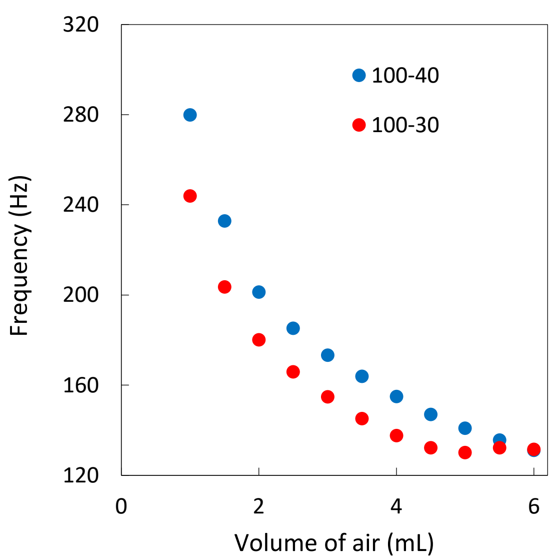

(c)

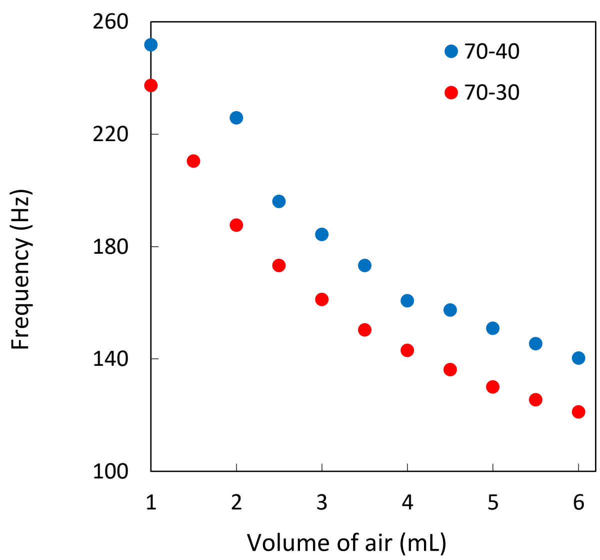

(d)

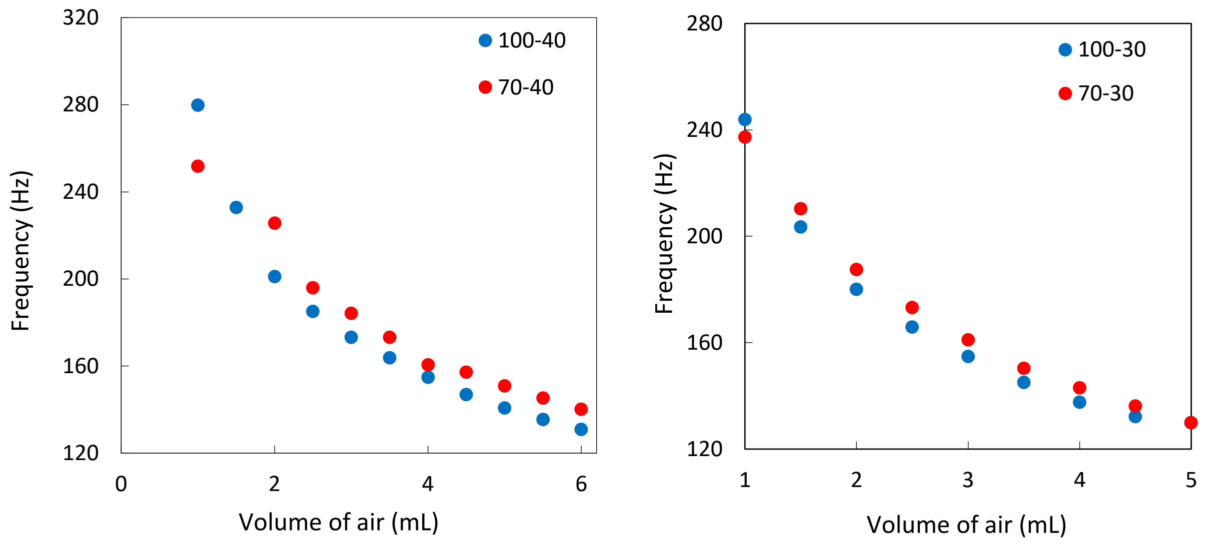

(e) (f)

Fig. C. Design optimization of a double cavity open Helmholtz resonator (a) with hollow screws on the side of the cavity acting as open necks. Table (b) shows the dimensions of the open neck and the diameter and length are varied. Fig. (c) shows, resonance frequency with increased volume of air in open necks of constant length of 100 mm but varying open neck diameter of 40 mm and 30 mm. Fig (d) shows constant length of 70 mm but varying diameter of 40 and 30 mm. Resonance frequency with increased volume of air in open necks of (e) constant diameter of 40 mm but varying the open neck length of 100 mm and 70 mm length and (f) constant diameter of 30 mm but varying the open neck length 70 and 100 mm.

Double cavity-based acrylic open resonator for fish volume measurement

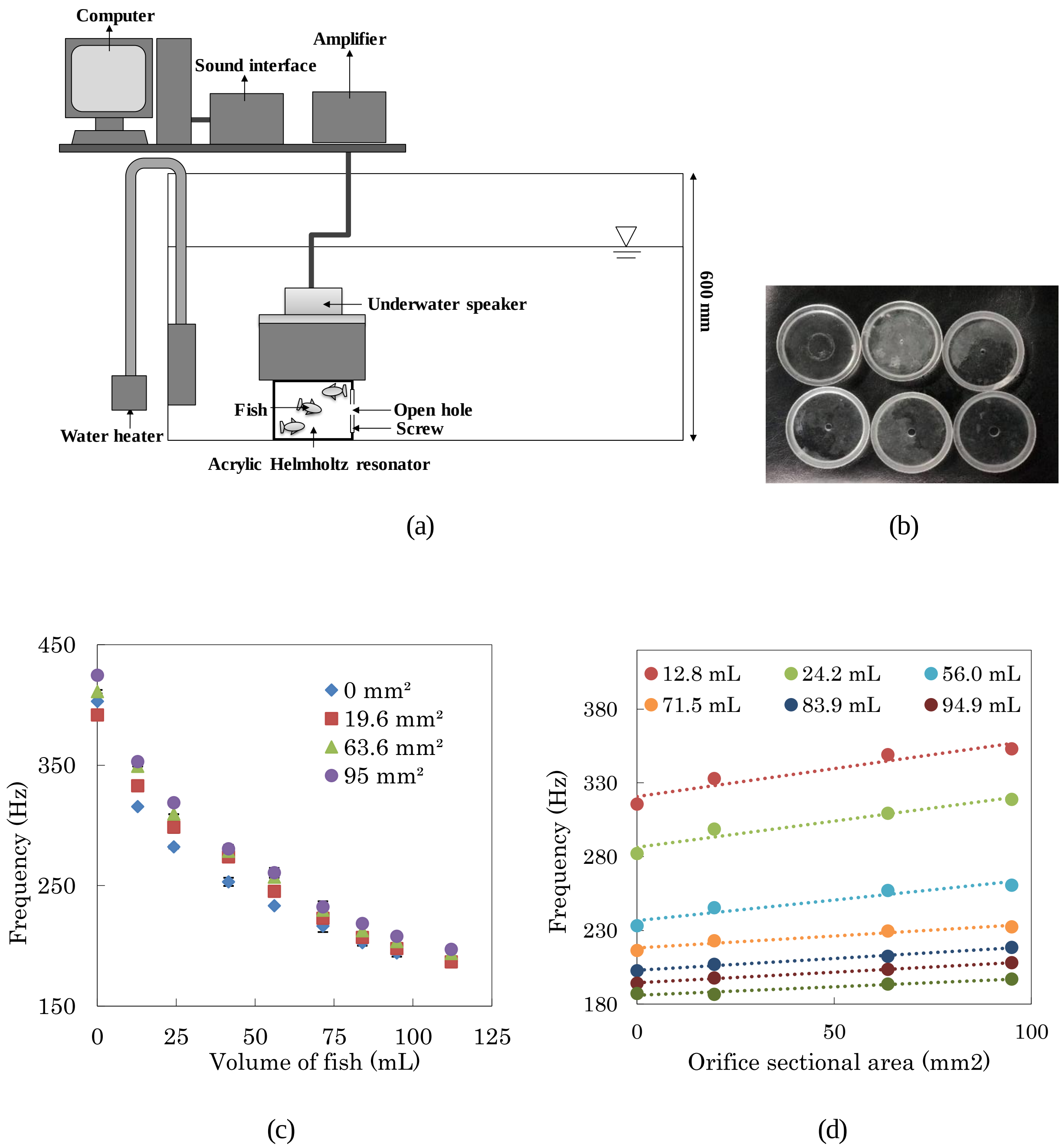

Fig. D. Set up Helmholtz resonator in water with fish inside the open holed-cavity (a) and screws of varying orifice diameter enclosing the cavity of the resonator (b): 0, 19.6, 63.6, 95 mm^2 holes. The graph (c) shows resonance frequency vs. cross sectional area of the opening on the screw of acrylic cavity. As the cross-sectional area increased, resonance frequency increased, in all air volume measured (d).

Double cavity-based acrylic open resonator for air volume measurement

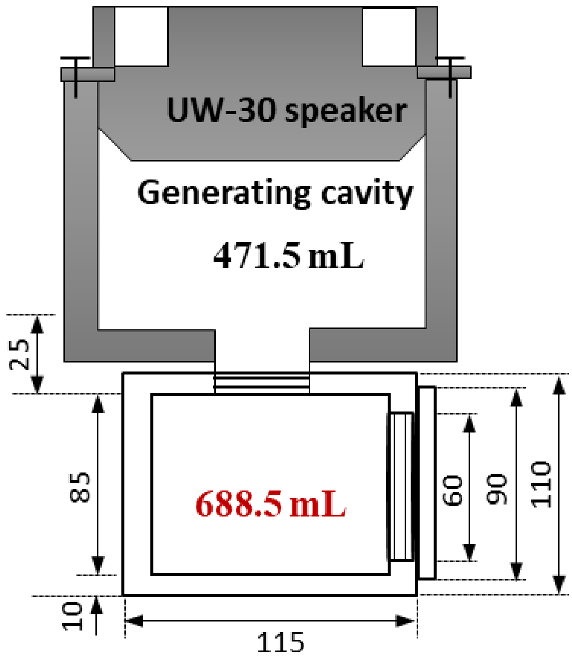

(a)

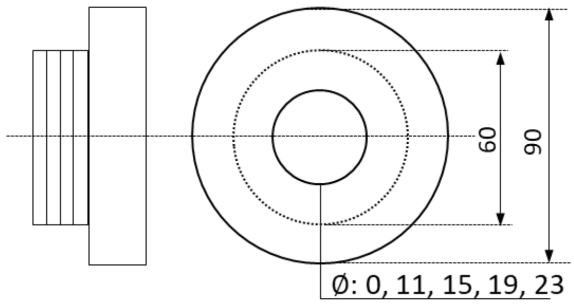

(b)

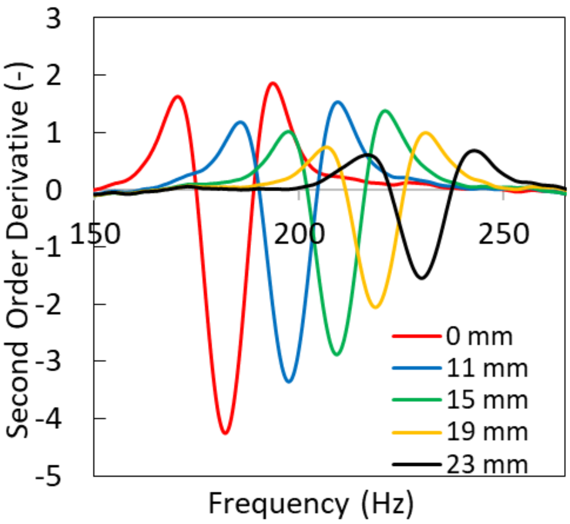

(c)

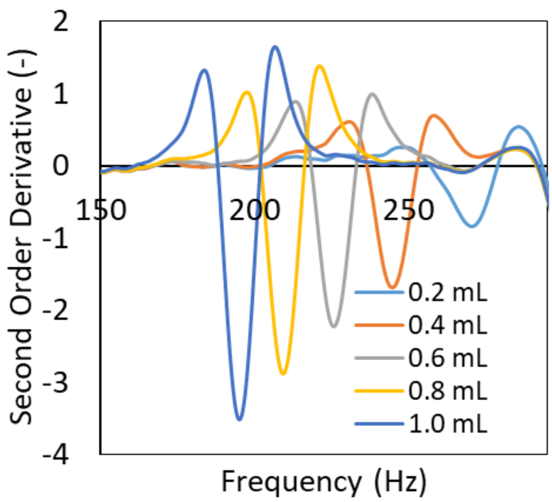

(d)

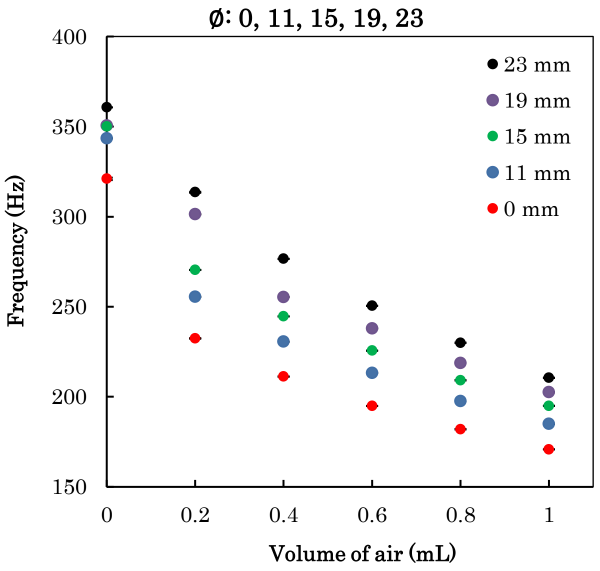

(c)

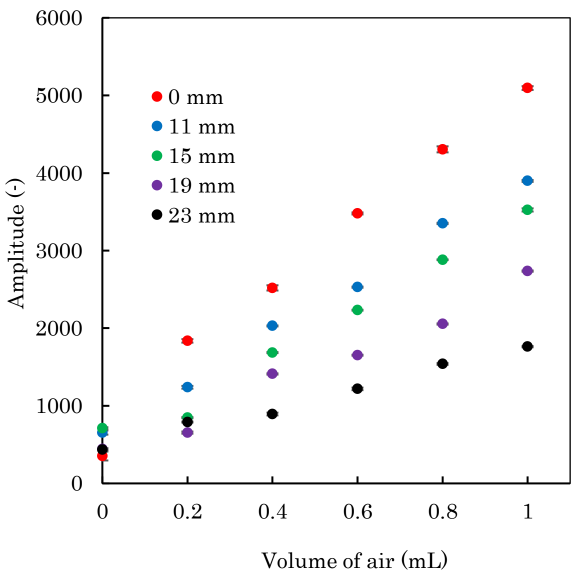

(d)

Fig. E. Double cavity-based resonator (a) with acrylic sample cavity that has open holes (b), with diameter varying 0 (closed), 11, 15, 19, 23 mm on the screw closing the east side of the resonator. As the diameter of the opening (c) increased resonance frequency peaks shifted (d) and for each opening, as the volume of air increased resonance frequency decreased while amplitude increased. As observed in (e), as the diameter of the opening increased, resonance frequency increased.

Effect of sample cavity material of Helmholtz resonators: Acryl vs. stainless-steel

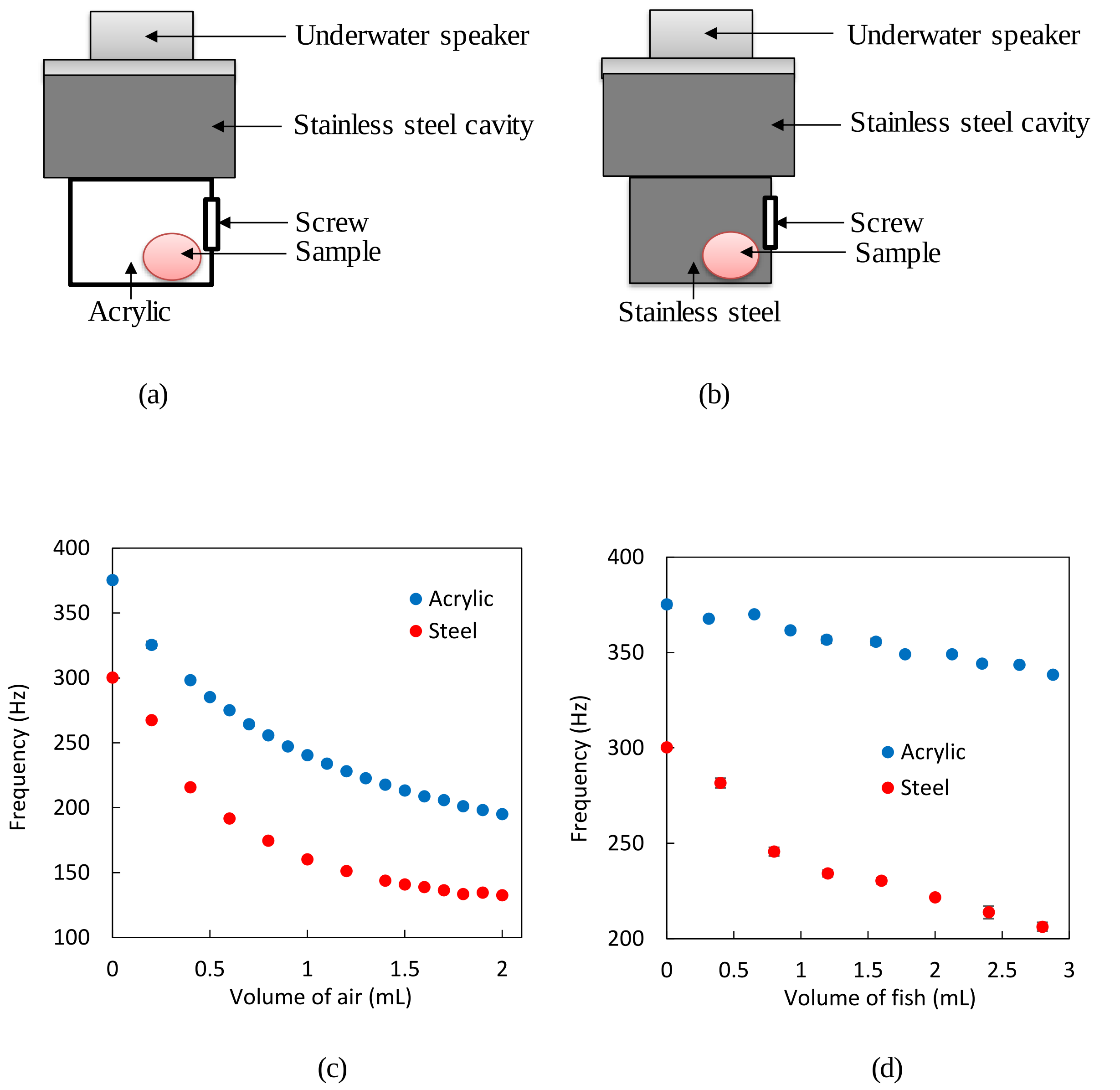

Fig. F. Equal volume (688.5 mL) sample cavity resonators with generating cavities attached on top (a) acrylic type and (b) stainless-steel type sample cavity resonator. Higher resonance frequencies were observed in the acrylic resonance compared to the stainless-steel resonator when both air (c) and fish (d) were measured in the sample cavities. Acrylic sample cavity has lower bulk modulus and thus less stiff compared to the stainless-steel resonator which is stiffer thus lower resonance frequency.

<u>**Water temperature vs. Helmholtz resonance: Water reed and double cavity resonator**</u>

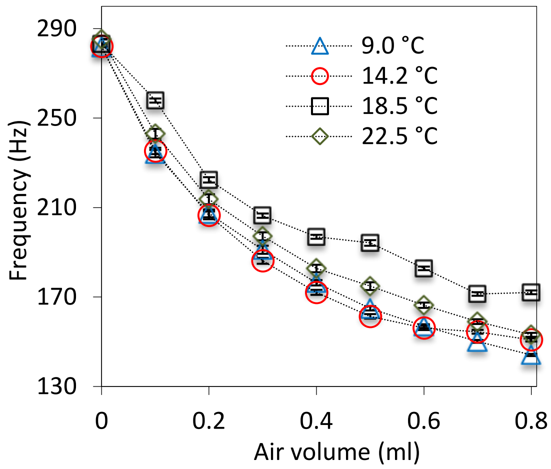

(a)

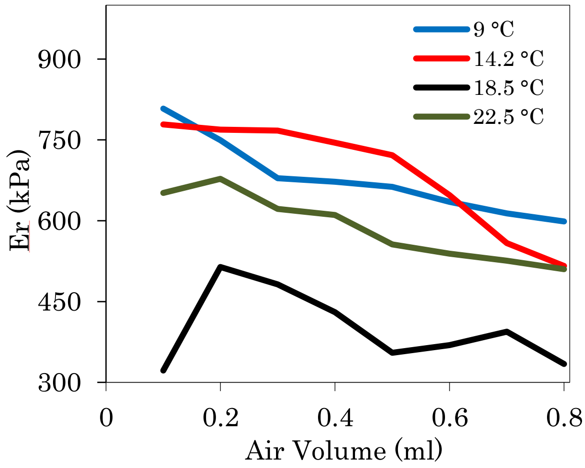

(b)

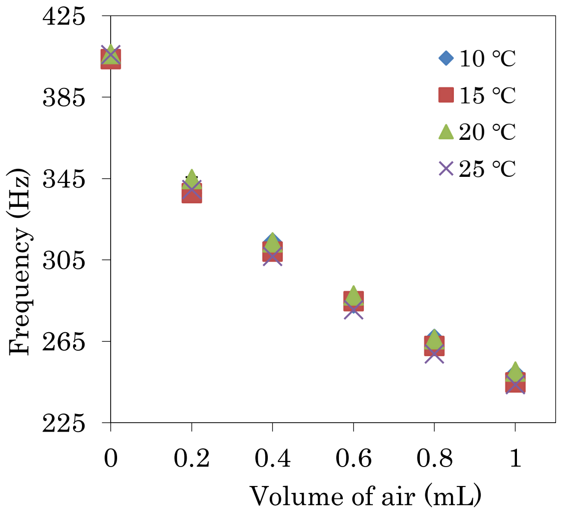

(c)

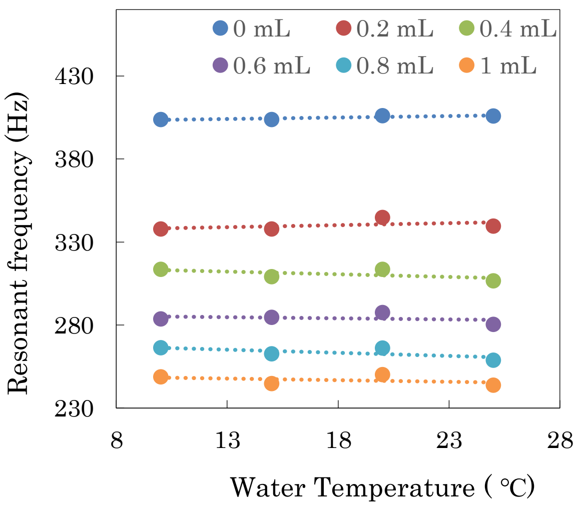

(d)

Fig. G. Resonance frequency change with (a) increased volume of air while varying the water temperature in water reed method and (b) the respective resonator's deflection, E_r (Pa). In the double cavity resonator using speaker impedance method (c) water temperature was varied and air volume measured (d). There was no correlation with the change in resonance frequency in both the water reed method and the speaker impedance technique. However, resonator should be calibrated for each water temperature that it is utilised in.

Water salinity variation with Helmholtz resonance: Water reed technique

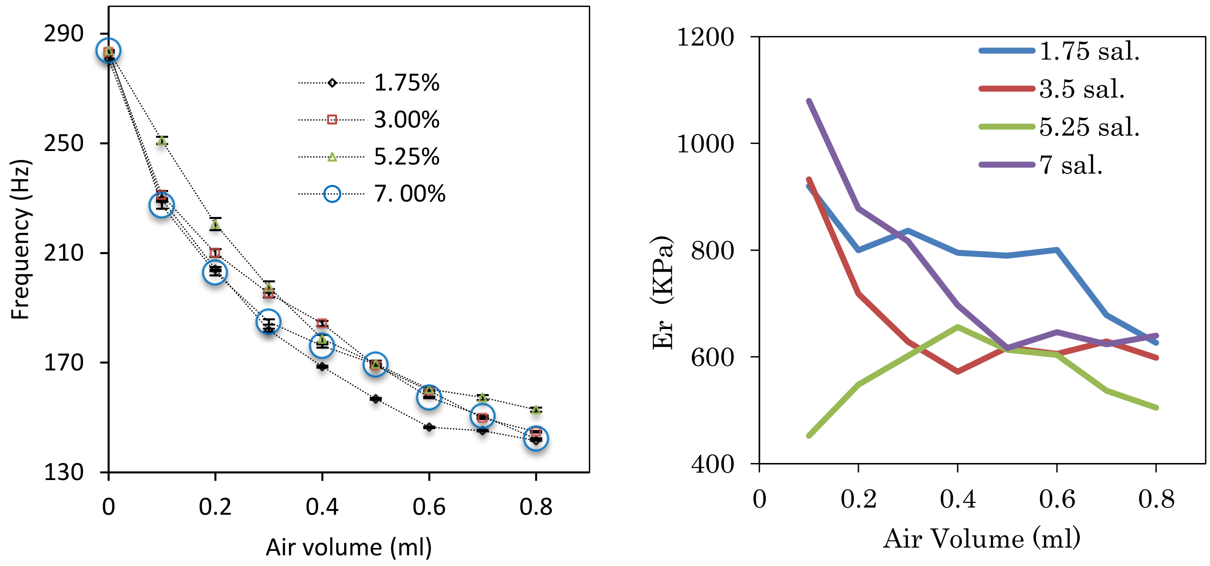

(a) (b)

Fig. H. Resonance frequency against volume of air in different salinity concentrations. There were no clear correlations between salinity level variation with resonance frequency. Fig. (b) shows the resonator deflection property E_r (Pa) in different salinity concentrations. Although there no clear tendencies, it is important to calibrate the fundamental frequency in each salinity level before measuring the sample volume.